8413690

Aytuna, Sezgin

FORMS OF LARGE FOLDS IN THE CENTRAL APPALACHIANS, PENNSYLVANIA

University of Cincinnati PH.D. 1984

University
Microfilms
International 300 N. Zeeb Road, Ann Arbor, MI 48106

PLEASE NOTE:

In all cases this material has been filmed in the best possible way from the available copy. Problems encountered with this document have been identified here with a check mark __√__.

1. Glossy photographs or pages _____
2. Colored illustrations, paper or print _____
3. Photographs with dark background _____
4. Illustrations are poor copy __√__
5. Pages with black marks, not original copy _____
6. Print shows through as there is text on both sides of page _____
7. Indistinct, broken or small print on several pages __√__
8. Print exceeds margin requirements _____
9. Tightly bound copy with print lost in spine _____
10. Computer printout pages with indistinct print _____
11. Page(s) __________ lacking when material received, and not available from school or author.
12. Page(s) __________ seem to be missing in numbering only as text follows.
13. Two pages numbered __________. Text follows.
14. Curling and wrinkled pages _____
15. Other ____

FORMS OF LARGE FOLDS IN THE CENTRAL APPALACHIANS, PENNSYLVANIA

A dissertation submitted to the
Division of Graduate Studies and Research
of the University of Cincinnati
in partial fulfillment of the
requirements for the degree of

DOCTOR OF PHILOSOPHY

in the Department of Geology of the
College of Arts and Sciences

January 1984

by

Sezgin Aytuna

B.S., University of Istanbul, 1974
M.S., West Virginia University, 1979

UNIVERSITY OF CINCINNATI

January 27 19 84

I hereby recommend that the thesis prepared under my supervision by Sezgin AYTUNA

entitled Forms of Large Folds in the Central Appalachians, Pennsylvania.

be accepted as fulfilling this part of the requirements for the degree of DOCTOR OF PHILOSOPHY

Approved by:

David M. Johnson

Attila Kilinc

Malcolm P. Annis

This dissertation is dedicated
to my wife, Ayfer, and my son,
Ali Selim.

FORMS OF LARGE FOLDS IN THE CENTRAL APPALACHIANS, PENNSYLVANIA

ABSTRACT

My Ph.D. dissertation is composed of three chapters, all based on studies of fold forms in the central Appalachians.

The first chapter is a study of the forms of 1st-order (wavelengths of 11 to 18 km) and 2nd-order (wavelengths of 2.5 to 3 km) folds in the central Appalachians of Pennsylvania. At various times, the folds have been stylized in cross sections as concentric, chevron or kink folds, and the current, prevailing interpretation is that the 1st-and 2nd-order folds are kink bands or conjugate kink bands. In part of the central Appalachians, northwest of Harrisburg, Pennsylvania, however, outcrop patterns, serial vertical sections, and structural cross sections indicate that kink-like forms are absent in the 1st-and 2nd-order folds. The folds are complicated, but they resemble combinations of chevron-like and concentric-like forms.

The second chapter is an application of folding theory to complex multilayers, composed of layers of different rheological properties, including the interaction caused by the simultaneous growth of folds with two different wavelengths, in order to study the origin of fold forms in the central Appalachians. An idealized stratigraphic section for rocks in the central Appalachians is divided into structural units with different viscosities and thicknesses based upon study of lithologic descriptions. Viscosities are estimated for various rock types.

The structural units define the mechanical multilayer. Theoretical analysis of folding of the multilayer indicates that the essential features of the forms of Tuscarora Mountain anticline and Berry-Buffalo syncline can be reproduced by horizontal shortening of the multilayer above a detachment surface in upper Ordovician rocks. Further, by moving the detachment surface into the Silurian rocks, the same mechanical multilayer produces theoretical folds with narrow anticlines and broad, flat-bottomed synclines, typical of folds in the Plateau Province.

The third chapter is a detailed field study of the Shikellamy fold, a 3rd-order fold near Northumberland, Pennsylvania. The Shikellamy fold is the largest kink-like fold known in the central Appalachians. The fold has three limbs: southern, central and northern. Bedding-surface faults are common in all the limbs, but they are abundant in the central limb. The sense of shear relative to layering is consistently right-lateral in the central and northern limbs, whereas it is left-lateral in the southern limb. The field evidence suggests that the Shikellamy fold is a monoclinal kink fold, but the structural setting of the fold is peculiar, so it is unclear how the fold formed.

ACKNOWLEDGEMENTS

This research was mainly supported by the National Science Foundation, Grant No. EAR 80-00053. The study was supported in part by the Geological Society of America, Sigma Xi, and the Turkish Educational Ministry.

I express appreciation to my advisor, Dr. Arvid Johnson, for friendship, patience, supervision and assistance. He was always available for consultation and always challenging me to carry new ideas just one step further. This dissertation would not be possible without him. I also would like to thank my Advisory Committee members, Dr. Attila Kilinc and Dr. Malcolm P. Annis, for critically reading the manuscript. Appreciation is also extended to other faculty members of the Department of Geology. I thank Virginia Pfaff for editing the entire manuscript and George Losonsky and Mary Riestenberg for critically reading the third chapter. I thank my wife, Ayfer, for many hours of drawing the figures and Joan Harman for typing the manuscript.

Last, but not least, I thank again my wife and son, Ali Selim, who provided much needed moral support and encouragement during my research.

TABLE OF CONTENTS

TABLE OF CONTENTS (continued) Page No:

TABLE OF CONTENTS (continued) Page No:

LIST OF FIGURES

Figure No: Page No:

CHAPTER I

CHAPTER II

LIST OF FIGURES (continued)

LIST OF FIGURES (continued)

Figure No. Page No:

APPENDIX I

LIST OF TABLES

INTRODUCTION

Modern structural geology is the study of mechanical and chemical processes responsible for geologic structures, such as faults, joints, folds and cleavage, and the application of knowledge of the processes to the understanding of particular structures. This dissertation is an application of the principles of folding theory to the study of several large folds in the Valley and Ridge Province of central Pennsylvania. The fold trains in the Valley and Ridge Province are classic structures, presented in elementary geology courses as typical of folded-mountain belts throughout the world. Field mapping and description of the folds since the middle 1800's have provided considerable information about the rocks involved in the folding as well as the forms of the folds, so the area is nearly ideal for an application of folding theory to the understanding of forms of folds. In order to apply folding theory, one must know or assume the rheological and dimensional properties of the rocks, the boundary conditions of the stack of layers being folded, and the type of deformation to which the rocks were subjected. Previous studies (e.g., Nickelsen, 1963) have shown that the rocks were subjected to layer-parallel compression (shortening ranging from about 10 to 15 percent), so I assume that layer-parallel compression was responsible for the generation of the large folds. The time of folding and the character of the overburden at the time of folding are known, so we can deduce the boundary conditions at the top of the stratigraphic sequence. Further, many studies (e.g., Rodgers, 1963; Gwinn, 1964) have indicated that there was a major zone of decollement or detachment in upper Ordovician rocks at the time of folding, so I can deduce the boundary conditions at the base of the stratigraphic sequence as well.

Folding theory provides many of the tools essential for analyzing low- or high-amplitude folding of simple or complex multilayers; indeed, folding theory is one of the most highly developed theories in geology (e.g., Biot, 1959, 1961; Ramberg, 1960, 1970; Fletcher, 1974, 1977; Smith, 1979; Johnson, 1977; Johnson and Fletcher, 1982). Theories are available for studying folding of elastic, viscous, power-law, elastic-plastic and the extremely general, Reiner-Rivlin fluid. Most of the theory is for low-amplitude folding, but theory is now available for producing theoretical folds with limb dips up to about 30 degrees, and theory is nearly finished for producing folds with limb dips up to 90 degrees (Johnson, personal communication).

My research has focused on the forms of large folds, with wavelengths of three to 18 km, in two areas northwest of Harrisburg, Pennsylvania. One area, about 30 km WNW of Harrisburg, contains the Tuscarora Mountain anticlinorium and the Berry-Buffalo and Cove synclinoria, and the other area, about 100 km NW of Harrisburg, contains the Northumberland synclinorium. There are relatively detailed maps available for the first area, so I measured attitudes of layering throughout the area in order to investigate fold forms (Chapter I). For the second area, near Northumberland, I mapped about 45 square km and used my data to investigate the shape of the Northumberland synclinorium (Chapter III). The folds are so large that their forms cannot be determined directly, but I used all relevant geometric techniques for analyzing fold forms in the two areas, including a new technique of examining serial vertical cross sections, which is described in Chapter I. I compare the fold forms with forms of idealized folds, concentric, chevron, and kink, in Chapter I, and conclude that the folds most closely resemble a combination of concentric-like and chevron-like forms. This result is significant because the prevailing view (e.g., Faill, 1969, 1973; Nickelsen, 1979) is that the large folds are kink-like. The geometric analysis show that the folds are definitely not kink-like in form; indeed, they show that none of the simple forms adequately describes fold shape. This, however, should not be surprising, because the rock multilayers involved in folding are complex, whereas folds resembling simple concentric, chevron and kink forms are known to develop in simple, repetitive multilayers (e.g., Johnson, 1977).

In order to investigate fold forms in complex multilayers one must apply theoretical analysis. This is done in Chapter II, where folding theory valid for limb dips up to about 30 degrees is used to simulate the growth of folds in a model of the mechanical multilayer for the central Appalachians. A summary of the theory and the computer programs necessary for applying the theory are presented in Appendices I, II, III and IV. Furthermore, one must know or assume dimensional and rheological properties of the complex multilayer. I assume that the layers behaved as viscous substances, with free slip between layers, and use published descriptions of stratigraphic sections in order to estimate relative dimensional and rheological properties. The method is explained in detail in Chapter II. Although the theoretical model of the mechanical multilayer is simplified, the results show that the essential features of fold forms deduced by geometric analysis of field data appear in the simulation of the folding.

Thus, Chapters I and II show that one can use a combination of geometric information obtained from the field and theoretical analysis of folding processes in order to estimate shapes of large folds at depth. This result is important academically and practically. It is important academically to structural geologists who wish accurately to portray folded structures in cross sections or to study mechanics of folding. It is important practically to economic and petroleum geologists who wish to exploit deposits controlled by folded structures. The methods of performing the theoretical analysis are made available through the computer programs, presented in Appendices II, III and IV. The computer programs are written in the relatively simple, Microsoft BASIC language so that they can be run on most microcomputers with modest amounts of memory.

Although most of the large folds in the central Appalachians appear to be repetitious folds of the forms described in Chapter I, many of the small folds with wavelengths of a few cm to a few m are kink-like, as can be observed in outcrops. The largest kink-like fold known in the central Appalachians is the Shikellamy fold, near Northumberland, Pennsylvania, which is described in Chapter III. The limb of this fold is about 150 m wide. I studied the structural setting, determined the cross-sectional form and examined minor structures within the Shikellamy fold in order to provide an example of the methods of deducing folding mechanics. The theory of kink folding in complex multilayers is still being developed so that the fold cannot be simulated. Nevertheless, sufficient theory of kink folding has been developed for simple, repetitive multilayers so that one can deduce much about the mechanics of folding where contact strengths between mechanical layers are significant. Most of the evidence suggests that the Shikellamy fold is a kink band, although the structural setting of the fold is peculiar. According to theoretical analyses (e.g., Johnson, 1977), kink folds form in multilayers with contact strength, so there must have been significant contact strength between structural members at the time the fold formed. It is unclear why the contact strength is not reflected in the forms of the large folds, but the answer to this question may lie in scaling; at the scale of the large folds, the contact strength may have been negligible, but at the scale of small folds the contact strength was significant. The most important contribution of Chapter III is the method of using theoretical understanding of folding in order to search for field evidence of various folding mechanisms.

CHAPTER I

ON THE FORMS OF FOLDS IN THE CENTRAL APPALACHIANS*

*Chapter 1 based on manuscript by Johnson, Aytuna and Pfaff (1982)

ABSTRACT

Fold forms in the central Appalachians of Pennsylvania typically are stylized in cross sections, and the styles of folds shown range widely, from concentric-like folds associated with splay faults, to parallel folds, to chevron and kink folds. The prevailing interpretation of fold form in the central Appalachians is that the folds are kink bands or conjugate kink bands. In part of the central Appalachians, however, in an area northwest of Harrisburg, Pennsylvania, and west of the Susquehanna River, the folds plunge so that the forms of folds can be determined by the down-structure method of constructing cross sections. Examination of the structural cross-sections indicates that the relatively simple, major folds, with wavelengths of about ten km, typically are a combination of chevron-like and concentric-like forms; nowhere do the major folds resemble kink bands or kink folds. The forms of smaller folds, with wavelengths of two to three km, are somewhat more complicated, but comparison of their forms with ideal forms developed in simple multilayers subjected to various boundary conditions indicates that the complications can be understood in terms of different structural units in different parts of the stratigraphic section, to simultaneous development and interference of folds with different wavelengths, and to relatively stiff confining media for some multilayered units.

INTRODUCTION

Determination of the causes of folding in the central Appalachians of Pennsylvania and parts of West Virginia, Virginia and Maryland is one of the classic problems of structural geology, a problem that has been the subject of much discussion in geological literature since the early 1800's, and solutions to which have been applied with some success to structures in other mountain belts such as the Canadian Rockies and the Jura Mountains. The earliest view was that the folds are similar to ocean waves, and that the earth's crust was violently disturbed and thrown into permanent waves (e.g., Rogers, 1858). Willis (1893) studied the folds and interpreted them as a result of layer-parallel, penetrative compressive strain and buckling of a rock sequence with contrasting rheological properties and thicknesses. Subsequently, John L. Rich (1934) recognized that the structural relief of the Powell Valley anticline in the Pine Mountain thrust block might reasonably be explained by repetition of section above ramp faults connecting thrust detachment zones. Rich's idea was applied by Rodgers (1949, 1963) to the central Appalachians, but Gwinn's (1964, 1970) application to folding throughout the Valley and Ridge and Allegheny Plateau provinces had greater impact, because it was based on considerable subsurface information. Further, Gwinn suggested that many of the folds are a result of repetition of strata as a result of splay faulting, not necessarily ramp faulting.

The forms of folds shown in cross sections of the central Appalachians largely reflect an investigator's conception of the origin of the folds. Thus, Gwinn's cross sections emphasize the ramp faults and splay faults, and fold forms appear to be drawn to be consistent with forms of the steps in the detachment faults. Jacobeen and Kanes (1974) have constructed similar cross sections for the Wills Mountain anticline. On the other hand, several investigators have assumed that the folds are a result of buckling of the rocks, particularly for folds in Silurian and Devonian rocks of the central Appalachians and of the Allegheny Plateau (Nickelsen, 1963, 1979; Faill, 1969, 1973; Sherwin, 1972; Wiltschko and Chapple, 1977), and have shown folds with a wide range of forms in cross sections. There is considerable evidence that some of the larger folds in the central Appalachains are a result of ramp or splay faulting, particularly the Wills Mountain anticline and the Nittany arch, near the Allegheny front (e.g., Gwinn, 1964, 1970; Jacobeen and Kanes, 1974). However, there is also considerable evidence for layer-parallel compressive strain in the rocks, even in the relatively flat-lying rocks of the Allegheny Plateau of western Pennsylvania (Nickelsen, 1966) and western New York (Englender, 1979). Multilayered rocks subjected to layer-parallel compression will tend to buckle into folds, so many of the folds in the Silurian and Devonian rocks of central Pennsylvania probably are results of unstable growth of perturbations in the layering of the rocks.

This chapter is concerned with forms of folds in Silurian and Devonian rocks in part of the central Appalachians northwest of Harrisburg, Pennsylvania. The folds may be a result of variable shortening in these rocks as a result of splay faulting in the deeper, Cambrian rocks, or may be a result of relatively uniform shortening of the rock sequence above a detachment in Ordovician rocks. In any case, in comparing ideal fold forms with actual fold forms, it is assumed that the folds are primarily a result of layer-parallel compressive strain in multilayered rocks.

Early investigators of the folds in the central Appalachians stylized the cross-sectional forms of folds, but it is unclear how to describe the style of folding depicted (Fig. 1A; Rogers, 1858; Willis, 1893). Perhaps the folds were stylized as sinusoidal folds (Fig. 2B). Sometime between 1900 and 1930, it became common practice to represent the folds as parallel or concentric folds (Fig. 2A). The first cross section of this type we have seen for the central Appalachians, Fig. 1B, was prepared by Chamberlin (1910), who was concerned with estimating the thickness of sections involved in folding in the Appalachians.

Subsequent investigators of folds in the Appalachians have described the folds in various ways. Gwinn (1964, 1970), whose primary interest was folding associated with ramp faulting, incidentally described the typical fold as concentric. According to Wood and others (1969, p. 85), "parallel folding is the principal style of fold deformation..." throughout the southern anthracite coal field. "Mining data indicate that many folds approach parallelism so closely that their shapes, as illustrated in the structure sections...could have been reconstructed mechanically with little error. Most folds die out at depth and show little stratigraphic thinning on their limbs. However, some large synclines locally are similar folds that exhibit pronounced thickening in their troughs and thinning on their limbs" (op. cit., p. 85).

Nickelsen (1963) indicated that the typical folds one can observe in large outcrops in the Valley and Ridge Province of central

Figure 1 - Cross sections of folds in central Appalachians, Pennsylvania.

A. Cross Section prepared in 1858 of folds between Blue Mountain, a few km north of Harrisburg to Jack's Mountain (from Rogers, 1858, x-sections, sheet 2)

B. Cross section prepared in 1910 of folds between Harrisburg (on right) to the Nittany Arch (on left). Folds stylized as parallel folds (from Chamberlin, 1910).

Figure 2 - Some idealized fold forms.

A. Parallel (or concentric) fold (after Van Hise, 1896, fig. 103a)

B. A typical similar fold in which contacts are deflected into sinusoidal curves (Van Hise, 1896, fig. 103b)

C. Chevron fold, another type of similar fold (Van Hise, 1896, fig. 3)

D. Combination of concentric and chevron folds

E. Kink fold comprised of intersecting kink bands. Chevron folds occur locally where bands intersect

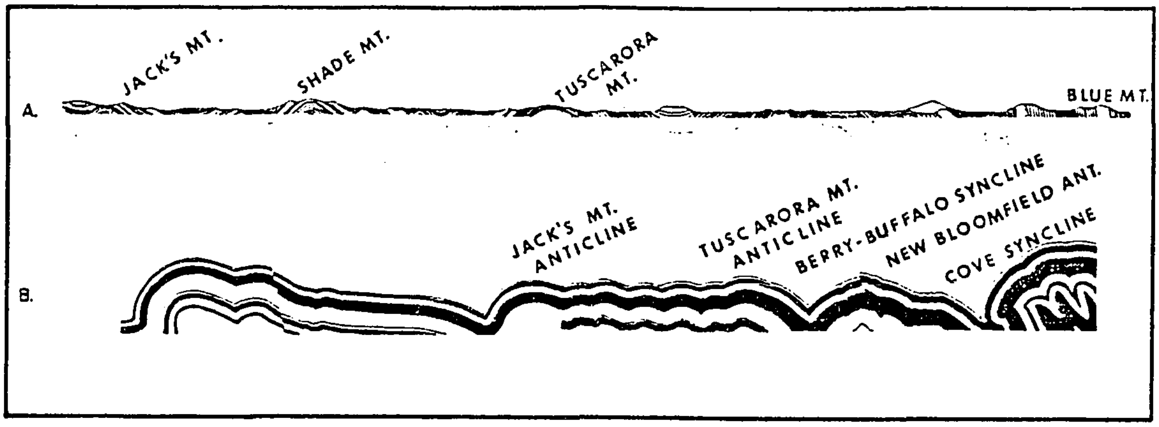

FIGURE 1

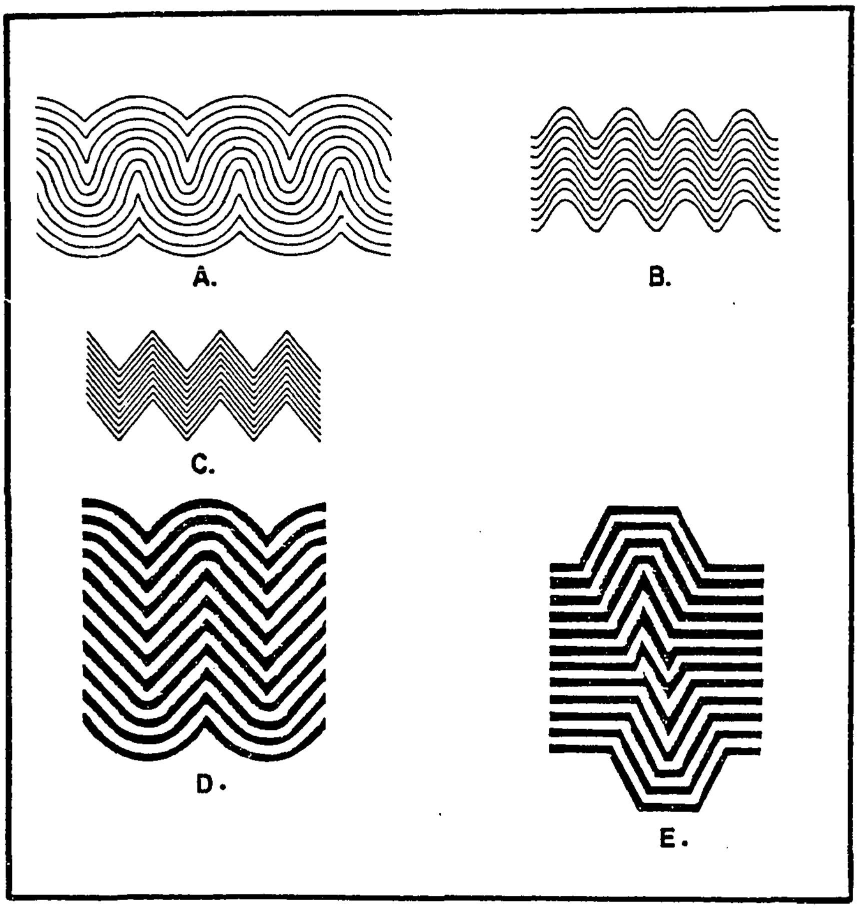

FIGURE 2

Pennsylvania are neither parallel (Fig. 2A) nor similar folds (Fig. 2B), "...but rather more like sine curves with nearly planar limbs and curved hinges..." (p. 19). His description implies the form of the idealized chevron fold (Fig. 2C), but with rounded hinges. He suggested that concentric-like folds might occur in some parts of the section, but he assumed that the larger folds, not directly observable, are also grossly sinusoidal with straight limbs (Nickelsen, 1963, p. 20), that is, are chevron-like. Wood and others (1969, p. 85) indicated that most large anticlines in the southern anthracite coal field are open folds with broad crests, whereas most large synclines are acute or chevron folds with V-shaped cross sections.

Faill (1969, 1973) reinterpreted most of the folds in the Appalachians as kink folds (Fig. 2E). The bases for the reinterpretation, according to Faill (1973, p. 1310), are that typical fold hinges are narrow and radii of curvature of the hinges are much smaller than wavelengths of folds, and that bedding in fold limbs is planar, so that the folds cannot be parallel. Finally, there is negligible thickening or thinning of beds in crests and limbs of folds, so that the folds cannot be of the similar variety such as that shown in Fig. 2B. The typical fold described by Faill (1969, p. 2540 and 2541; 1973, p. 1310 and 1312) closely resembles the idealized chevron fold (Fig. 2C). The chevron fold, of course, is a type of similar fold. However, Faill specifically envisioned the typical fold in the central Appalachians to be a chevron fold formed by the intersection of conjugate kink bands (1969, figs. 3, 4, 5, 7 ; figs. 6, 8, 9, 20, 22, 27-31). Furthermore, most folds shown in cross sections of areas in Pennsylvania recently mapped by Faill have been stylized as kink forms and chevron forms (Faill and Wells, 1974, 1977).

Thus, there have been widely divergent interpretations of the styles of folding in the Central Appalachians.

The purposes of this chapter are to re-examine fold forms in the central Appalachians, using a variety of methods of structural analysis, and to compare the reconstructed fold forms with the idealized forms shown in Fig. 2.

A program of detailed quadrangle mapping by the Pennsylvania Geological Survey has provided a series of geological maps of five adjacent 15-minute quadrangles in an area north and northeast of Harrisburg, Pennsylvania, and west of the Susquehanna River. I examined small folds and bedding characteristics in outcrops in the area, and measured attitudes of bedding at strategic locations in order to estimate plunge angles of folds. Many of the folds in this area plunge at angles ranging from five to twenty degrees, so that down-plunge, structural cross-sections can be constructed to determine fold forms. Further, changes in forms of folds through the various rock units can be recognized by examining serial, vertical cross-sections prepared by the investigators who mapped the quadrangles.

FORMS OF LARGE FOLDS IN THE CENTRAL APPALACHIANS

Folds are necessarily three-dimensional structures, because they die out along their axes, but most folds are highly elongate so that most of the structural information about fold form is contained in cross sections, transverse to axes. The outcrops in the central Appalachians are too small to show the cross-sectional forms of 1st- and 2nd-order* folds, which range from about 2 to 18 km in wavelength, so one necessarily must rely upon indirect methods of determining fold shapes. Where folds are plunging, as in many areas of the central Appalachians, one can obtain some information about the forms of folds by observing the gross outcrop patterns of the layers, by examining serial cross sections constructed roughly normal to fold axes, and by using the down-plunge method of constructing structural cross sections. I will discuss each of these methods in the following paragraphs.

Map Patterns

As stated by Bailey and Robin Wills, "The pattern made by the erosion of folded strata to an approximately plane surface may reveal

*The concept of orders of folds is an old one (e.g., Rogers, 1858, p. 887; Van Hise, 1896); the notion is that folds of distinctly different sizes form roughly at the same time in a complex multilayered rock sequence. Nickelsen (1963) has provided a useful classification of sizes or orders of folds in the Appalachians: 1st-order folds are anticlinoria and synclinoria with wavelengths of 11 to 18 km (7-11 mi.) and involve rocks from the Cambrian to the Pennsylvanian. 2nd-order folds have wavelengths of 2.5 to 3 km (1.5-2 mi.); they are best developed at the levels of the Tuscarora and Bald Eagle formations. 3rd-order folds have wavelengths of several meters to one km. They are best developed in the middle Silurian and middle Devonian rocks above the Rose Hill Shale and below the Hamilton group. 4th-order folds have wavelengths ranging from a few tens of centimeters to a few meters. 5th-order folds are smaller than these.

many facts in regard to the character and classification of...folds. Relative curvature of different contacts around the axis of a plunging fold indicates concentric or similar folding. The actual shape of the fold in cross-section is indicated by the degree of curvature and variations in it from bed to bed" (Willis and Willis, 1934, p. 370). The patterns are visible on space imagery (Fig. 3) and in map patterns of contacts between rock units in the Central Appalachians (Fig. 4, after Gray and others, 1960). The rounded form of hinges of some 2nd-order anticlines is particularly well shown for Shade Mountain anticline and Tuscarora Mountain anticline (Fig. 3; for locations, see Fig. 4), by relief made visible by shadows on the space imagery. Also, the outcrop patterns of the Tuscarora Sandstone and Juniata Formation in a series of anticlines and synclines of 2nd-order size, the Green Valley and Kennedy Valley synclines, and the Barkley Ridge and Mt. Dempsey anticlines (Fig. 4), suggest an alteration of open synclines and tight anticlines within the same stratigraphic units.

The map patterns suggest that the forms of the folds change not only in the same unit, from adjacent anticlines to adjacent synclines, but also from unit to unit within a single fold. For example, the lower contact of the Catskill Formation in the North Trough of the Minersville Synclinorium, west of the Juniata River (Figs. 3 and 4), forms an open hinge whereas the lower contacts of the Pocono Group and the Mauch Chunk Formation form tight hinges. The changes in tightness of hinges from unit to unit are more apparent in a detailed map of the area west of the Susquehanna River (Fig. 5). For example, the hinge area in the Rose Hill Formation (cross-hatched pattern) is an open flexure, whereas in overlying Silurian and Devonian rocks, there

Figure 3 - Space image of part of Valley and Ridge Province in central Pennsylvania, showing rounded profile of Tuscarora Mountain (T) and Shade Mountain (S).

FIGURE 3

Figure 4 - Traces of contact between some of rock units shown on part of Pennsylvania State Geological Map (after Gray and others, 1960)

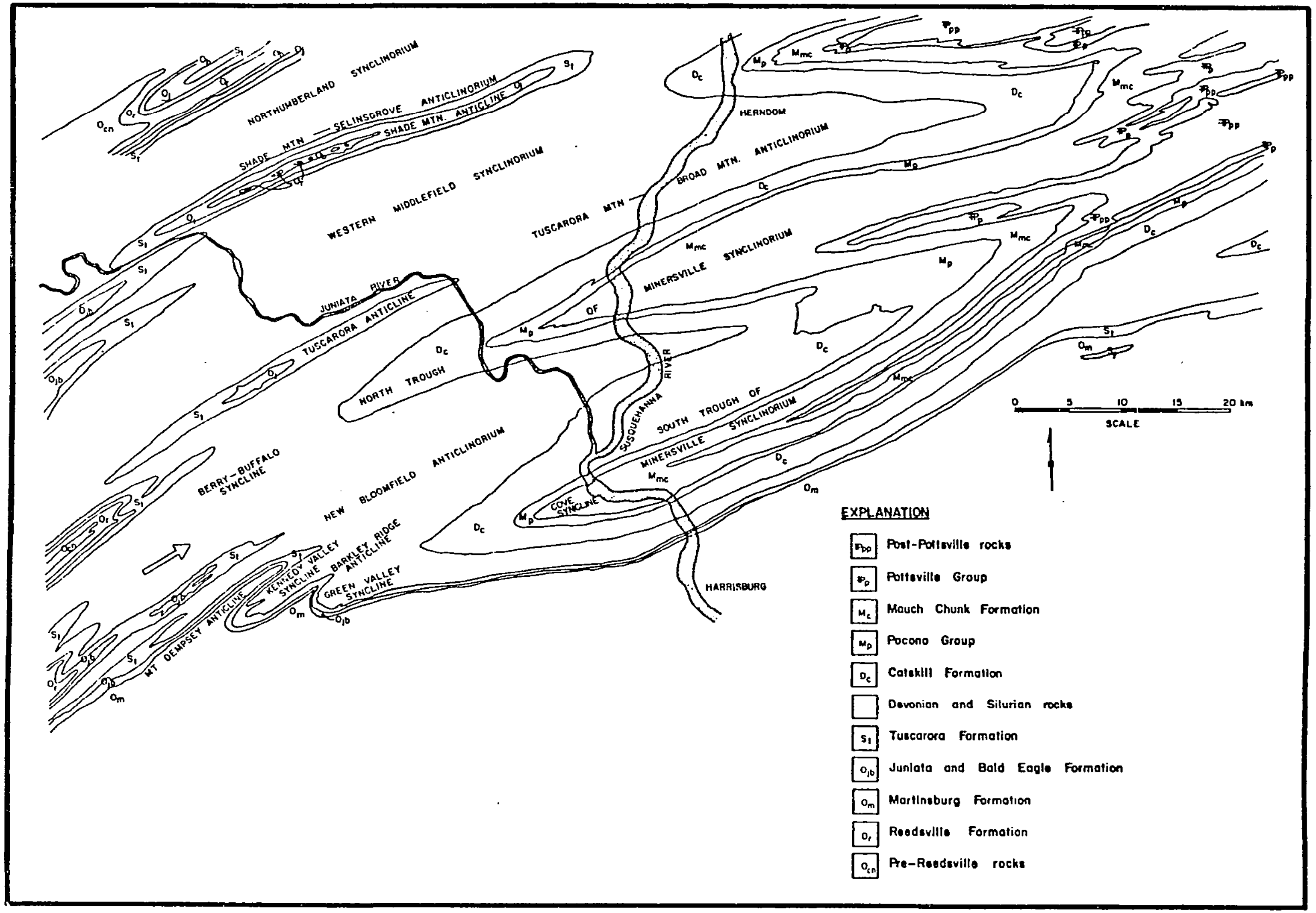
NORTHUMBERLAND SYNCLINORIUM
SHADE MTN — SELINSGROVE ANTICLINORIUM
SHADE MTN. ANTICLINE
WESTERN MIDDLEFIELD SYNCLINORIUM
TUSCARORA MTN
BROAD MTN. ANTICLINORIUM
HERNDOM
MINERSVILLE SYNCLINORIUM
JUNIATA RIVER
TUSCARORA ANTICLINE
NORTH TROUGH OF
SUSQUEHANNA RIVER
SOUTH TROUGH OF
MINERSVILLE SYNCLINORIUM
BERRY–BUFFALO SYNCLINE
NEW BLOOMFIELD ANTICLINORIUM
COVE SYNCLINE
KENNEDY VALLEY SYNCLINE
BARKLEY RIDGE ANTICLINE
GREEN VALLEY SYNCLINE
MT DEMPSEY ANTICLINE
HARRISBURG
0 5 10 15 20 km
SCALE
EXPLANATION
Post-Pottsville rocks
Pottsville Group
Mauch Chunk Formation
Pocono Group
Catskill Formation
Devonian and Silurian rocks
Tuscarora Formation
Juniata and Bald Eagle Formation
Martinsburg Formation
Reedsville Formation
Pre-Reedsville rocks

FIGURE 4

Figure 5 - Composite geologic map of parts of Loysville, Millerstown and New Bloomfield, 15-minute quadrangles (after Miller, 1961; Faill and Wells, 1974; and Dyson, 1963, 1967) and composite structural cross-section (down-plunge) of 1st-order synclines and associated 2nd-order folds.

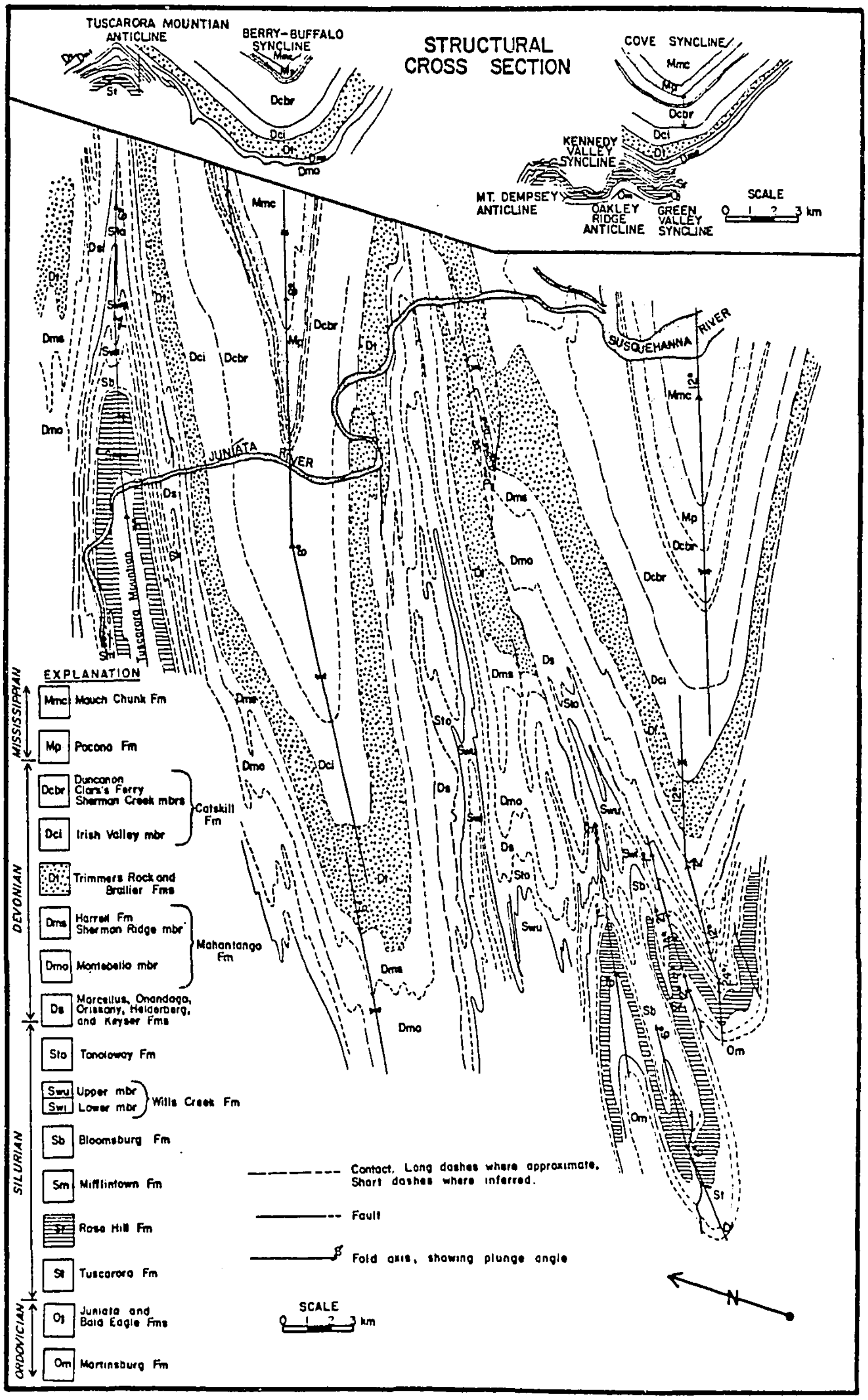
STRUCTURAL CROSS SECTION
TUSCARORA MOUNTAIN ANTICLINE
BERRY-BUFFALO SYNCLINE
COVE SYNCLINE
KENNEDY VALLEY SYNCLINE
MT. DEMPSEY ANTICLINE
OAKLEY RIDGE ANTICLINE
GREEN VALLEY SYNCLINE
SCALE 0 1 2 3 km
SUSQUEHANNA RIVER
JUNIATA RIVER
Tuscarora Mountain
EXPLANATION
MISSISSIPPIAN
Mmc Mauch Chunk Fm
Mp Pocono Fm
DEVONIAN
Dcbr Duncanon Clark's Ferry Sherman Creek mbrs
Dci Irish Valley mbr
Catskill Fm
Dt Trimmers Rock and Brallier Fms
Dms Harrell Fm Sherman Ridge mbr
Dmo Montebello mbr
Mahantango Fm
Ds Marcellus, Onondaga, Oriskany, Helderberg, and Keyser Fms
SILURIAN
Sto Tonoloway Fm
Swu Upper mbr
Swl Lower mbr
Wills Creek Fm
Sb Bloomsburg Fm
Sm Mifflintown Fm
Sr Rose Hill Fm
St Tuscarora Fm
ORDOVICIAN
Oj Juniata and Bald Eagle Fms
Om Martinsburg Fm
Contact. Long dashes where approximate, Short dashes where inferred.
Fault
Fold axis, showing plunge angle
SCALE 0 1 2 3 km
N

FIGURE 5

are numerous narrow hinges, and in the overlying Trimmers Rock Formation (stippled pattern), the hinge area is again an open flexure.

Let us compare the map patterns of contacts with the map patterns of some idealized folds. Figure 6A shows, below, an idealized kink band in structural cross-section and above, the map pattern of the kink band plunging toward the top of the figure at 15 degrees; the ground surface is assumed to be flat, so that topographic effects, present in the geologic maps in Figs. 4 and 5, are absent in the idealized maps. The kink band forms a distinctive pattern. Although the layers in the limbs and crests are of equal thickness, they appear to change thickness in the map pattern of the plunging kink band. The hinges are shown as angular forms, but the gross pattern would be unchanged if the hinges were rounded. I would note that the ideal map pattern shown in Fig. 6A does not resemble, even approximately, the patterns shown in the geologic maps in Figs. 4 or 5. Figure 6B shows an idealized concentric fold, of low amplitude. The structural cross-section was constructed with a drafting compass, so the form is known to be concentric. The idealized map pattern in plunging, concentric folds is shown above the structural cross section in Fig. 6B. Except for the core of the anticline, the hinges are all smooth curves. In the map pattern, the curvature appears to be concentrated in the hinges and the limbs appear to be nearly straight. But, in fact, we know that, along each contact, the curvature is constant between inflection points, and that the curvature changes abruptly at inflection points separating an anticline from an adjacent syncline. Thus, even relatively sharp map patterns do not necessarily imply that the fold, as viewed down its axis, has a sharp hinge, and even relatively straight contacts do not necessarily imply that the

Figure 6 - Outcrop patterns of some idealized folds.

A. Above, outcrop pattern of kink band plunging 15°; below, down-plunge, structural cross-section of fold.

B. Above, outcrop pattern of concentric fold of low amplitude plunging 15°; below, structural cross section.

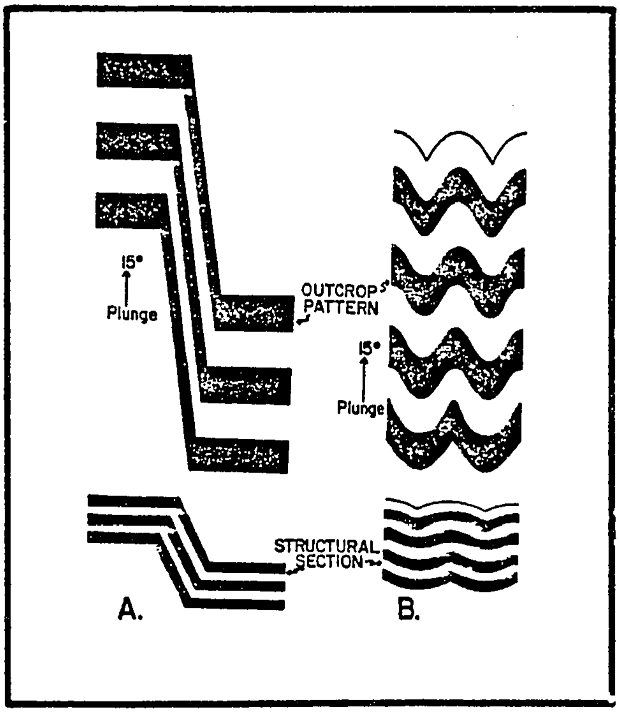

FIGURE 6

limbs, as viewed down the fold axis, are straight. This example illustrates some of the difficulties of recognizing the cross-sectional form of a fold plunging at a low angle, as for the folds in the central Appalachians, by merely examining the map patterns of contacts between layers.

Figures 7A and 7B show structural cross sections and map patterns for plunging folds of idealized kink-fold form (7A) and idealized chevron and concentric forms (7B). Where the kink bands intersect, the forms are locally chevron folds, but elsewhere they are distinct kink bands, as in Fig. 6A. The concentric folds appear in anticlines at the upper contact of the multilayer with the medium in which the folds formed, and in synclines at the lower contact. The folds are of chevron shape elsewhere in the idealized fold pattern. As in the previous diagram, I could have shown the hinges of chevron folds and kink folds as rounded forms, with short radii of curvature, rather than as sharp forms; but, again, the basic pattern would not have been changed and one can readily imagine the fold patterns with rounded hinges. The idealized map patterns of folds in Figs. 7A and 7B are distinctly different. There is apparent thinning on limbs of folds and apparent thickening in hinges of folds for both patterns, but the axial regions of the concentric folds appear as rounded forms whereas the axial regions of kink folds appear as flat forms. Furthermore, except for the localized area where the kink bands intersect, there are distinct kink-band forms elsewhere in the map pattern. In contrast, in the combination of chevron folds and concentric folds, the chevron folds dominate the map pattern and the rounded folds representing the concentric forms appear along the axes of the anticline and synclines.

Figure 7 - Outcrop patterns of some idealized folds.

A. Above, outcrop pattern of kink-fold plunging 15°; below, down-plunge, structural cross-section.

B. Above, outcrop pattern of combination of concentric and chevron folds plunging 15°; below, structural cross-section.

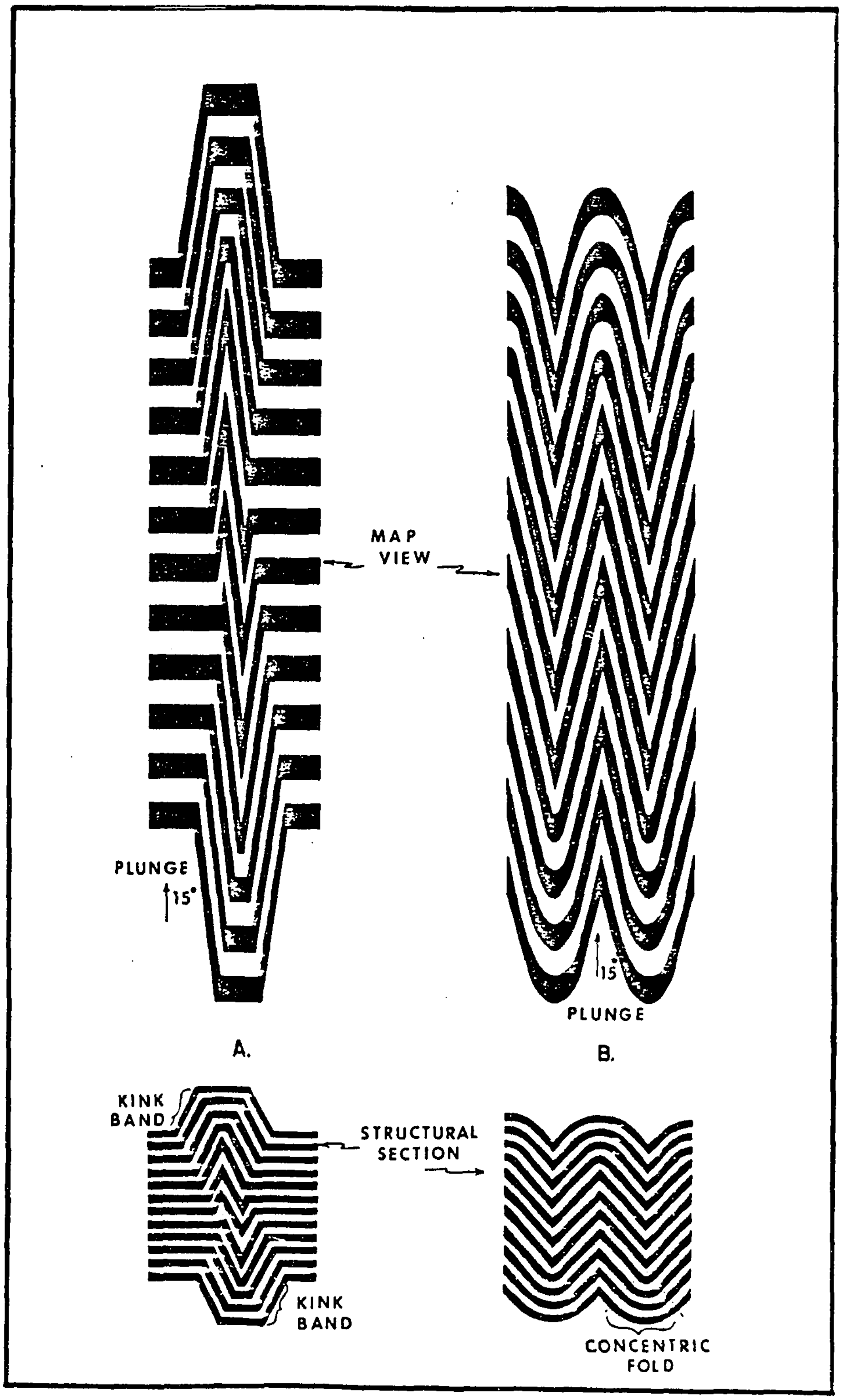
MAP
VIEW
PLUNGE
15°
15°
PLUNGE
A.
B.
KINK
BAND
STRUCTURAL
SECTION
KINK
BAND
CONCENTRIC
FOLD

FIGURE 7

Comparing the idealized map patterns of plunging folds with the geologic maps, Figs. 4 and 5, one is impressed with the similarity of the gross outcrop patterns of the 1st-order folds with the idealized pattern for chevron folds. Further, the geologic map patterns for the 2nd-order folds (e.g., the Green Valley syncline and the Barkley Ridge anticline, Fig. 5) closely resemble idealized patterns for synclines of concentric form and anticlines of chevron form, as shown near the bottom of the idealized map pattern in Fig. 7B. Finally, nowhere in the map can we recognize the distinctive pattern of a kink band.

Vertical Cross Sections

Now let us examine fold forms as shown in vertical cross sections by various investigators for the general areas shown in Figs. 4 and 5. Vertical cross sections of folds largely represent assumptions about the shapes of the folds at depth. Many investigators use the Busk method (Busk, 1957; Raga, 1973), assuming that the folds are parallel. Some (e.g., Faill and Wells, 1974; Hoskins, 1976; Laubscher, 1976; Thompson, 1979) assume that most of the folds are kink bands or kink folds in constructing cross sections. The primary data used in constructing vertical cross sections are positions of contacts at the ground surface along the cross section, apparent dips of contacts projected onto the cross section, and apparent dips determined for attitudes measured near the line of cross section.

Commonly, vertical cross sections are drawn assuming that the folds exposed at the surface extend indefinitely to depth, except where the folds are assumed to be of parallel form (Fig. 1B). For example, in some of the earliest cross sections of the central Appalachians prepared by Rogers (1858, p. 345 and 355), small asymmetric folds that crop out near Fio Forge on the NW (left) limb of the Cove syncline (Fig. 8A) are shown throughout the depth of the cross section. Other examples are shown in serial cross sections of Tuscarora Mountain (Figs. 9A, B and C) prepared during a modern program of quadrangle mapping in central Pennsylvania. In Fig. 9A the outcrop of the fold in the Wills Creek Formation (Sw) suggests a chevron form, and the chevron form is extended to depth through the Tuscarora Sandstone (St). In Fig. 9B the outcrop of the fold in the Bloomsburg Formation (Sb) suggests two sharp anticlines and an intervening flat syncline, and these forms are extended to depth into the Tuscarora Sandstone. In Fig. 9C the outcrop of the Tuscarora Sandstone suggests an open, concentric-like form, and this form is extended to depth into the Reedsville (Or). The three cross sections shown in Fig. 9 were prepared by different investigators in three adjacent quadrangles (A from Hoskins, 1979; B from Faill and Wells, 1974; C from Conlin and Hoskins, 1962). I would emphasize that the three different fold forms shown in the cross sections are displayed at different stratigraphic horizons near the ground surface along the cross sections, so that there is evidence that the folds change shape from one stratigraphic unit to another, but no evidence that the fold forms change significantly along fold axes.

Figure 8 - Vertical cross sections of folds in central Appalachians according to Rogers (1858, Vol. I).

A. Section from northeastern end of Tuscarora Mountain to Blue Mountain (fig. 63)

B. Section from Shade Mountain (fig. 62)

C. Section from Shade Mountain through Mifflintown to Tuscarora Mountain (fig. 67)

Figure 9 - Serial vertical cross sections of Tuscarora Mountain anticline and Berry-Buffalo syncline in several adjacent quadrangles. Symbols for units defined in Fig. 5.

A. Millersburg quadrangle (Hoskins, 1976)

B. Millerstown quadrangle (Faill and Wells, 1974)

C. Mifflintown quadrangle (Conlin and Hoskins, 1962)

D. New Bloomfield quadrangle (Dyson, 1963)

E. Loysville quadrangle (Miller, 1961)

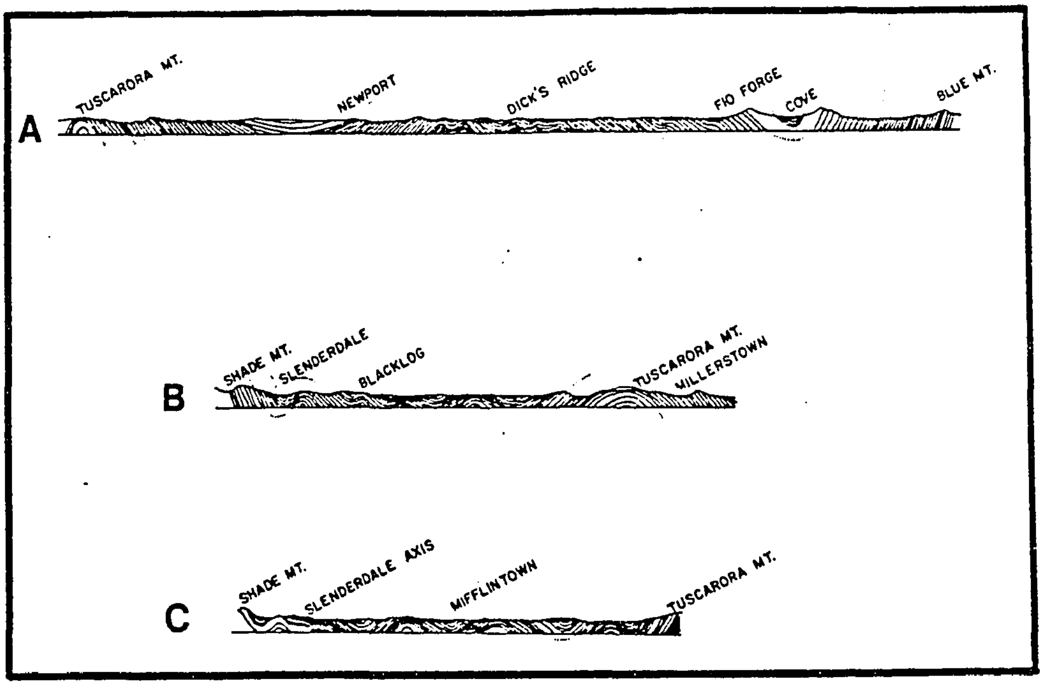

FIGURE 8

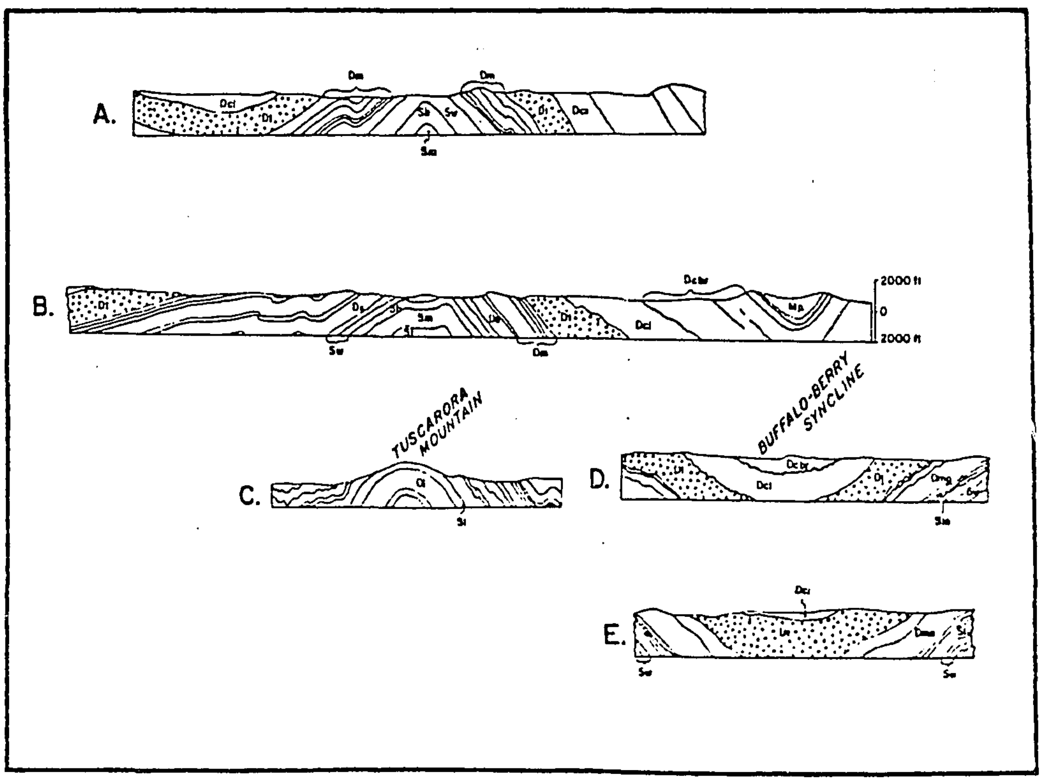

FIGURE 9

Down-Plunge Structural Cross Sections

Another, quite different, approach to the construction of cross sections of plunging folds is to project geometric elements of folds along the plunge direction to a common cross section; this is the so-called down-structure or down-plunge method of structural geology, explained clearly in principle by J. Hoover Mackin (1950). The method of constructing such cross sections is explained in some structural textbooks (e.g., Ragan, 1973). This powerful method is uncommonly used in constructing cross sections, so I will quote Mackin's discussion at some length (Mackin, 1950, p. 58):

> The use of the down-structure method...is obviously based on the assumption that the structural features in individual beds and corresponding parts of folds are continuous down the plunge. The extent to which this assumption is justified varies widely, of course, from district to district, depending on the rock types involved and local structural habits; the only generalization that can be made is that it is usually preferable to the alternative assumption that subsurface structures can be drawn in a structure section solely on the basis of graphical or mathematical manipulation of dip measurements recorded at the surface along the line of section... In an area of plunging folds, strikes measured at the surface up-plunge and down-plunge from a given line of section have quite as significant a bearing on the structure beneath the surface in the section as do dips measured along the line. To draw a structural section across plunging folds, it is usually necessary to map a zone, with as much attention to precision in strike measurements as in dip measurements.

The advantage of the down-plunge method, in comparison to the vertical-section method, is that one does not have to assume the shapes of folds at depth, rather one estimates the shapes of folds at depth by projection of forms exposed at the surface. The method works only where folds are plunging, and it works well only where fold forms maintain nearly constant profiles along the plunge direction. As a rule of thumb, I would recommend projecting attitudes and contacts, by the down-plunge method, at distances from the cross section less than about one wavelength of the fold. Thus, I would project attitudes and contacts defining 1st-order folds in the Appalachians no farther than about 15 km, and the 2nd-order folds no farther than about three km.

I have graphically constructed structural cross sections using parts of geologic and topographic maps of the Loysville (Miller, 1961), the New Bloomfield (Dyson, 1963, 1967) and the Millerstown (Faill and Wells, 1974) quadrangles. A reduced and somewhat simplified composite geologic map and the structural cross section, and average trends and plunge angles of fold axes used in constructing the sections are shown in Fig. 5. Orientations of fold axes were determined with attitudes I measured throughout the area specifically for the purpose of structural analysis, except for the area of 2nd-order folds in the southwestern corner of the area (Fig. 5) where outcrops are rare. These plunges were determined largely graphically, by assuming that selected sedimentary units are of constant thickness. As indicated on the map, directions and plunge angles of fold axes vary from place to place throughout the area. Therefore, structural cross sections were constructed for local areas and projected onto a common cross section. The trends of 3rd-order folds in the Silurian and Devonian rocks commonly are oblique to those of the 2nd-order and 1st-order folds, so that 3rd-order folds generally could not be shown on the structural cross section. The 3rd-order folds and several faults dominate the central part of the New Bloomfield anticlinorium, between the Cove and Berry-Buffalo synclinoria, so that folds were not reconstructed in the anticlinorium. Furthermore, apparent thicknesses of units are rather variable locally in the structural cross sections, but many of the thickness changes probably are results of the construction method and are therefore unreal. Nevertheless, the down-plunge method provides general forms of 1st- and 2nd-order folds in the area.

DISCUSSION

The structural cross sections for the Cove syncline and associated 2nd-order folds, and for the Berry-Buffalo syncline and the Tuscarora anticline, are shown in Fig. 10. Let us compare the composite structural section of the Tuscarora Mountain anticline and Berry-Buffalo syncline with the serial vertical cross sections prepared by others (Fig. 9). The forms shown in the composite section (Fig. 10A) are clear in the serial cross sections (Fig. 9). Both the serial and composite sections for the Berry-Buffalo syncline suggest a concentric-like form at the levels of the Trimmers Rock (Dt) and the Catskill (Dci and Dcbr) formations, and a chevron-like form at the levels of the Pocono Group (Mp) and the Mauch Chunk Formation (Mmc). Thus, the gross form is strikingly similar to that of the combination of idealized concentric and chevron folds (Fig. 2D). The limbs of the reconstructed Berry-Buffalo syncline are relatively straight, as they are in the idealized example. However, the fold pattern shown in Fig. 2D is regular, whereas that in the field example is irregular, probably because the fold involves rocks with different properties at different stratigraphic levels. Thus, although one might project the Trimmers Rock Formation as a chevron-like anticline over the Tuscarora Mountain anticline, it is also possible that the Trimmers Rock Formation forms the inner arc of a concentric-like fold developed above the stratigraphic level shown in Fig. 10A.

The fold shown in the structural cross section of the Tuscarora Mountain anticline is quite different from the folds shown in the serial vertical cross sections (Fig. 9). According to the serial sections,

Figure 10 - Structural cross-sections of Berry-Buffalo and Cove synclinoria constructed by the down-plunge method. Symbols for units defined in Fig. 5.

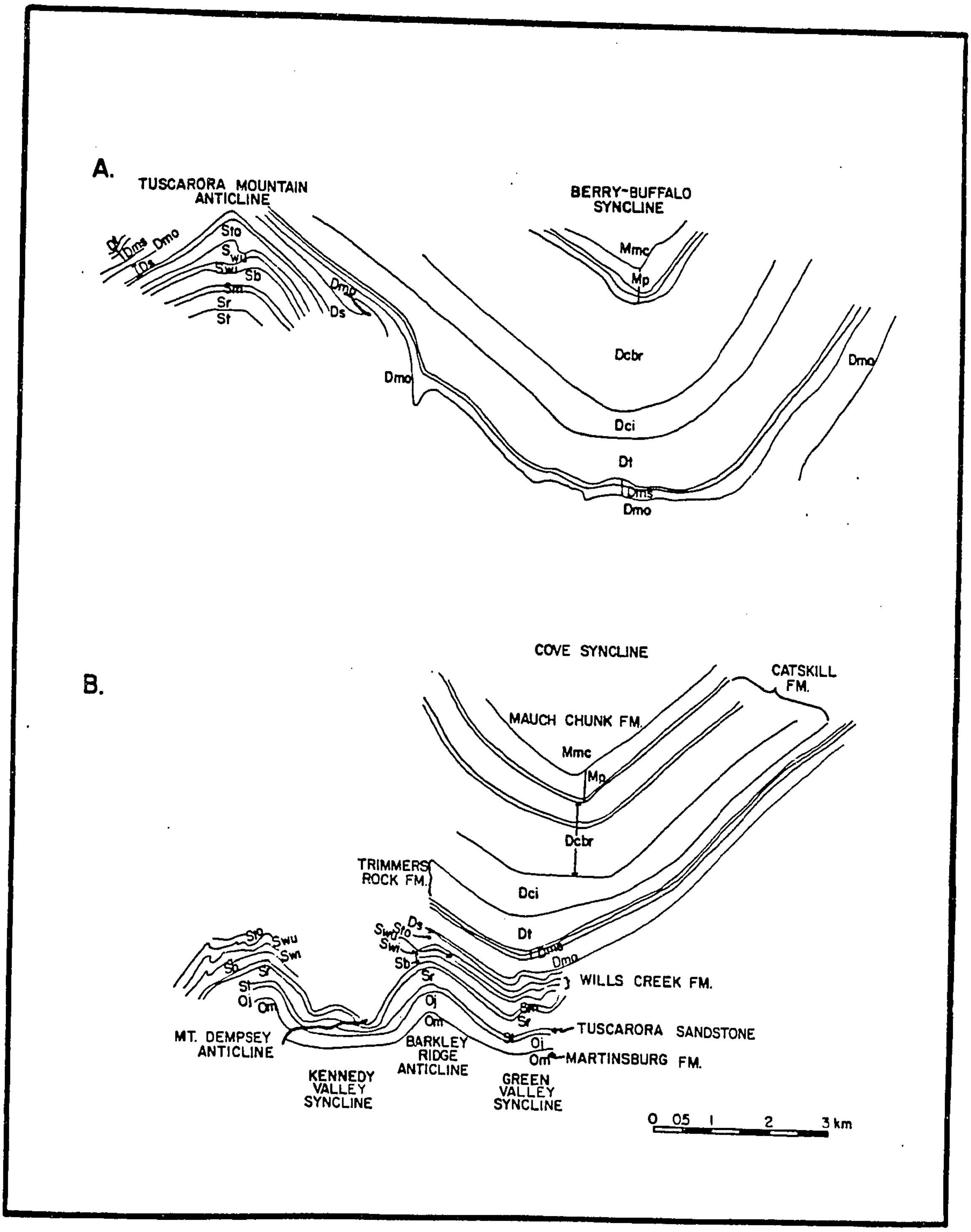
A.
TUSCARORA MOUNTAIN ANTICLINE
BERRY-BUFFALO SYNCLINE
Sto
Swu
Swi
Sb
Sm
Sr
St
Dmo
Ds
Dms
Mmc
Mp
Dcbr
Dci
Dt
B.
COVE SYNCLINE
CATSKILL FM.
MAUCH CHUNK FM.
Mmc
Mp
Dcbr
TRIMMERS ROCK FM.
Dci
Dt
Dms
Dmo
WILLS CREEK FM.
TUSCARORA SANDSTONE
MARTINSBURG FM.
Sto
Swu
Swi
Sb
Sr
St
Oj
Om
MT. DEMPSEY ANTICLINE
KENNEDY VALLEY SYNCLINE
BARKLEY RIDGE ANTICLINE
GREEN VALLEY SYNCLINE
0 05 1 2 3 km

FIGURE 10

the fold form changes markedly along the fold axis, whereas, according to the structural section (Fig. 10), the fold form changes markedly with position within the stratigraphic section. Thus, the double anticlinal crest developed in the lower member of the Wills Creek Formation (Swl) dies out downward into a flattened crest at the level of the Rose Hill Formation (Sr). The northern anticline of the pair dominates in the upper member of the Wills Creek Formation (Swu) and a single hinge is developed at the level of the top of the Tonoloway Formation (Sto).

The form of the fold in Tuscarora Mountain does not correspond to any of the idealized folds shown in Fig. 2. Rather, the anticline appears to change from a chevron-like form above to a concentric-like form below. This example, however, is by no means unique. The Huasna syncline, California, which has the same general form (Johnson, 1977, p. 297), changes from a concentric-like syncline in massive sandstones of the Santa Margarita Formation, to a chevron-like syncline in the underlying, relatively well-bedded Monterey Formation, to a concentric-like syncline in the underlying, massive sandstones of the Vaqueros Sandstone.

The cross-sectional form of the cove syncline is not as simple as that of the Berry-Buffalo syncline. In some respects, the fold is a combination of chevron-like and concentric-like forms but the forms are complicated by two distinct fold hinges at the level of the Catskill Formation (contact between Dci and Dcbr, Fig. 10B). I would not classify the Cove syncline as any of the simple fold forms, because of complicated forms.

The smaller folds in the Silurian rocks, shown in Fig. 10B, are examples of the 2nd-order folds of Nickelsen (1963). The Barkley Ridge anticline appears to be roughly chevron-like at the level of the Juniata Formation (Oj) and roughly concentric-like at the level of the Rose Hill and Tuscarora formations (Sr and St). A similar association of fold forms and stratigraphy can be recognized in the Mt. Dempsey anticline. The Kennedy Valley syncline apparently is flat-bottomed at the level of the Juniata Formation. The flattened forms reflect interference between 2nd- and 3rd- order folds developed in the Mifflintown Formation (Sm). The Green Valley syncline similarly has a flat bottom at the level of the Juniata, and 3rd-order folds with a shorter wavelength are clear in the Mifflintown Formation.

CONCLUSIONS

Examination of folds shown in cross sections prepared by many different structural geologists for central Pennsylvania shows an astonishing range of interpretations of fold forms at depth.

I have examined outcrop patterns of folded layers, examined serial vertical cross sections prepared by other geologists, and constructed down-plunge structural sections in order to estimate forms of 1st- and 2nd-order folds in several quadrangles northwest of Harrisburg, Pennsylvania. The structural cross sections suggest that 1st- and 2nd-order folds are grossly a combination of chevron-like and concentric-like forms but that the shapes of the actual folds are more complicated than the ideal folds. Perhaps many of the complications are the result of irregularities in the structural units involved in the folding. I will address this question in the next chapter.

It is clear that 1st- and 2nd-order folds in central Pennsylvania do not resemble kink folds, as suggested by Faill (1969, 1973). However, there are excellent examples of 4th- and 5th-order kink-like folds. Faill and Wells (1974, figs. 56 and 58) and Faill (1973, fig. 10) show examples of classic, monoclinal and symmetric, conjugate kink-like folds in the Rose Hill and Wills Creek formations.

REFERENCES CITED

Busk, H. G., 1957, Earth flexures: William Trussell, N. Y., 106 p.

Chamberlain, R. T., 1910, The Appalachian folds of central Pennsylvania:: Jour. Geology, v. 18, p. 228-251.

Conlin, R. R., and Hoskins, D. M., 1962, Geology and Mineral Resources of the Mifflintown quadrangle: Pennsylvania Topographic and Geologic Survey, Atlas 126.

Dyson, J. L., 1963, Geology and mineral resources of the New Bloomfield quadrangle: Pennsylvania Topographic and Geologic Survey, Atlas 137 A & B, 63 p.

Dyson, J. L., 1967, Geology and mineral resources of the southern half of the New Bloomfield quadrangle, Pennsylvania: Pennsylvania Topographic and Geologic Survey, Atlas 137 C & D, 86 p.

Engelder, T., 1979, Mechanisms for strain within the upper Devonian clastic sequence of the Appalachian Plateau, western New York: Amer. Jour. Sci., v. 279, p. 527-542.

Faill, R. T., 1969, Kink band structures in the Valley and Ridge Province, central Pennsylvania: Geol. Soc. Amer. Bull., v. 80, p. 2539-2550.

Faill, R. T., 1973, Kink band folding, Valley and Ridge Province, Pennsylvania: Geol. Soc. Amer. Bull., v. 84, p. 1298-1314.

Faill, R. T., and Wells, R. B., 1974, Geology and mineral resources of the Millerstown quadrangle, Perry, Juniata, and Snyder Counties, Pennsylvania: Pennsylvania Topographic and Geologic Survey, Atlas 136, 276 p.

Faill, R. T., and Wells, R. B., 1977, Geology and mineral resources of the Salladasburg and Cogan Station quadrangles, Lycoming County, Pennsylvania: Pennsylvania Topographic and Geologic Survey, Atlas 134 C & D.

Gray, C., Conlin, R. R., Hoskins, D. M., and Shepps, V. C., 1960, Geologic map of Pennsylvania, 1/250,000. Pennsylvania Topographic and Geologic Survey, 4th series.

Gwinn, V. E., 1964, Thin-skinned tectonics in the Plateau and northwestern Valley and Ridge Province of the central Appalachians: Geol. Soc. America Bull., v. 75, p. 863-900.

Gwinn, V. E., 1970, Kinematic patterns and estimates of lateral shortening, Valley and Ridge and Great Valley provinces, central Appalachians: In: G. W. Fisher, F. J. Pettijohn, J. C. Reed, Jr., and K. N. Weaver, eds., Studies in Appalachian Geology, Central and Southern: Intersci. Publisher, N. Y., p. 127-146.

Hoskins, D. M., 1976, Geology and mineral resources of the Millersburg 15-minute quadrangle, Dauphin, Juniata, Northumberland, Perry, and Snyder Counties, Pennsylvania: Pennsylvania Topographic and Geologic Survey, Atlas 146, 38 p.

Jacobeen, F., Fr., and Kanes, W. H., 1974, Structure of the Broadtop synclinorium and its implications for Appalachian structural style: Amer. Assoc. Petrol. Geologists Bull., v. 58, p. 362-375.

Johnson, A. M., 1977, Styles of Folding: Elsevier Sci. Publ. Co., N.W., 406 p.

Laubscher, H. P., 1976, Fold development in the Jura: Tectonophysics, v. 37, p. 337-362.

Mackin, J. H., 1950, The down-structure method of viewing geologic maps: Jour. Geology, v. 58, p. 55-72.

Miller, J. T., 1961, Loysville quadrangle: Pennsylvania Topographic and Geologic Survey, Atlas 127, 47 p.

Nickelsen, R. P., 1963, Fold patterns and continuous deformation mechanisms of the central Pennsylvania folded Appalachains. In: Guidebook to Tectonics and Cambro-Ordovician stratigraphy, central appalachians of Pennsylvania: Pittsburgh Geol. Soc., Sept. 1963, p. 13-29.

Nickelsen, R. P., 1966, Fossil distortion and penetrative rock deformation in the Appalachian Plateau, Pennsylvania: Jour. Geology, v. 74, . 924-931.

Nickelsen, R. P., 1979, Sequence of structural stages of the Allegheny Orogeny at the Bear Valley Strip Mine, Shamokin, Pennsylvania: American Jour. of Science, v. 279, p. 225-271.

Ragan, D. M., 1973, Structural Geology: John Wiley & Sons, N.Y., 208 p.

Rich, J. L., 1934, Mechanics of low-angle overthrust faulting as illustrated by Cumberland thrust block, Virginia, Kentucky and Tennessee: Amer. Assoc. Petrol. Geol. Bull., v. 18, p. 1584-1596.

Rodgers, J., 1949, Evolution of thought on structure of middle and southern Appalachians: Amer. Assoc. Petrol. Geol. Bull., v. 33, p. 1634-1654.

Rodgers, J., 1963, Mechanics of Appalachian foreland folding in Pennsylvania and West Virginia: Amer. Assoc. Petrol. Geol. Bull., v. 47, p. 1527-1536.

Rogers, H. D., 1858, The geology of Pennsylvania: First Pennsylvania Geological Survey (1836-1841) 2 vols. and atlas.

Sherwin, J., 1972, Decollement folding: Unpublished Ph.D. dissertation, Brown University, Providence, R. I., 150 p.

Thompson, R. I., 1979, A structural interpretation across part of the northern Rocky Mountains, British Columbia, Canada: Canadian Jour. Earth Sci., v. 16, p. 1228-1244.

Van Hise, C. R., 1896, Principles of North American pre-Cambrian geology: 16th Ann. Rept. U.S. Geological Survey, p. 571-874.

Van Hise, C. R., 1898, Estimates and causes of crustal shortening: Jour. Geology, v. 6, p. 10-64.

Willis, B., 1893, The mechanics of Appalachian structure: 13th Ann. Rept. U. S. Geological Survey, p. 211-281.

Willis, B., and Willis, R., 1934, Geologic Structures: McGraw-Hill Book Co., N. Y., 544 p.

Wiltschko, D. V., and Chapple, W. M., 1977, Flow of weak rocks in the Appalachian Plateau folds: Amer. Assoc. Petrol. Geol. Bull., v. 61, p. 653-670.

Wood, G. H.,Jr., Trexler, J. P., and Kehn, T. M., 1969, Geology of the west-central part of the southern anthracite field and adjoining areas, Pennsylvania: U.S. Geol. Survey Prof. Paper 602, 150 p.

CHAPTER II

APPLICATION OF FOLDING THEORY TO THE FOLDS IN THE PLATEAU AND VALLEY AND RIDGE PROVINCES OF THE CENTRAL APPALACHIANS

ABSTRACT

Application of second-order folding theory to rocks involved in folding in the Plateau and Valley and Ridge provinces in the central Appalachians suggests that the flat-bottomed synclines and narrow anticlines typical of folds in this region can be explained as a result of buckling of layers overlying a detachment surface. Furthermore, a change in the position of the detachment surface can result in a change, from folds that resemble those in the Plateau, to folds that resemble those in the Valley and Ridge. Analysis of preferred wavelengths for the Valley and Ridge Province suggests that wavelengths of the large folds (wavelengths of 11 to 18 km) are controlled by the Catskill and Trimmers Rock formations, whereas wavelengths of the intermediate folds (wavelengths of 2.5 to 3 km) are controlled by the Tuscarora and Juniata formations.

INTRODUCTION

Folding theory has advanced very quickly during the last 20 years, starting with the early work by Biot (1959, 1961, and 1965) and Ramberg (1959, 1960, 1962 and 1970) on wavelengths of single-layer and multilayered folds. Fletcher (1974) and Smith (1979) have developed the theory of low-amplitude folding of power-law materials. Analyses of the forms of folds were initiated by Ramberg (1963) and by Johnson (e.g., 1977), and the method of second-order analysis of fold forms in viscous materials was introduced by Fletcher (1979).

Relatively recently Johnson and Fletcher (manuscript, 1982) have introduced a series of methods of deriving fold forms in multilayered viscous materials. Nobody, however, has compared forms of theoretical folds with forms of folds shown in structural cross sections. The purpose of this chapter is to do so for parts of the Valley and Ridge and Allegheny Plateau provinces of the central Appalachians.

Since the very early descriptions of folds in the central Appalachians by Rogers (1858), there have been widely divergent interpretations of the forms of the folds and the causes of the folding. Willis (1893) imagined that the folds were produced by layer-parallel shortening and interpreted the folds to be results of buckling of "strut members". He introduced the important idea of structural units. Rich (1934) suggested that the folding associated with the Pine Mountain thrust block was a result of repetition of strata by thrusting of passive blocks of rocks over steps in detachment surfaces. His suggestion was later applied to folds throughout the Allegheny Plateau and Valley and Ridge Provinces by Gwinn (1964, 1970) and Rodgers (1963).

For example, Fig. 1A shows part of a cross section presented by Gwinn (1964) as evidence that the Horton, Glady and Elkins Valley anticlines in West Virginia are a result of splay faulting near a basal decollement. A distinguishing characteristic of folds produced by splay faulting is supposed to be broad, flat synclinal troughs and narrow anticlinal bumps. Rodgers (1963) suggested that the anticlines are passive structures, resulting from repetition of strata by thrusting within the cores of the anticlines, whereas Gwinn (1964) suggested that the anticlines initiated before thrusting in the core but the thrusting was largely responsible for the structural relief of the anticlines. Sherwin (1972), however, pointed out that structural interpretations of folds on the Plateau based solely on gliding of blocks along a decollement cannot explain the regular wavelengths or the development of thrusts in the cores of the anticlines. Wiltschko and Chapple (1977) re-examined the folds and showed that only part of the structural relief of the folds is accounted for by thrusting in the cores, and that there must have been flow of relatively soft units into cores of anticlines from adjacent synclines. Furthermore, they suggested that the flat-bottomed synclines and narrow anticlines can be explained as a result of folding of a sequence of rocks underlain by relatively stiff rocks, but they did not present theoretical analysis to support their suggestion. One purpose of this section is to perform a theoretical analysiss to second-order in the maximum slopes of interfaces in order to show that, indeed, flat-bottomed synclines and narrow anticlines can form under the conditions envisioned by Wiltschko and Chapple.

It is generally agreed that most of the folds in the Valley and Ridge Province of the central Appalachians are a result of buckling of a multi-

Figure 1 - Fold forms in the Allegheny Platau of central Appalachians.

A. Interpretive vertical cross section of some folds in Plateau Province of central Appalachian mountains in West Virginia (after, Gwinn, 1964).

B. Theoretical fold forms derived through second-order analysis of growth of low-amplitude perturbation in Plateau Province of central Appalachians. Normalized viscosities of structural units are indicated by numbers at right-hand side.

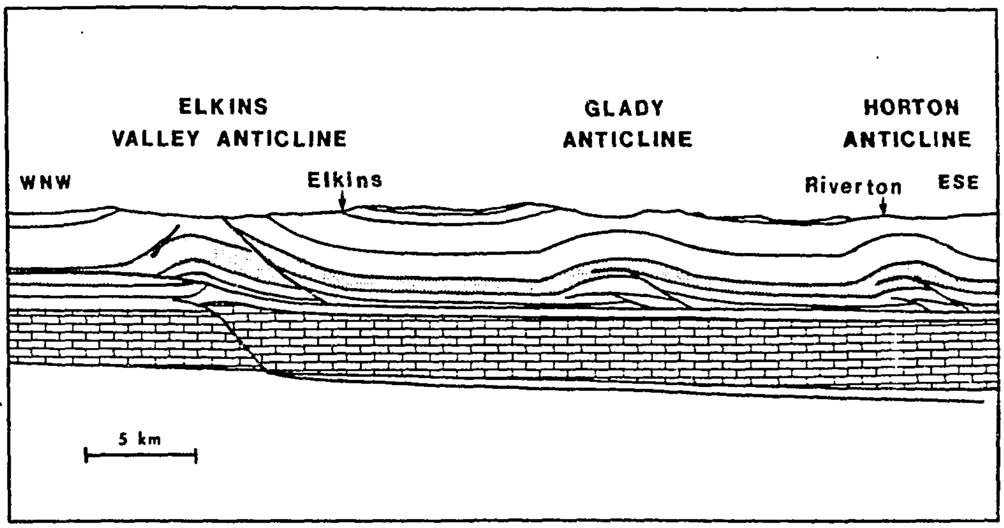
ELKINS
VALLEY ANTICLINE
GLADY
ANTICLINE
HORTON
ANTICLINE
WNW
Elkins
Riverton
ESE
5 km

A

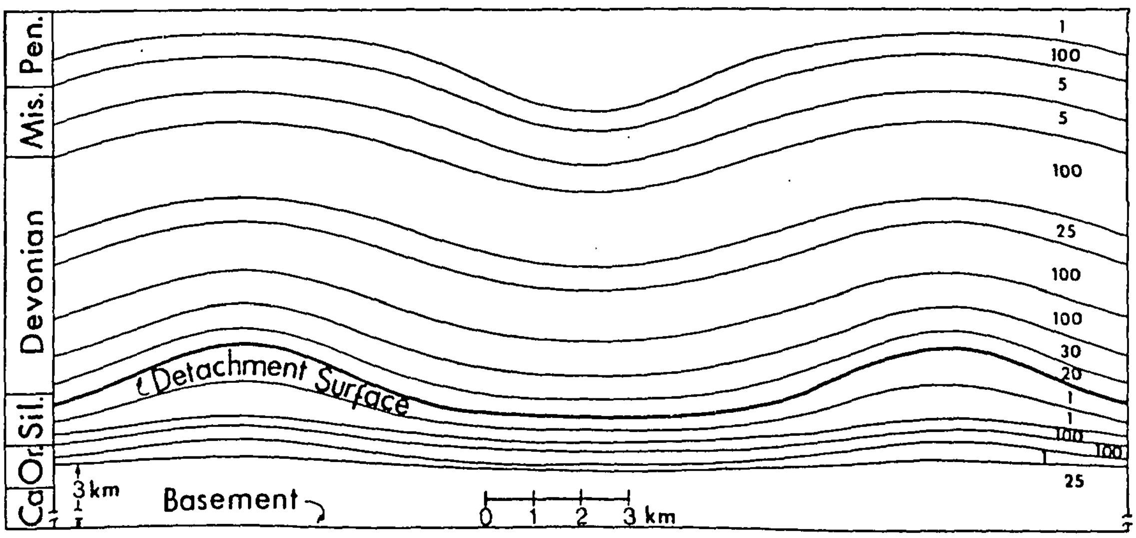
Pen.
Mis.
Devonian
Sil.
Or.
Ca.
Detachment Surface
3 km
Basement
0 1 2 3 km
1
100
5
5
100
25
100
100
30
20
1
1
100
100
25

B

FIGURE 1

layered rock sequence subjected to layer-parallel compression (Willis, 1983; Nickelsen, 1963, 1966; Faill, 1969, 1973). There is considerable disagreement, however, about the forms of the folds. Evidence was presented in Chapter I that the typical, large folds are roughly concentric-like and chevron-like, but that the folds are complicated. The folds have been interpreted to be kink bands by Faill (e.g., 1973) and co-workers of the Pennsylvania Geological Survey. It is well known that kink folds form in multilayers with moderate contact strength at interfaces between layers, and that repetitious folds, such as concentric-like and chevron-like folds, form in multilayers or interbedded soft and stiff layers or multilayers with very low or zero contact strength at interfaces between layers (Honea and Johnson, 1976; Reches and Johnson, 1976; Ramberg and Johnson, 1976). The theoretical model used in the computer programs (Appendix II, III and IV) assume zero contact strength at interfaces. Therefore, it will be of interest to determine whether one theoretically can develop complicated folds resembling those in the central Appalachians by means of the computer programs. Indeed, one can, as will be shown in following paragraphs.

First, I will present a representative stratigraphic section for the central Appalachians and propose possible structural units that can be used for analysis of large- and intermediate-sized folds as well as suggest estimates of relative viscosities of the structural units. Then I will use the structural units to simulate the growth of folds under conditions that appear to have prevailed during folding on the Valley and Ridge Province, using a computer program (Appendix IV), which deals with second-order analysis of the simultaneous growth of waveforms with two distinct wavelengths. Finally, I will use the same structural units but change the level of the detachment surface to simulate the growth of folds under conditions inferred for the Allegheny Plateau in central Pennsylvania, using another computer program (Appendix III), which deals with second-order analysis of folds with a single wavelength.

ESTIMATION OF THICKNESSES AND VISCOSITIES OF STRUCTURAL UNITS

Structural units involved in folding in the central Appalachians have been discussed by Willis (1893), Currie and others (1962), Nickelsen (1963) and Faill and others (1973). In an analysis of folding viscous multilayers, the problem of characterizing structural units is a problem in identifying thicknesses of layers that have markedly different coefficients of viscosity or that have slipped readily at interfaces between layers and in estimating coefficients of viscosity for the different layers. I will propose structural units based upon descriptions of stratigraphic units by Wood and others (1969), Nickelsen (1973), Faill and Wells (1974, 1977) and Faill (1979), and based upon theoretical analyses of relations between grain size and effective viscosity of rocks.

Some guidance for estimating viscosities of rocks can be obtained from theoretical analyses in which it is asumed that rock deforms primarily by pressure solution, diffusion and deposition along grain boundaries (e.g., Fletcher, 1982). For example, based on a model proposed by Weyl (1959) and Fletcher (1982), Kilinc and Johnson (unpublished class notes, 1980) have shown that the effective viscosity of an aggregate of cubic grains is,

$$\mu_{eff} = (\alpha/14.2)\, a^3 \qquad (1a)$$

where μ_{eff} is the effective coefficient of viscosity, a is the length of a side of a cube (a meassure of grain size) and α is,

$$\alpha = 2RT/(DC_o\overline{V}_o^2 w) \qquad (1b)$$

$\underline{R}$ is the gas constant, $\underline{T}$ is temperature (°K), $\underline{D}$ is diffusion coefficient for the fluid, $\underline{C_0}$ is mean concentration of solid dissolved in the fluid, $\underline{w}$ is thickness of the fluid film, and $\underline{V_0}$ is the specific volume of the solid being dissolved.

These equations show that the effective viscosity for the ideal rock would depend on the grain size, temperature and pressure and on the compositions of the fluid and solid phases. The effective viscosity would be sensitive to differences in grain size because it is proportional to the cube of the grain size. Thus the coefficient of viscosity for one rock with a grain size of one mm would be 1000 times that for another rock with a grain size of 0.1 mm, if other parameters in eq. (1b), such as temperature and diffusion coefficient, are the same for the two rocks. One can use this relation between effective viscosity and grain size as a guide for estimating relative coefficients of viscosity.

Another useful relation is the dependence of effective viscosity of averged viscosities of interbedded stiff and soft layers. The effective normal viscosity, μ_n, for multilayered materials is (e.g., Johnson, 1970),

$$\mu_n = ((t_1/t_2)\mu_1+\mu_2)/((t_1/t_2)+1) \qquad (2)$$

in which $\underline{t}$ is thickness and μ is coefficient of viscosity of stiff, 1, and soft, 2, layers in a multilayer. The effective viscosity of a multilayer depends on the fractions $t_1/(t_1+t_2)$ of stiff and $t_2/(t_1+t_2)$ of soft layers as well as the coefficients of viscosity of the stiff and soft layers according to eq. (2). This relation can be used to estimate relative viscosities of packages of interbedded units such as sandstone and shales in a turbidite sequence which behave collectively as a single structural unit during folding.

The relative viscosities of the structural units in central Pennsylvania have been estimated by using eqs. (1) and (2). The thickness of formations and thickness ratios of stiff-to-soft layers, t_1/t_2, were obtained from the studies of Nickelsen (1973), Wood and others (1969), Faill and Wells (1974, 1977), Faill and others (1973) and Faill (1979). The grain sizes were assumed according to the classifications of Wentworth (1922). I assume that the effective viscosity of medium grained sandstone ($a \approx 0.5$ mm) is $\mu \approx 2 \times 10^{21}$ poises (e.g., Crittenden, 1963 p. 5526). Thus, according to eq. (1a) $\alpha \approx 2.27 \times 10^{23}$ poises/mm^3. Results of sample normal viscosity calculations will be given for the Llewellyn (Pl), Tuscarora (St), Wills Creek (Sw) and Bloomsburg (Sb) formations.

The Llewellyn Formation is described by Wood and others (1969). The stiff layers (1) are fine to medium grained sandstone ($a \simeq 0.13$ mm) and the soft layers (2) are shale, siltstone ($a \simeq 0.03$ mm) and coal. I assume that the viscosity of coal is the same as that of shale. The thickness ratio of stiff-to-soft layers is $t_1/t_2 \approx 1$. According to eq. (1a) the effective viscosity is $\mu_1 \approx 3.5 \times 10^{19}$ poises for the stiff layers, and $\mu_2 \approx 4.3 \times 10^{17}$ poises for the soft layers. Thus, from eq.(2) the normal viscosity of the Llewellyn Formation is,

$$\mu_{Pl} \approx 1.77 \times 10^{19} \text{ poises} \tag{3a}$$

The normalized viscosity ratio for the formation is, $\mu_{Pl}/\mu_{Pl}=1$. This value is recorded in Table I.

The calculation of normal viscosity of the Tuscarora Formation is based upon descriptions by Faill and Wells (1974). The stiff layers are medium grained sandstone ($a\approx0.5$ mm) and the soft layers are very fine grained sandstone ($a\approx0.125$ mm). The thickness ratio of stiff-to-soft layer is $t_1/t_2\approx7$. The effective viscosity is $\mu_1\approx2\times10^{21}$ poises for the stiff layers, and $\mu_2\approx3.1\times10^{19}$ poises for the soft layers, so the normal viscosity of the Tuscarora Formation is,

$$\mu_{Sr}\approx1.75\times10^{21} \text{ poises} \tag{3b}$$

The normalized viscosity ratio of the Tuscarora and Llewellyn formations, eqs. (3b) and (3a) , is $\mu_{Sr}/\mu_{Pl}\approx100$. This value is recorded in Table I.

The Wills Creek Formation is described by Nickelsen (1973). The stiff layers are medium to fine grained sandstone ($a\approx0.125$ mm) and limestone. The soft layers are shale and siltstone ($a\approx0.0625$ mm). I assume the limestone is as stiff as sandstone. The thickness ratio of stiff-to-soft layers is $t_1/t_2\approx4$. The effective viscosity is $\mu_1\approx3.1\times10^{19}$ poises for the stiff layers and $\mu_2\approx3.9\times10^{18}$ poises for the soft layers, so the normal viscosity of the Wills Creek Formation is,

$$\mu_{Sw}\approx2.6\times10^{19} \text{ poises.} \tag{3c}$$

TABLE I

Average thicknesses and normalized viscosity ratios of the structural units in the central Appalachians

				Average thickness (km)	Normalized viscosity ratio	
PENNSYLVANIA		Pl	Llewellyn Formation	1	1	*I=0
		Pp	Pottsville Formation	0.45	100	
MISSISSIPPIAN		Mp	Mauch-Chunk Formation	0.7	5	
		Mp	Pocono Formation	0.6	5	I=3
DEVONIAN	CATSKILL FORMATION	Dcbr	Duncanon Member Clark's Ferry Member	1.5	100	
			Sherman Creek Member	0.5	25	I=5
		Dci	Irish Valley Member	1	100	
		Dtr	Trimmers Rock For.	0.7	100	I=7
	MAHANTANGO FORMATION or HAMILTON GROUP	Dms	Harrell Member Sherman Ridge Member	0.5	30	
		Dmo	Montebello Member			
		DS	Marcellus Formation Onandago Formation Oriskany Formation Helderberg Formation Keyser Formation	0.375	20	
SILURIAN		Sto	Tolonoway Formation			I=9
		Sw	Wills Creek Form.	0.4	1	
		Sb	Bloomsburg Formation			I=10
		Sm	Mifflintown Form.	0.365	1	
		Sr	Rose Hill Formation			I=11
		St	Tuscarora Formation	0.2	100	I=12
ORDOVICIAN		Oj	Juniata Formation Bald Eagle Form.	0.25	100	I=13
		Om	Martinsburg Form. (Reedsville Form.)	1	1	I=14
CAMBRO-ORDOVICIAN				3	25	

TOTAL THICKNESS 12.54 km

*I is an interface number

The normalized viscosity ratio of the Wills Creek and Llewellyn formations, eqs. (3c) and (3a), is $\mu_{Sw}/\mu_{Pl} \simeq 1.5$.

The calculation of normal viscosity of the Bloomsburg Formation is based upon descriptions by Faill and Wells (1974). The stiff layers are fine to very fine grained sandstone ($a \approx 0.1$ mm) and soft layers are shale and claystone ($a \approx 0.0625$ mm). The thickness ratio of stiff-to-soft layer is $t_1/t_2 \simeq 12$. The effective viscosity is $\mu_1 \simeq 1.6 \times 10^{19}$ poises for the stiff layers and $\mu_2 \simeq 3.9 \times 10^{18}$ poises for the soft layers, so that normal viscosity of the Bloomsburg Formation is,

$$\mu_{Sb} \simeq 1.5 \times 10^{19} \text{ poises.} \tag{3d}$$

Thus, the normalized viscosity ratio of the Bloomsburg and Llewellyn formations, eqs. (3d) and (3a), is $\mu_{Sb}/\mu_{Pl} \simeq 0.85$.

The normalized ratios of the Wills Creek and Bloomsburg are similar, so I have elected to combine them into a single structural unit with a normalized viscosity ratio of 1, as shown in Table I.

A total of 12.54 km section of rocks has been grouped into 16 structural units, using the methods discussed in the examples above. The thicknesses and normalized viscosities for the units are shown in Table I.

The structural units that I have selected to describe folding in the central Appalachians (Table I) are related to <u>structural-lithic units</u> defined for the same area by Nickelsen (1963), based on the definition of such units by Currie and others (1962). According to Currie and others (1962, p. 670), a structural-lithic unit is a part of a stratigraphic section that contains a dominant member or dominant members and that contains both stiff and soft ("competent" and "incompetent") layers. The dominant members are individual stiff layers or groups of stiff layers that control the wavelength of folds within the structural-lithic units, according to Currie and others (1962, p. 667). Furthermore, Currie and others discuss several field examples in order to illustrate how one is to identify dominant members. For example, for folds in interbedded siltstone and shale in the Pottsville Group, they assume that the dominant members are the siltstone layers. They suggest that, where continuous surfaces of bedding-parallel slip separate a rock section into units, the thicknesses of units bounded by slip surfaces should define the thicknesses of dominant members (Currie and others, 1962, p. 667).

Nickelsen (1963, p. 17) describes wavelengths of folds and identifies several structural-lithic units in the central Appalachians (Fig. 2). According to Nickelsen, wavelengths of 1st-order folds are 11 to 18 km, of 2nd-order folds are about 3 km, of 3rd-order folds are about 1 km, of 4th-order folds are about 10 m, and of 5th-order folds are a few mm to a few cm. He indicates that the 1st-order folds extend throughout the stratigraphic column from Ordovician to Pennsylvanian and implies that the structural-lithic unit for 1st-order folds is the entire column. He identifies the stratigraphic section between the Keefer Sandstone (lower member of Mifflintown Formation) and lower Ordovician Beekmantown Group as a structural-lithic unit within which 2nd-order folds have developed (unit II, Fig. 2), and suggests that sandstones and carbonate rocks are the dominant members of the unit. I have assumed that the stiff members are the

Figure 2 - Structural-lithic units and size orders of folds in central Appalachians of Pennsylvania (after, Nickelsen, 1963, fig. 2). The 1st-order folds involved rocks from the Cambrian to the Pennsylvanian. The 2nd-order folds are best developed at the levels of Tuscarora (St) and Bald Eagle formations (Oj). The 3rd-order folds are best developed in the middle Silurian and middle Devonian rocks above the Rose Hill Formation (Sr) and below the Hamilton Group (Dms and Dmo).

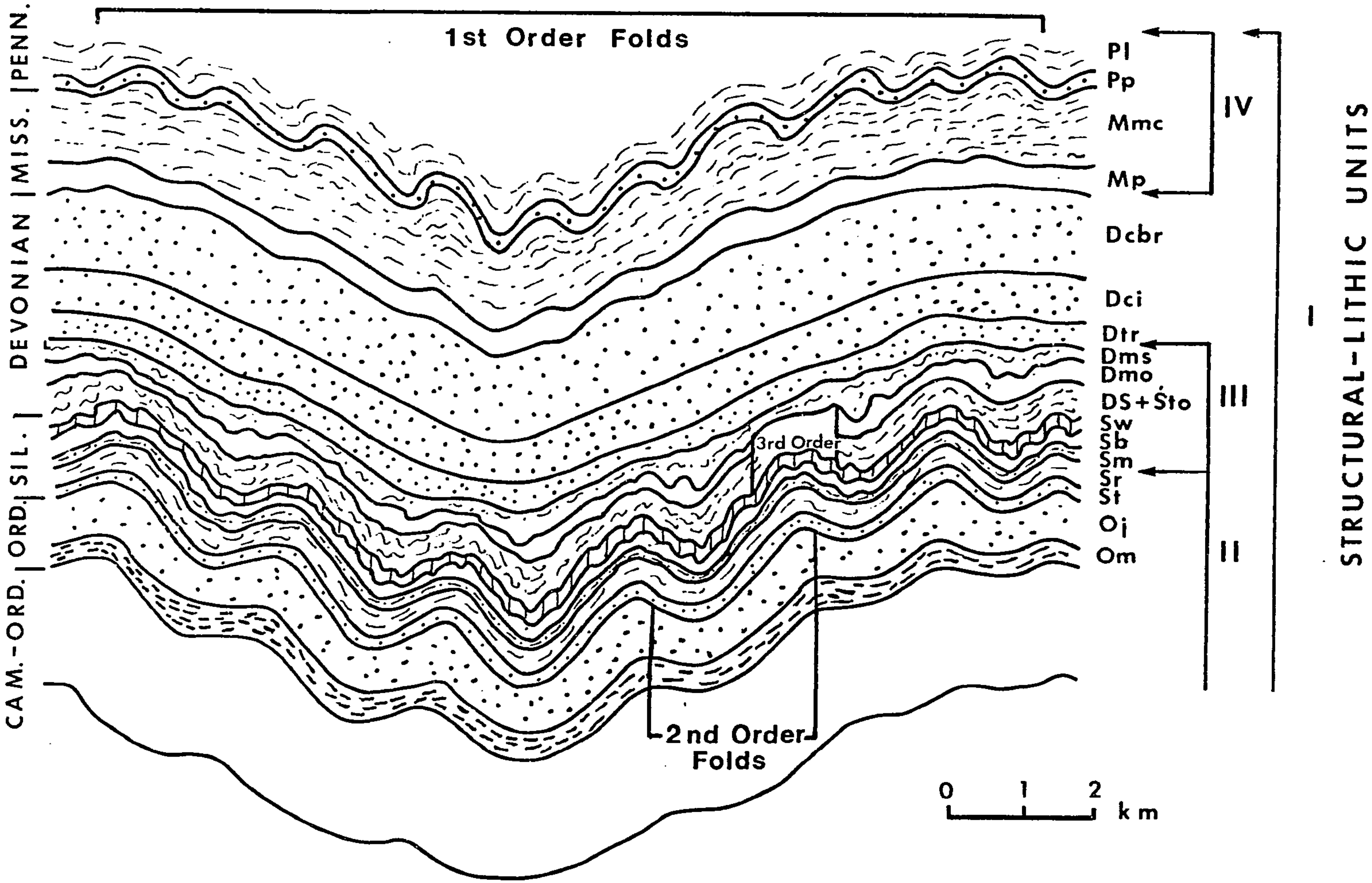
1st Order Folds
PENN.
MISS.
DEVONIAN
SIL.
ORD.
CAM.-ORD.
Pl
Pp
Mmc
Mp
Dcbr
Dci
Dtr
Dms
Dmo
DS+Śto
Sw
Sb
Sm
Sr
St
Oj
Om
IV
III
II
I
STRUCTURAL-LITHIC UNITS
3rd Order
2nd Order Folds
0
1
2
km

FIGURE 2

Tuscarora and Juniata formations (Table I), and that the Martinsburg, Mifflintown and Rose Hill formations are the soft members in this part of the section.

Another structural-lithic unit recognized by Nickelsen extends from the Silurian Bloomsburg Formation up through the Hamilton Group. This unit contains 3rd-order folds (unit III, Fig. 2). I have assumed that the lower one-third of this section is very soft and that the upper two thirds are moderately stiff structural units (Table I). However, if I were to examine 3rd-order folds, I would subdivide this part of the section into many structural units. I will do this in following pages where I analyze 3rd-order folding in the Wills Creek Formation. Nickelsen briefly discusses the folds in Pennsylvanian rocks, noting that the wavelengths of folds there are one to two km, so that the folds are 2nd-order. He suggests that the folds occur within the Llewellyn and Mauch Chunk formations and the Pottsville Group, so that these rocks would be a fourth structural-lithic unit (unit IV, Fig. 2). I have assumed that the Llewellyn and Mauch Chunk formations are soft and the Pottsville is stiff and that this part of the section can be described in terms of three structural units. As I will show, 2nd-order folds are not developed in the Pottsville Group in theoretical simulations of folding, whereas 2nd-order folds are well developed in the Juniata and Tuscarora formations. Apparently the Pottsville would have to be subdivided into two or more structural units in order for 2nd-order folds to develop in that part of the section.

Thus the structural units shown in Table I are generally compatible with the structural-lithic units and the dominant members discussed by Currie and others (1962) and by Nickelsen (1963) for the central Appalachians.

PREFERRED WAVELENGTH AND FOLD FORMS IN VALLEY AND RIDGE PROVINCE

One crude check on the estimates that one must make in order to specify structural units is that the wavelengths of folds developed in the idealized multilayer correspond approximately to the wavelengths of folds observed in the field. Field observations and study of structural cross sections indicte that 1st, 2nd and 3rd-order folds occur in the Valley and Ridge Province (Fig. 2).

Let us begin with the 3rd-order folds in the Wills Creek Formation. Nickelsen (1973) has described these folds in detail where they are well exposed at Rainbow Rocks, near Mifflintown, Pennsylvania. Measurements made on a cross section prepared by Nickelsen (1973, fig. 11) indicate that the wavelength of the folds is about 300 m. The sequence of rocks involved in the folding is apparently the Wills Creek, Bloomsburg and Mifflintown formations, a total thickness of about 465 m. Thus, the ratio of wavelength to total thickness is about L/T=0.65. The folded sequence is overlain by the moderately stiff, Tonoloway Formation and underlain by the soft, Rose Hill Formation. The ratio of thicknesses of soft and stiff layers within the folded sequence is about 0.5 and the viscosity ratio of soft-to-stiff layers is about 0.01. Using these values and a graph presented by Johnson (1982, unpublished manuscript), I computed a ratio of viscosity of media to normal viscosity, μ_m/μ_n, of 0.05 and a ratio of viscosity of media to viscosity of stiff layers, μ_m/μ_1, of 0.03. Thus, using reasonable estimates for the physical properties of the rocks involved in folding and of the rocks overlying and underlying the folded sequence, one can compute a dominant wavelength equal to the observed wavelength of 3rd-order folds in the Wills Creek Formation.

The remainder of the discussion of large folds will be restricted to 1st- and 2nd-order folds because the round-off errors in computations of wavelengths and forms are very large for problems where there is a wide range of fold sizes. A computer program (discussed in Appendix II) was used to determine relations between amplification, A/A_0, and wavelength-to-thickness ratio, L/T, for the structural units shown in Table I. Here $\underline{A}_0$ is the initial amplitude of a perturbation and $\underline{A}$ is the final amplitude, after layer-parallel shortening. $\underline{L}$ is the wavelength of the perturbation and $\underline{T}$ is the total thickness of section involved in the folding. The relations between amplification and wavelength-to-thickness ratio for some of the interfaces betwen structural units are shown in Fig. 3A. The interfaces are identified in Table I. For example, interface $\underline{I}$=11 is the contact between the Rose Hill and the Tuscarora formation. Figure 3A shows that perturbations in different interfaces become amplified by different amounts for each wavelength of perturbation. Furthermore, Fig. 3A shows that there are two maxima in the relations between amplification and wavelength-to-thickness ratio. For example, interface $\underline{I}$ =11 has maxima at L/T ratios of about 0.35 and 1.8. These L/T ratios correspond to wavelengths of 3.3 km and about 17 km. Interface $\underline{I}$=0, however, has only one maximum amplification, at a L/T ratio of about 1.8, or a wavelength of 17 km. Thus Fig. 3A already suggests some of the features of the fold forms in the multilayer of structural units shown in Table I. I would expect folds with two wavelengths to form simultaneously deep in the section, at the level of the Tuscarora Formation, whereas I would expect folds with a single wavelength to form high in the section, in the Pottsville Formation.

The wavelengths associated with the maxima in relations between amplification, A/A_0, and wavelength-to-thickness ratio, L/T, are the <u>preferred</u>

Figure 3 - Relations among ratio of wavelength-to thickness and amplification of interfaces in central Appalachians of Pennsvylania.

I: Interface number (intefaces defined in Table I).

L_p: Preferred wavelength.

T: Total thickness.

T/T_0: Thickening ratio (final thickness-to-initial thickness).

A/A_0: Amplification (final amplitude-to-initial amplitude).

A - For the Valley and Ridge Province.

B - For the Plateau Province.

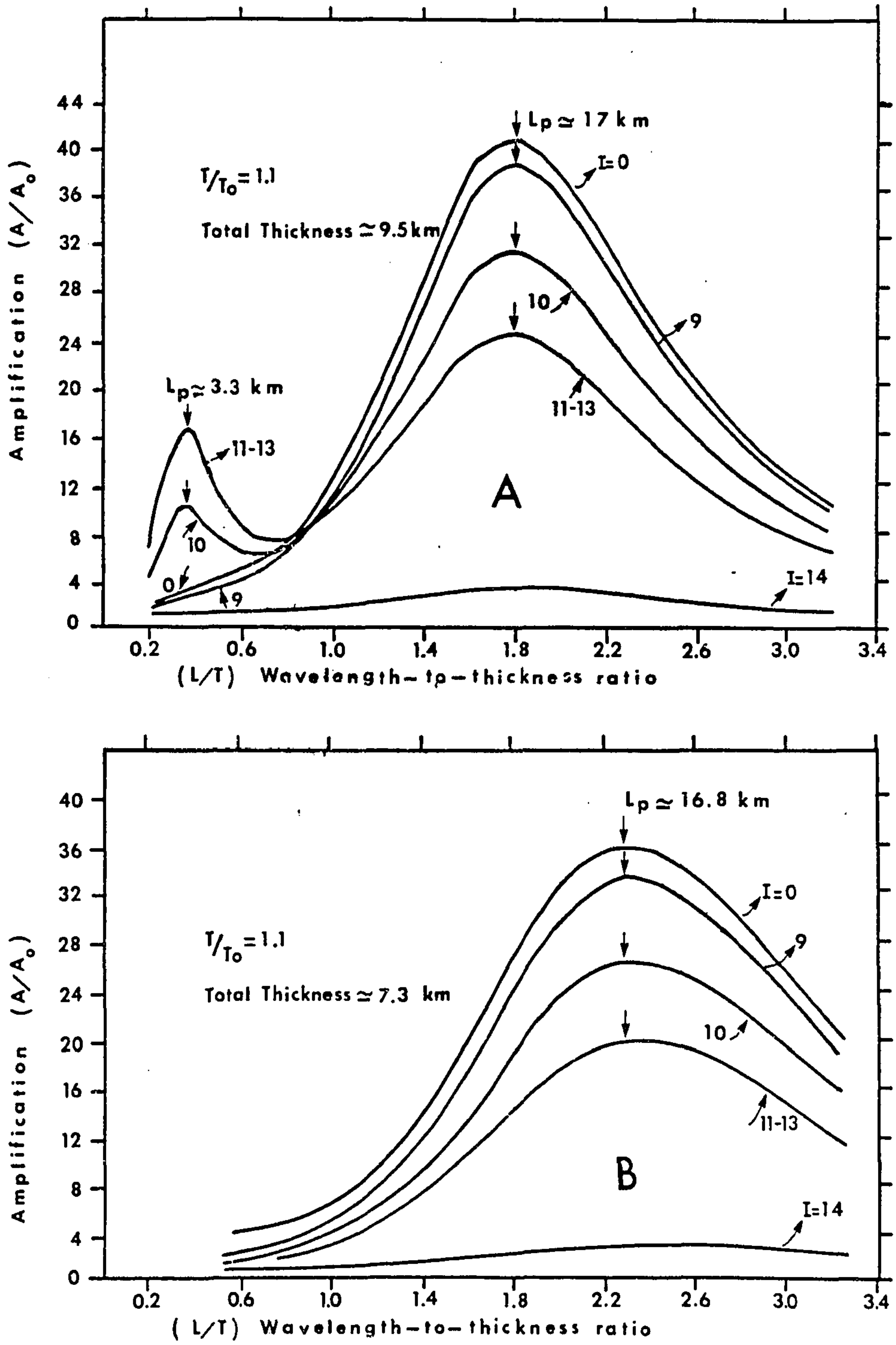
44
40
36
32
28
24
20
16
12
8
4
0
Amplification (A/A₀)
T/T₀ = 1.1
Total Thickness ≃ 9.5 km
Lp ≃ 17 km
I=0
9
10
11-13
Lp ≃ 3.3 km
11-13
10
0
9
I=14
A
0.2
0.6
1.0
1.4
1.8
2.2
2.6
3.0
3.4
(L/T) Wavelength-to-thickness ratio
40
36
32
28
24
20
16
12
8
4
0
Amplification (A/A₀)
T/T₀ = 1.1
Total Thickness ≃ 7.3 km
Lp ≃ 16.8 km
I=0
9
10
11-13
I=14
B
0.2
0.6
1.0
1.4
1.8
2.2
2.6
3.0
3.4
(L/T) Wavelength-to-thickness ratio

FIGURE 3

<u>wavelengths</u> (L_p) for the folds. The preferred wavelength is the wavelength of the perturbation that becomes amplified the most during shortening of the multilayer. The preferred wavelength is a function of the amount of shortening, the number of layers and the viscosities and thicknesses of individual layers composing a multilayer, as explained and illustrated in Appendix I. The computer program presented in Appendix II calculates the amplificatins of perturbations of all the interfaces for each wavelength selected, and one can determine the preferred wavelengths by plotting relations between amplification and L/T, as shown in Fig. 3A.

The results presented in Fig. 3A are based on the assumption that there is a detachment surface within the structural unit corresponding to the Martinsburg (Reedsville) Formation, as suggested by Rodgers (1963) and Gwinn (1964). The practical consequence of the assumption of a detachment surface is that rocks above the detachment are shortened whereas rocks below are not. The rocks below act merely as a medium underlying a stack of layers being shortened. The amount of shortening is assumed to be about nine percent, in accord with measurements reported by Nickelsen (1966), Faill and others (1973) and Englender (1979).

The two preferred wavelengths of about 3.3 km and 17 km correspond closely with the wavelengths of 1st- (11 to 18 km) and 2nd-order (2.5 to 3 km) folds in the region (Nickelsen, 1963). The correspondence suggests that the structural units selected for the analysis, Table I, satisfactorily predict the preferred wavelengths, so the selection of structural units passes this first test.

The second requirement of the selection of structural units is that the fold forms in the theoretical multilayer resemble those in structural cross sections. The fold forms were determined by using computer program III (Appendix IV), and are shown in Fig. 4B. The forms clerly show 2nd-order folds at the levels of the Tuscarora (St) and Juniata formations (Oj). The overall fold form is complex. However, in Devonian and younger rocks the anticline changes from a rounded, chevron-like fold with a narrow hinge and nearly straight limbs at the level of the Montebello Member (Dmo) to an open, concentric-like form in the lower part of the Catskill Formation (Dci), to a flat-topped form in the Pocono Group (Mp). In the same units, the syncline is concentric-like in the Pottsville Group (Pl) through Trimmers Rock Formation (Dtr). The hinge is tighter in the Pottsville than in the Trimmers Rock, and the trough is flat at the level of the Montebello Member (Dmo).

In these respects, the theoretical large folds resemble the folds shown in the structural cross section, Fig. 4A. The Berry-Buffalo syncline (Fig. 4A) is roughly concentric-like, with a flattened trough below the level of the Trimmers Rock Formation. The limbs are steeper and the hinge zones are tighter in the actual syncline than in the theoretical model, but the thoeretical model is near the limit of validity of the second-order approximation so that it could not be folded further without including terms of higher order. Nevertheless, the theoretical folds suggest the actual folds, and the theoretical model shows the probable fold form of rocks above the Trimmers Rock Formation in the Tuscarora Mountain anticline.

In the theoretical model (Fig. 4B), the 2nd-order folds are in phase with the 1st-order folds at Tuscarora Mountain and out of phase with the Berry-Buffalo syncline. Such seems to be the case in the actual folds. Examination of the geological map of central Pennsylvania (fig. 4, Chapter

Figure 4 - Fold forms in the Valley and Ridge Province of central Pennsylvania

A. Down-plunge structural cross section of the Berry-Buffalo syncline and the Tuscarora Mountain anticline. Symbols are defined in Table I.

B. Theoretical fold forms derived through second-order analysis of low amplitude perturbation. The layers are shortened about 9 percent above a detachment surface (lower interface of the Martinsburg Formation). Normalized viscosities of structural units are indicated by numbers at the right hand side.

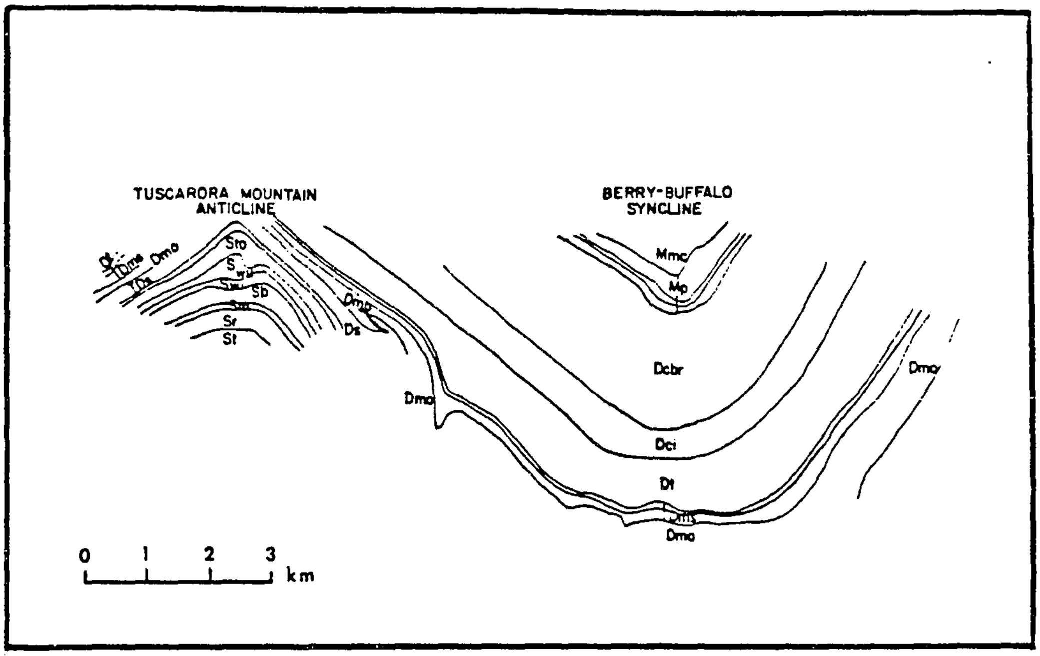
TUSCARORA MOUNTAIN ANTICLINE
BERRY-BUFFALO SYNCLINE
Sto
Sb
Sr
St
Ds
Dmo
Mmc
Mp
Dcbr
Dci
Dt
Dms
0 1 2 3 km

A

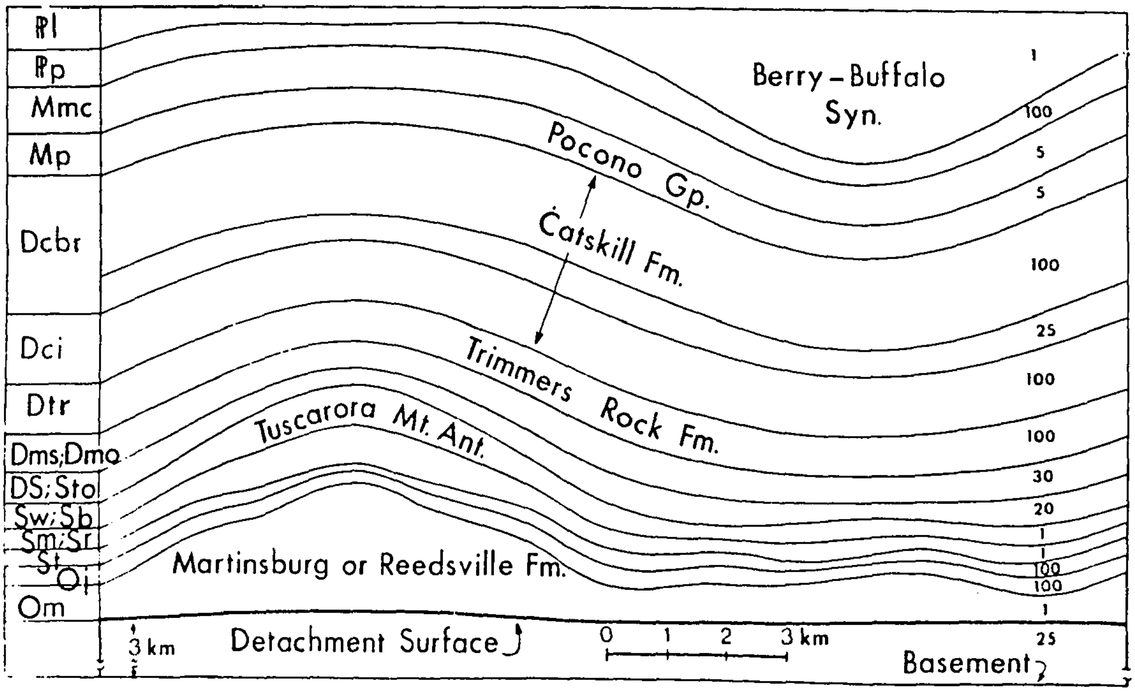
Pl
Pp
Mmc
Mp
Dcbr
Dci
Dtr
Dms;Dmo
DS;Sto
Sw;Sb
Sm;Sr
St
Oi
Om
Berry-Buffalo Syn.
Pocono Gp.
Catskill Fm.
Trimmers Rock Fm.
Tuscarora Mt. Ant.
Martinsburg or Reedsville Fm.
Detachment Surface
3 km
0 1 2 3 km
Basement?
1
100
5
5
100
25
100
100
30
20
1
1
100
100
1
25

B

FIGURE 4

I) indicates that the Tuscarora Mountain anticline reflects the superposition of 1st- and 2nd-order waveforms; the 2nd-order waveforms are apparent in the outcrop pattern of the Tuscarora Formation (figs. 3 and 4, Chapter I).

Examination of serial cross sections for central Pennsylvania (figs. 8 and 9, Chapter I) and the structural cross section (Fig. 4A) suggests that the fold form in the Tuscarora Mountain anticline changes from a rounded hinge at the level of the Tuscarora Formation (St) to a sharp hinge at the level of the Tonoloway Formation (Sto) back to an open, rounded hinge at the level of the Trimmers Rock Formation (Dtr). This change of fold is also developed in the theoretical model, Fig. 4B, although the amplitude of folding is lower in the theoretical model than in the actual folds. The extra, 3rd-order folds in the Wills Creek Formation (Fig. 4A) are absent in the theoretical model (Fig. 4B) because the Wills Creek and Bloomsburg formtions were treated as a single structural unit in the theoretical model. For a similar reason, the 3rd-order folds with short wavelengths in the Mahantango Formation (Dmo and Dms), shown in Fig. 4A, were not produced in the theoretical multilayer, Fig. 4B.

This theoretical analysis of some of the large folds in the central Appalachians shows that the essential features of the fold patterns can be understood in terms of the simultaneous development of folds with several wavelengths, in different parts of the stratigraphic section, and in terms of interactions between these folds. The fold pattern can be simulated, essentially, with a relatively simple multilayer of structural units with different viscosities separated by interfaces along which there is free slip. Contact strengths between structural units almost certainly were low relative to the scale of folding, so that one would not expect kink-like folds to develop at the scale of the 1st- and 2nd-order folds. Indeed, nobody has described kink-like folds with widths greater than 150 m in the central Appalachians. The flat bottoms of synclines such as the Berry-Buffalo (Fig. 4A) and the Northumberland (fig. 5, Chapter III) can readily be explained in terms of folding above a zone of decollement which overlies relatively stiff rocks that are not undergoing shortening. This is demonstrated in Fig. 4B.

PREFERRED WAVELENGTH AND FOLD FORMS IN PLATEAU PROVINCE

One of the striking results that one obtains from folding is that wavelengths and fold forms in a complex multilayer are sensitive to minor changes in the configuration of the multilayer. I will show that, by merely moving the detachment surface from the top of the Martinsburg Formation to near the top of the Silurian rocks, one eliminates the 2nd-order folds and produces a fold pattern that resembles the fold pattern on the Allegheny Plateau.

Fig. 3B shows the preferred wavelength for the multilayer of structural units shown in Table I, but with the detachment surface at the level of the base of the Tonoloway Formation. According to Fig. 3B, the preferred wavelength is about 17 km, which falls within the range of wavelengths of 9 to 21 km for folds on the Allegheny Plateau (Wiltschko and Chapple, 1977). Figure 1B shows the theoretical fold pattern, computed to second-order in the maximum slope of interfaces using Program II (Appendix III).

The theoretical fold pattern shows marked thickening in cores of anticlines. The thickening is due to flow of relatively soft materials from synclines into anticlines, as has been documented by Wiltschko and Chapple (1977) for folds on the Plateau. The model, of course, excludes faulting in the cores of anticlines but Sherwin (1972) has already explained that the faulting can be considered to be merely a means of achieving some of the thickening. That is, the faulting can be considered to be a result of folding rather than a cause of folding. The theoretical model also shows the narrow anticlines and broad synclines near the detachment surface which are typical of folds on the Allegheny Plateau. In the model (Fig. 1B) the narrow anticlines and broad synclines are the result of relatively stiff rocks below that are not subjected to layer-parallel shortening.

Thus the essential features of the folds on the Allegheny Plateau can be understood in terms of the folding of a multilayer with a detachment surface placed at a certain stratigraphic level.

CONCLUSIONS

Application of folding theory to complex multilayers, such as those in the central Appalachians, shows that theory can predict the wavelengths and forms of folds. For example, the pattern of folds, consisting of narrow anticlines and broad synclines, on the Allegheny Plateau can develop in a multilayer bounded below by a detachment surface.

In the Valley and Ridge Province, the wavelength of 1st-order folds (wavelengths of 11 to 18 km) apparently were controlled by relatively thick and stiff units in the Catskill and Trimmers Rock formations, and the wavelength of the 2nd-order folds (wavelengths of 2.5 to 3 km) were controlled by the stiffness of the Tuscarora and Juniata formations (Fig. 4B). Relatively soft beds above the Tuscarora Formation and below the Hamilton Group probably allowed the 3rd-order folds (wavelengths less than 1 km) to develop.

The forms of theoretical folds in the Plateau and Valley and Ridge provinces of central Pennsylvania resemble the forms of the actual folds, but one certainly can improve the correspondence between theoretical and actual forms by using higher-order approximations.

REFERENCES CITED

Biot, M. A., 1959. On the instability of folding deformation of a layered viscoelastic medium under compression. J. Appl. Mech., 26:393-400.

Biot, M. A., 1961, Theory of folding in stratified viscoelastic media and its implication in tectonics and orogenesis. Geol. Soc. Am. Bull., 72:1595-1620.

Biot, M. A., 1965, Further development of the thoery of internal buckling of multilayers. Geol. Sco. Am. Bull., 75:833-840.

Crittenden, M. D., 1963, Effective viscosity of the earth derived from isostatic loading of Pleistocene Lake Bonneville. Jour. Geophys. Res., 68:5517-5530.

Currie, J. B., Patnode, A. W. and Trump, R. P., 1962. Development of folds in sedimentary strata. Geol. Soc. Am. Bull., 73:461-472.

Englender, T., 1979. Mechamisms for strain within the upper Devonian clastic sequence of the Appalachians Plateau, west New York. Amer. Jour. Sci., 279: 527-542.

Faill, R. T., 1969. Kink band structures in the Valley and Ridg Province, central Pennsylvania. Geol. Soc. Am. Bull., 80:2539-2550.

Faill, R. T., 1973. Kink band folding, Valley and Ridge Province, Pennsylvania. Geol. Sco. Am. Bull., 84:1298-1314.

Faill, R. T., 1979. Geology and mineral resources of the Montoursville South and Muncy quadrangles and part of the Hughesville quadrangle. Penn. Geo. Sur. Atlas 146ab. 114 p.

Faill, R. T. and Wells, R. B., 1974. Geology and mineral resources of the Millerstown quadrangles, Perry, Juniata and Synder counties, Penn. Top. and Geol. Sur. Atlas 136, 276 p.

Faill, R. T. and Wells, R. B., 1977. Bedrock geology and mineral resources of the Linden and Williamsport quadrangles, Lycoming County, Pennsylvania. Penn. Top. and Geol. Sur. Atlas 134ab, 66 p.

Faill, R. T., Wells, R. B., Nickelsen, R. R. and Hoskins, D. M., 1973. Structure and Silurian-Devonian stratigraphy of the Valley and Ridge Province, central Pennsylvania. Guide book for 38th Annual Field Conference of Pennsylvania Geologist. Penn. Top. and Geol. Sur., Oct. 5-6, 1973, 168 p.

Fletcher, R. C., 1974, Wavelength selection in the folding of a single layer with power-law rheology. Am. Jour. Sci., 274:1029-1043.

Fletcher, R. C., 1979, The shape of single-layer folds at small but finite amplitude. Tectonophysics, 60:77-87.

Fletcher, R. C., 1982, Coupling of diffusional mass transport and deformation in a tight rock. Tectonophysics, 83:275-291.

Gwinn, V. E., 1964, Thin-skinned tectonics in the Plateau and northwestern Valley and Ridge Province of the central Appalachians. Geol. Soc. Am. Bull., 75:863-900.

Gwinn, V. E., 1970, Kinematic patterns and estimates of lateral shortening, Valley and Ridge and Great Valley Province, central Appalachians: In: G. W. Fisher, F. J. Pettijohn, J. C. Reed, Jr. and K. N. Weaver, editors. Studies in Appalachian Geology central and southern: Intersec. Publisher, N.Y., p. 127-146.

Honea, E. and Johnson, A. M., 1976, Part IV. Development of sinusoidal and kink folds in multilayers confined by rigid boundaries. Tectonophysics, 30:197-239.

Johnson, A. M., 1970, Physical Processes in Geology, 577 p., Freeman, Cooper and Company, San Francisco.

Johnson, A. M., 1977, Styles of Folding, 406 p. Elsevier Scientific Publishing Company, Amsterdam.

Johnson, A. M., 1982, Fold forms in multilayers. Presented to Geological Society of London on April 28, 1982. Unpublished manuscript, University of Cincinnati.

Johnson, A. M. and Fletcher, R. C., 1982, Final report to Earth Science Division, Geology Program of the National Science Foundation. Grant No.: EAR 80-00053, Volume II.

Kilinc, A. I. and Johnson, A. M., 1980, Diffusion and folding. Unpublished class notes, University of Cincinnati.

Nickelsen, R. P., 1963, Fold patterns and continuous deformation mechanisms of the central Pennsylvania folded Appalachians, In: Guidebook to tectonics and Cambro-Ordovician stratigraphy, central Appalachians of Pennsylvania: Pittsburgh Geol. Soc. and Appalachians Geol. Soc., p. 13-30.

Nickelsen, R. P., 1966, Fossil distortion and penetrative rock deformation in the Appalachians Plateau, Pennsylvania. Jour. Geol., 74:924-931.

Nickelsen, R. P., 1973, "Rainbow Rocks", an example of fold geometry and minor structure in the Wills Creek Formation. In: R. T. Faill, R. B. Wells, R. P. Nickelsen, D. M. Hoskins (editors). Guidebook for the 38th Annual Field Conference of Pennsylvania Geologist. Penn. Top. Sur., Oct. 5-6, 1973, p. 68-74.

Ramberg, H., 1959, Evolution of ptymatic folding. Nor. Geol. Tidsskr., 39:99-151.

Ramberg, H., 1960, Relationship between arch length and thickness of ptymatically folded veins. Am. Jour. Sci., 258:36-46.

Ramberg, H., 1962, Contact strain and folding instability of a multilayered body under compression. Geol. Rundsch., 51:405-439.

Ramberg, H., 1963, Evolution of drag folds. Geol. Mag., 100:97-106.

Ramberg, H., 1970, Folding of lateral compressed multilayers in the field of gravity. Phys. Earth Planet. Inter., Part I, 2:203-232; Part II. 4:83-120.

Ramberg, I. B. and Johnson, A. M., 1976, Part V. Asymmetrical folding interbedded chert and shale of the Franciscan Complex, San Francisco Bay area California. Tectonophysics, 32:295-320.

Reches, Z. and Johnson, A. M., 1976, Part VI. Asymmetric folding and monoclinal kinking. Tectonophysics, 35:295-334.

Rich, J. L., 1934, Mechanics of low-angle overthrust faulting illustrated by Cumberland thrust block, Virginia, Kentucky and Tennessee. Amer. Assoc. Pet. Geol. Bull., 18:1584-1596.

Rodgers, J., 1963, Mechanics of Appalachians foreland in Pennsylvania and West Virginia. Amer. Assoc. Pet. Geol. Bull., 47:1527-1536.

Rogers, H. D., 1858, The geology of Pennsylvania. First Pennsylvania Geological Survey (1836-1841) 2 vols. and Atlas.

Sherwin, J., 1972, Decollement folding: Unpublished Ph.D. dissertation, Brown University, Providence, R. I., 150 p.

Smith, R. B., 1979, The folding of a strongly non-Newtonian layer. Amer. Jour. Sci., 279:272-287.

Wentworth, C. K., 1922, A scale of grade and class terms for clastic sediments. Jour. Geol., 30:377-392.

Weyl, R. L., 1959, Pressure solution and force of crystallization-a-phenomenological theory. Jour. Geophys. Res., 64:2001-2025.

Willis, B., 1893, The mechanism of Appalachians Structure, 13th Annual Rept. U.S. Geol. Sur. (1891-2), p. 211-281.

Wiltschko, D. V. and Chapple, W. N., 1977, Flow of weak rocks in Appalachians Plateau folds. Amer. Ass. Pet. Geol. Bull., 61:653-670.

Wood, G. H., Jr., Trexler, J. P. and Kehn, T. M., 1969, Geology of the west-central part of the southern anthracite field and adjoining area, Pennsylvania. U.S. Geol. Sur. Prof. Paper 602, 150 p.

CHAPTER III

THE SHIKELLAMY FOLD

A Large Kink-Like Fold in the Trough of the Northumberland Synclinorium, East-Central Pennsylvania

ABSTRACT

The Shikellamy fold, near Northumberland, Pennsylvania, is the largest kink-like fold known in central Pennsylvania. Its central limb is about 150 m long. It is an asymmetric fold, gently plunging southwest, with a sharp anticlinal bend and a broad synclinal bend. It has three limbs; the southern limb gently dips towards the north, the central limb steeply dips towards the south and the northern limb is horizontal. The central and northern limbs are planar whereas the southern limb is warped. Several small-scale structural features occur within the fold zone. Bedding-surface faults are the most common structures in all the limbs, but they are more abundant in the central limb than in the others. The sense of shear relative to layering is consistently right-lateral on the central and northern limbs, whereas the sense of shear is left-lateral on the southern limb. Conjugate faults in the central limb indicate that the direction of maximum compression plunged about 5° towards the southeast, and field evidence and structural analyses suggest that the Shikellamy fold is a monoclinal kink fold.

INTRODUCTION

In central Pennsylvania, kink-like folds have been recognized in a variety of stratigraphic sequences (Nickelsen, 1963; Faill, 1969, 1973; Faill and others, 1973; Faill and Wells, 1974, 1977, and Pfaff, in preparation). The kink-like folds are conjugate types or a series of monoclinal types, whereas others are single, isolated folds. Most of the kink-like folds in the region are 3rd-order* and have planar limbs less than 10 m in length.

Kink-like folds have been studied in a variety of structural settings throughout the world, and kink folding has been experimentally as well as theoreticaly studied by many investigators. Kink folding has been observed experimentally by Turner (1964) in mica schist, by Patterson and Weiss (1966) in phyllite, by Donath (1968) and Anderson (1974) in slate, by Gay and Weiss (1974) in card decks and foliated rocks, and by Honea and Johnson (1976) and Reches and Johnson (1976) in multilayers of rubber. Kinking has been theoretically analyzed by Biot (1965), by Johnson and Ellen (1974), by Honea and Johnson (1976), by

*Nickelsen (1963, p. 16) has provided a useful classification of sizes or orders of folds in the central Appalachians: 1st order folds are anticlinoria and synclinoria with wavelengths of 11 to 18 km and involve rocks from the Cambrian to the Pennsylvanian. 2nd-order folds have wavelengths of 2.5 to 3 km; they are best developed at the levels of the Tuscarora and Bald Eagle Formations. 3rd-order folds have wavelengths of of several meters to one km. They are best developed in the middle Silurian and middle Devonian rocks above the Rose Hill Shale and below the Hamilton Group. 4th-order folds have wavelengths ranging from a few tens of centimeters to a few meters. 5th-order folds are smaller than these.

Reches and Johnson (1976), by Ramberg and Johnson (1976), by Collier (1978) and by Weiss (1980). Kink-like folds have been studied in the field by Dewey (1965), by Anderson (1968), by Reches and Johnson (1976), and by Johnson and Honea (1975). It is generally agreed that contact strength between stiff layers, layer-parallel compression and layer-parallel and layer-normal shear are necessary to monoclinal kink folding. Also, it has been shown that monoclinal flexures in sedimentary and metamorphic rocks can be genetically similar to kink bands (Johnson and Pollard, 1973; Reches, 1977; Koch, Pollard and Johnson, 1981).

I briefly examined many kink-like folds in central Pennsylvania, and then decided to study the Shikellamy fold because it is the largest kink-like fold known in the region and because nearly perfect exposures appeared to provide an opportunity to map most of the section of the fold. The Shikellamy fold is exposed in an abandoned railroad cut at the west end of the Northumberland Bridge, on State Route 11, near Northumberland, Pennsylvania, between the junction of the west and east branches of the Susquehanna River (Figs. 1 and 2). The region around the fold was first mapped by the Pennsylvania Geological Survey in 1980 as preliminary geologic maps of the Sunbury and the Northumberland 7½ minute quadrangles. Faill and others (1973) cited the Shikellamy fold as an excellent example of a large kink-like fold in the central Appalachians. However, no detailed work has previously been done for this structure.

Figure 1 - Location map of study area and traces of contacts between some of the rock units shown on part of the Pennsylvania Geologic Map along the Susquehanna River (after Gray and others, 1960). The figure shows outcrops of 1st- and 2nd-order folds.

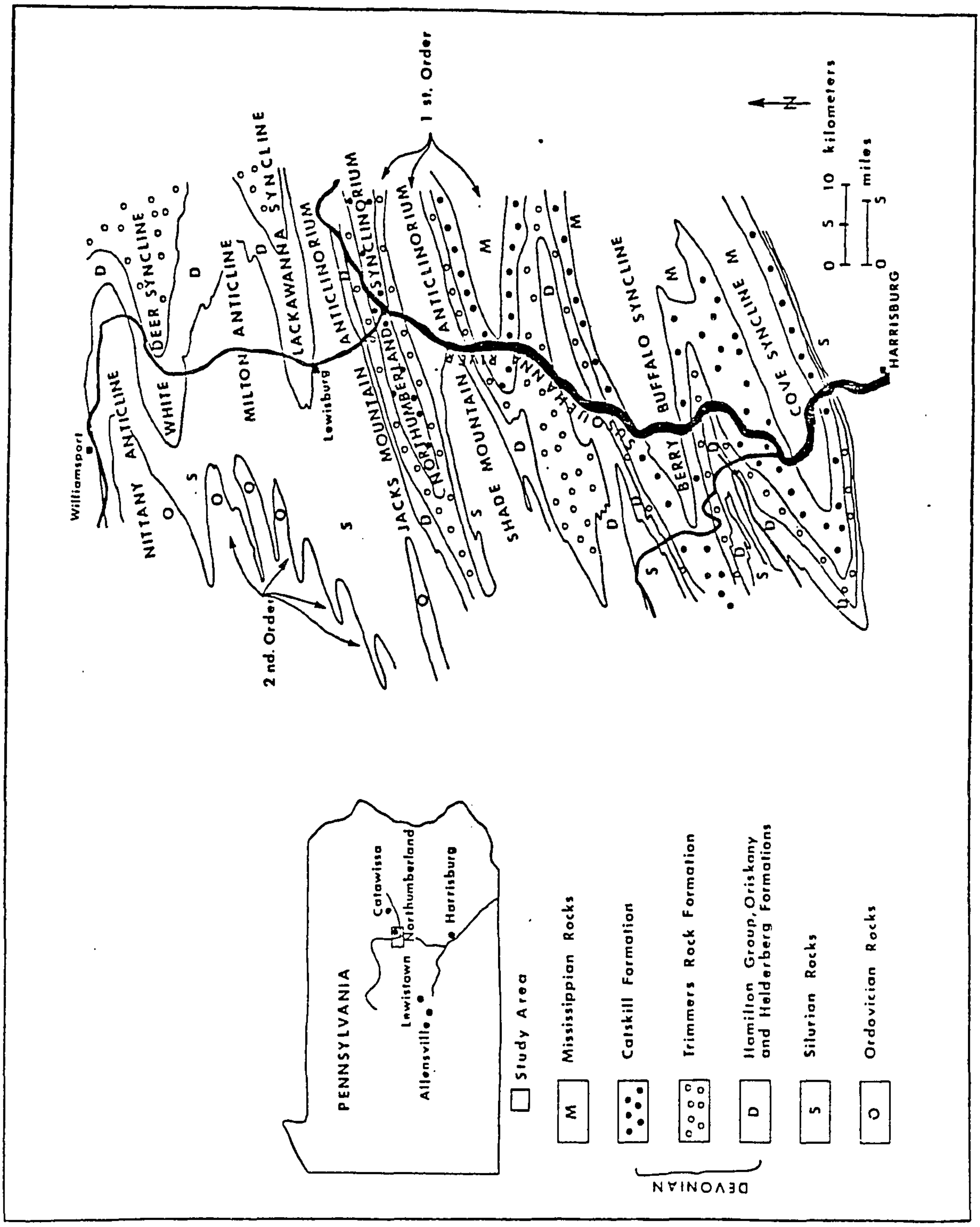

Williamsport
NITTANY ANTICLINE
WHITE DEER SYNCLINE
MILTON ANTICLINE
LACKAWANNA SYNCLINE
Lewisburg
ANTICLINORIUM
SYNCLINORIUM
JACKS MOUNTAIN
NORTHUMBERLAND
ANTICLINORIUM
SHADE MOUNTAIN
SUSQUEHANNA RIVER
BUFFALO SYNCLINE
BERRY
COVE SYNCLINE
HARRISBURG
2 nd. Order
1 st. Order
N
0 5 10 kilometers
0 5 miles
PENNSYLVANIA
Catawissa
Northumberland
Harrisburg
Lewistown
Allensville
Study Area
M Mississippian Rocks
Catskill Formation
Trimmers Rock Formation
D Hamilton Group, Oriskany and Helderberg Formations
S Silurian Rocks
O Ordovician Rocks
DEVONIAN

FIGURE 1

The main objective of this chapter is to present a comprehensive and detailed field study of the Shikellamy fold. The results are presented via an accurate geologic map of the area of the fold, a description of 1337 m of stratigraphic section, a detailed outcrop map of rocks within the central limb of the fold and structural data. The stratigraphic section is described in Appendix V. Cross sections were prepared in order to relate the Shikellamy fold to the Northumberland synclinorium.

STRATIGRAPHIC AND STRUCTURAL SETTING OF THE SHIKELLAMY FOLD

Stratigraphy:

The rocks exposed near Northumberland, Pennsylvania are of Late Devonian age, and include the Trimmers Rock Formation and the Catskill Formation (Fig. 2). The Catskill Formation is divided into two members, the Irish Valley and Sherman Creek (Faill and Wells, 1974, 1977).

The Trimmers Rock Formation is predominantly olive-gray siltstone and mudshale, with minor interbedded very fine-grained sandstone in the upper part. The siltstone and sandstone are cemented with silica. The mudshale has fissile parting and commonly grades into silty mudshale. The bedding is generally thinly laminated to thickly bedded and planar. The thickness of the formation in the study area exceeds 500 m according to my measurements (Fig. 3). In the surrounding region, the thickness is 570 m in the Millersburg quadrangle (Hoskins, 1976), about 15 km south of the area, and is 560 m in the Montoursville and Muncy quadrangles (Faill, 1979), about 25 km north of the area.

The Catskill Formation rests conformably upon the Trimmers Rock Formation, and consists of red and gray clastic rocks. The fractions of rocks of red color and of finer detrital sediments increase towards the top. The total thickness of the Catskill Formation is more than 904 m in the Northumberland area according to my measurements. In the surrounding region, the thickness is 1760 m about 15 km south of the area in the Millersburg quadrangle (Hoskins, 1976), and is 435 m about 30 km north of the area in the Linden and Williamsburg quadrangles

Figure 2 - Geologic map of Northumberland synclinorium and Shikellamy fold in the study area. The Shikellamy fold is exposed near the southern hinge zone of the Northumberland synclinorium.

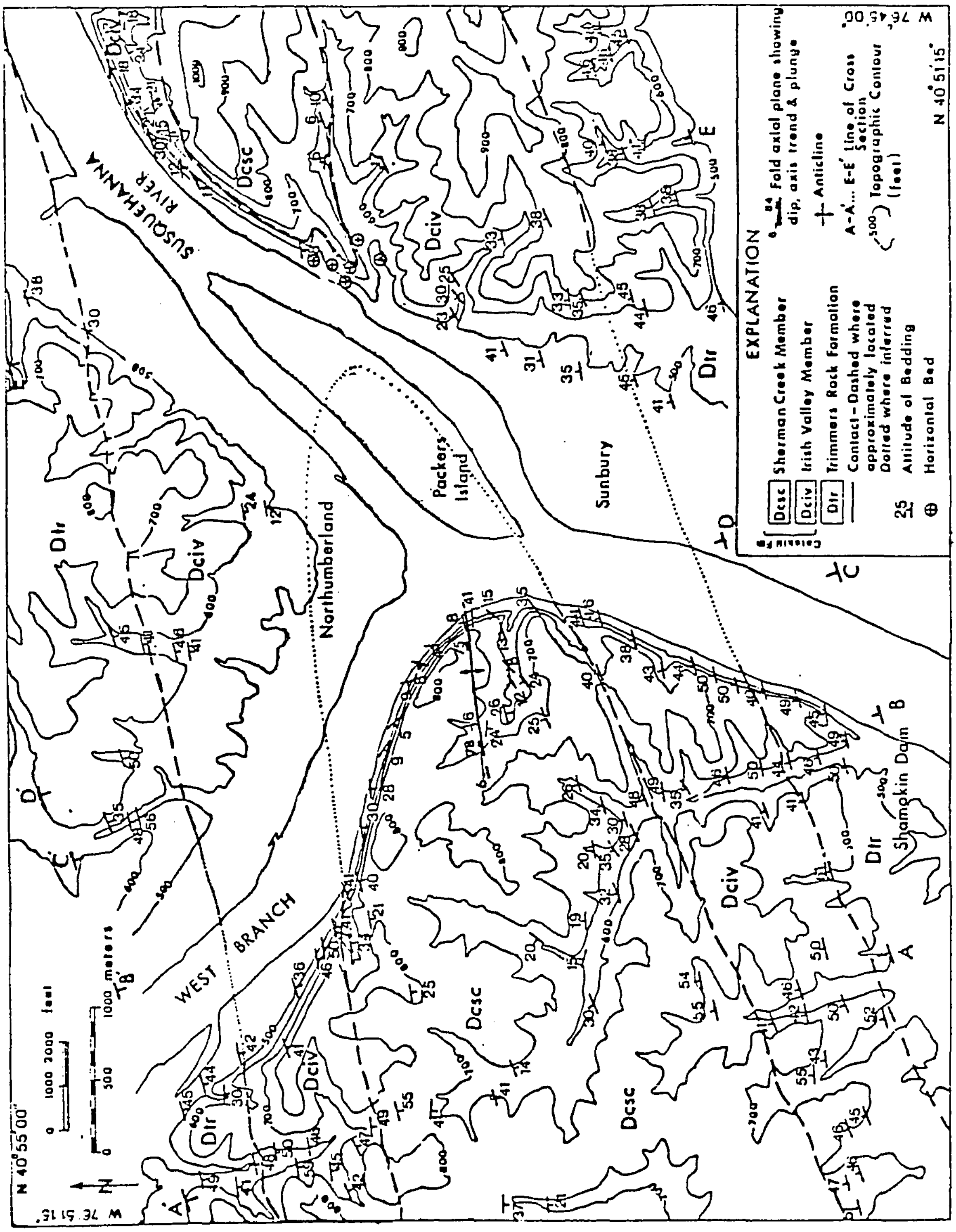
EXPLANATION
Dcsc Sherman Creek Member
Dciv Irish Valley Member
Catskill Fm
Dtr Trimmers Rock Formation
Contact–Dashed where approximately located Dotted where inferred
Attitude of Bedding
Horizontal Bed
Fold axial plane showing dip, axis trend & plunge
Anticline
A–A'... E–E' Line of Cross Section
Topographic Contour (feet)
SUSQUEHANNA RIVER
WEST BRANCH
Northumberland
Packers Island
Sunbury
Shamokin Dam
N 40°55'00"
W 76°51'15"
W 76°45'00"
N 40°51'15"
1000 2000 feet
500 1000 meters

FIGURE 2

(Faill and Wells, 1977).

The lower part of the Catskill is the Irish Valley Member, which includes marine and non-marine rocks. The thickness of the Irish Valley Member is 704 m in the Northumberland area (Fig. 3). The marine rocks are olive gray to grayish brown and consist of siltstone, sandstone and minor mudshale. The non-marine rocks are dusky red to brown and consist of siltstone and sandstone. They are very fine-grained and cemented with silica. The bedding is generally medium laminated to thin bedded (5-20 cm).

The upper part of the Catskill is the Sherman Creek Member which is dominated by dusky red to blackish red sandstone interbedded with siltstone. There are minor amounts of red mudshale in the member. The sandstones are generally thinly to thickly bedded (10-50 cm), but, at four locations, the sandstones are very thickly to massively bedded (units 56, 57, 59, 67, Fig. 3). Some beds are cross-bedded. The siltstones are thickly laminated to thinly bedded (0.5-25 cm) and the mudshales are laminated. The Sherman Creek Member is more than 200 m thick in the Northumberland area (Fig. 3). The member is 945 m thick south (Hoskins, 1976) and 150 m thick north (Faill and Wells, 1977) of the area.

Structural Setting:

The Northumberland synclinorium, which is a 1st order fold, and the Shikellamy fold are the major structural features in the Northumberland area. Axes of both folds parallel the general Appalachian trend. The Northumberland synclinorium is about 160 km long and 35 to 15 km wide, and is bounded on the south by the Shade Mountain anti-

Figure 3 - Measured stratigraphic section on an abandoned railroad cut along State Route 11, near Northumberland, Pennsylvania. Descriptions are given in Appendix V.

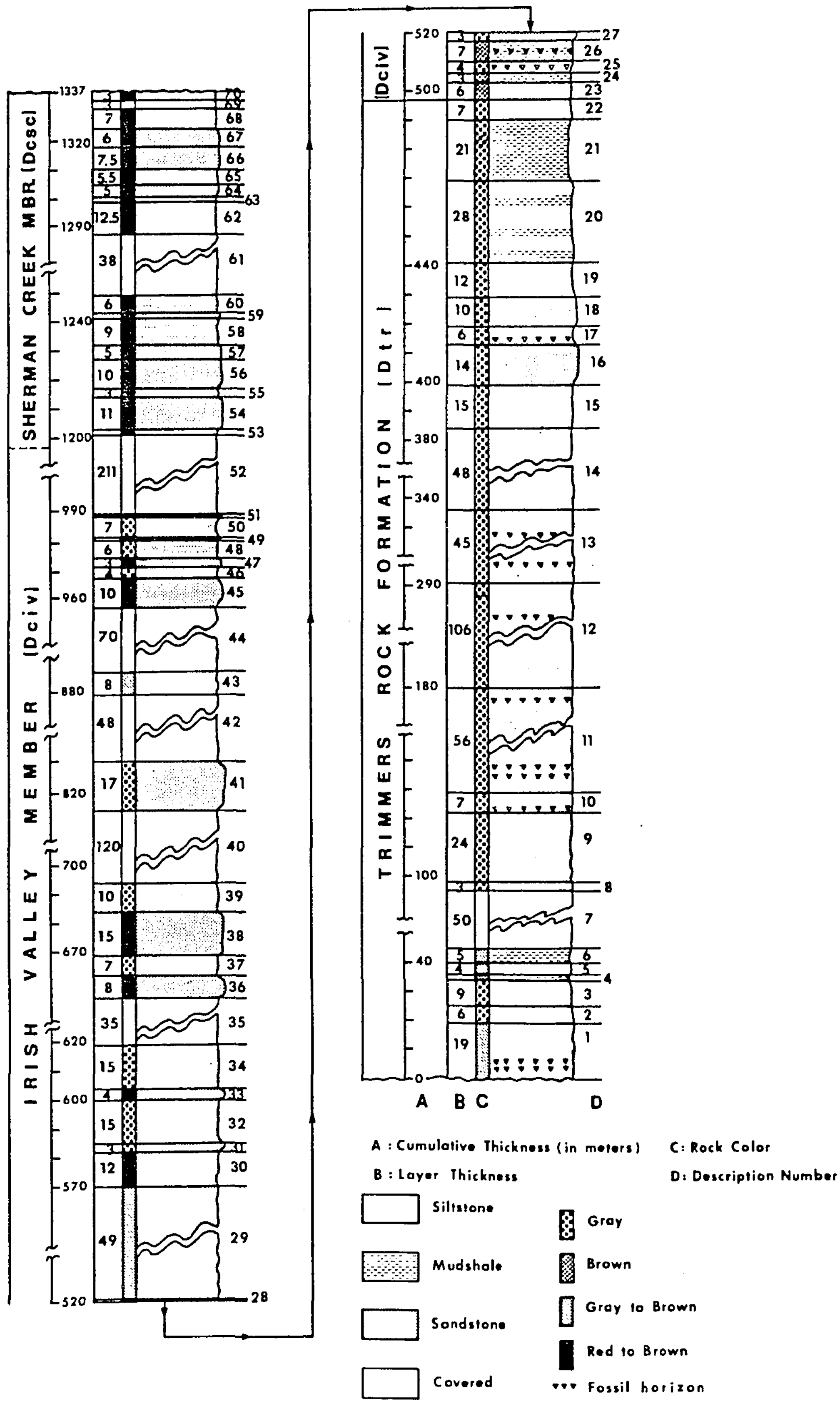
SHERMAN CREEK MBR. (Dcsc)
IRISH VALLEY MEMBER (Dciv)
(Dciv)
TRIMMERS ROCK FORMATION (Dtr)
A B C D
A : Cumulative Thickness (in meters)
B : Layer Thickness
C: Rock Color
D: Description Number
Siltstone
Mudshale
Sandstone
Covered
Gray
Brown
Gray to Brown
Red to Brown
Fossil horizon

FIGURE 3

clinorium and on the north by the Jack's Mountain anticlinorium. It extends in the N70-80°E direction from Allensville to Catawissa, Pennsylvania (Fig. 1). Southwest of Northumberland, the fold plunges 5-10° towards the northeast; however, near Northumberland, the plunge reverses its direction. In the study area, the Northumberland synclinorium axis trends S75°W. At the east branch of the Susquehanna River, the plunge is zero. Between the two branches, the plunge is 2°, and, at the west branch, the plunge becomes 6° to the southwest.

The cross-sectional form of the Northumberland synclinorium apparently does not change significantly in central Pennsylvania. The form of the fold is shown as concentric-like in cross sections accompanying geologic maps of Pennsylvania (1960, 1980) prepared by the Pennsylvania Geologic Survey. The southwestern extension of Northumberland synclinorium, the Northern synclinorium, was studied in the Mifflintown quadrangle by Conlin and Hoskins (1962), who described the synclinorium as a flat-bottomed concentric form.

In order to estimate the form of the Northumberland synclinorium near Northumberland, I constructed serial vertical cross sections and a down plunge structural cross section. Attitudes of layers were mapped at many places and fold axes and plunges were determined by the usual method, utilizing a stereographic net.

One way to determine the form of Northumberland synclinorium is to construct vertical cross sections. For this purpose, five different sets of cross sections were made. Two of them, B-B' and D-D', were superimposed onto cross sections A-A' and C-C', respectively (Fig. 4). The data used in constructing the vertical cross sections were positions of contacts at the ground surface along the cross sections and apparent

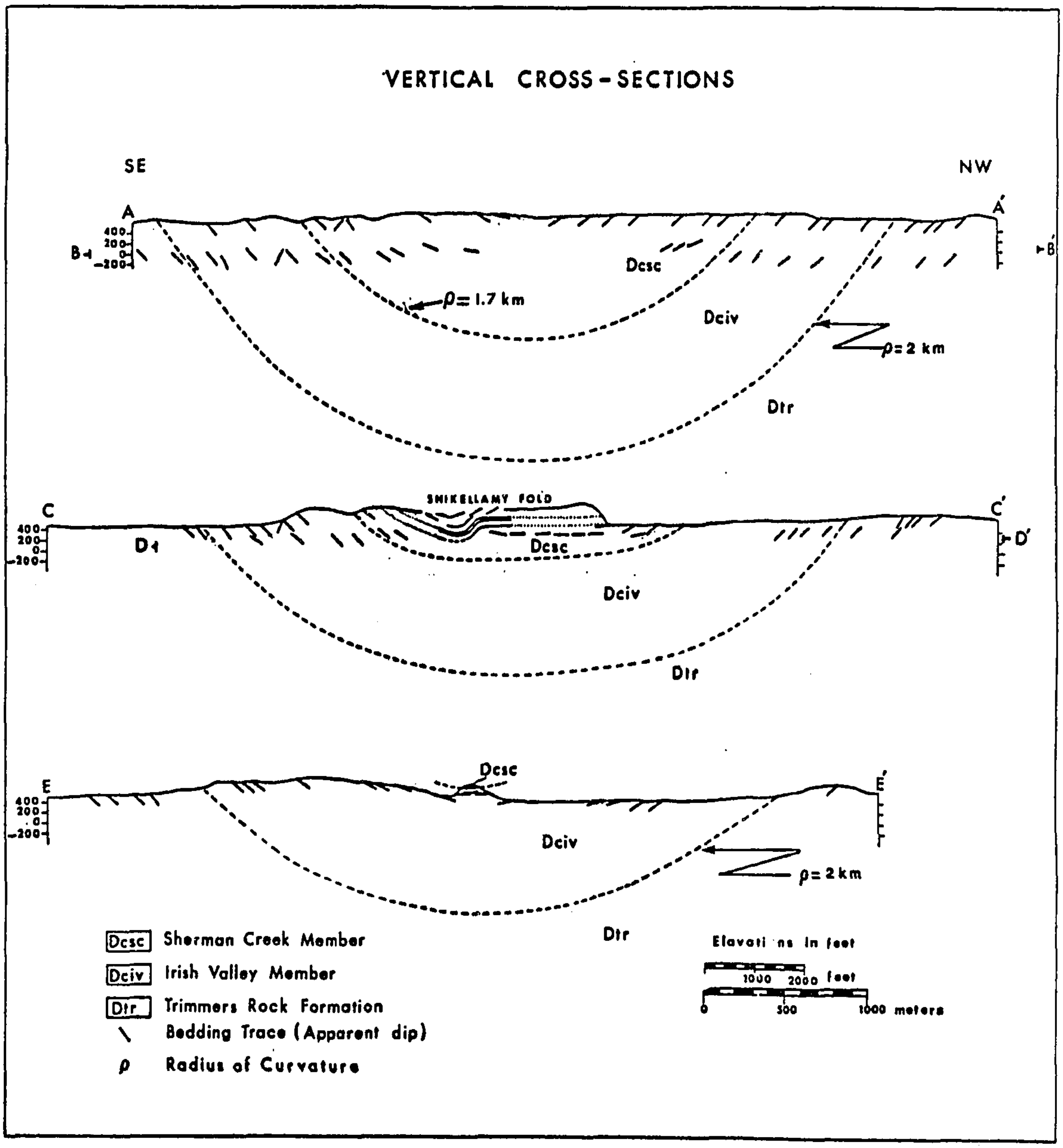

FIGURE 4

Serial vertical cross sections. Locations of cross sections are shown in the geologic map (Fig. 2).

dips determined for attitudes measured near the lines of the cross sections. The vertical cross sections were drawn assuming that the folds extend indefinitely at depth and that the thicknesses of beds are essentially constant. Data shown in cross sections A-A' and E-E' are consistent with concentric-like forms whereas data shown in cross section C-C' suggest a flat-bottomed form. Thus, according to this method, the fold would change form from concentric-like to flat-bottomed to concentric-like along the fold axis.

Another way to determine fold form is to construct a down-plunge structural cross section (Mackin, 1950; Ragan, 1973) using the geologic map of the study area (Fig. 2). The area was divided into three parts, according to plunge angles, and 225 attitudes were projected onto a common cross section (Fig. 5A). The formation contacts are shown in only a few places to give one the freedom to interpret the form of Northumberland synclinorium. According to my interpretation, shown in Figure 5B, the Northumberland synclinorium has a broad synclinal bend with a radius of curvature of about 2 km at the contact between the Irish Valley Member (Dciv) and the Trimmers Rock Formation (Dtr). The fold has two rather straight limbs, the southern limb and the northern limb, and a flat trough separated by two rounded hinge zones (Fig. 5B). The two limbs dip 45° towards each other; the interlimb angle is 90°. On both limbs, dip angles of bedding within the Irish Valley and the lower part of the Sherman Creek decrease towards the center of the synclinorium, where they become zero. However, within the southern hinge zone of the synclinorium, in the lower part of the Sherman Creek, the dip changes direction, reflecting the Shikellamy fold (Fig. 5A).

Figure 5 - Down-plunge structural cross section of the Northumberland synclinorium.

A- Attitudes of bedding traces and formation contacts in some locations.

B- Form of Northumberland synclinorium.

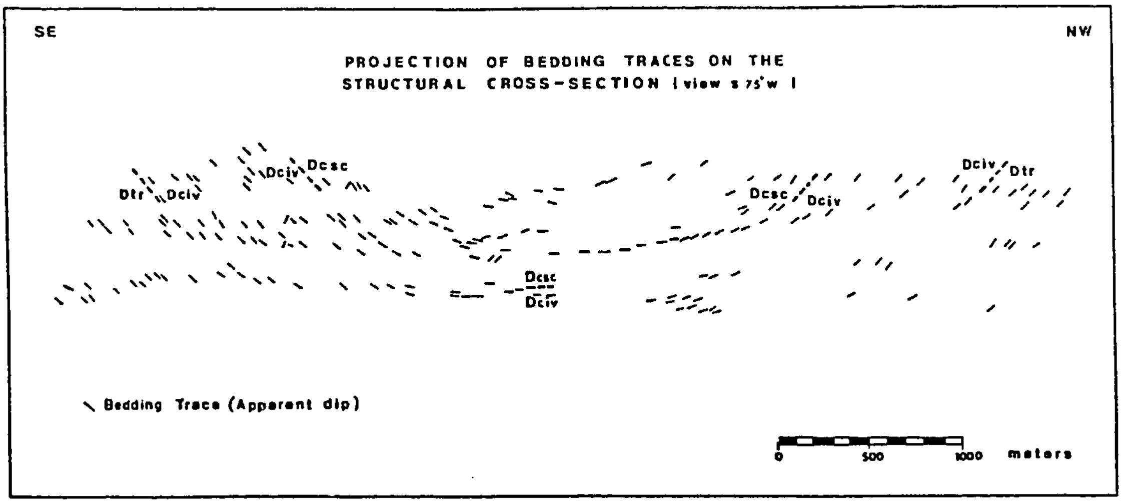
SE
NW
PROJECTION OF BEDDING TRACES ON THE STRUCTURAL CROSS-SECTION (view s 75°w)
Dtr
Dciv
Dcsc
Bedding Trace (Apparent dip)
0 500 1000 meters

A

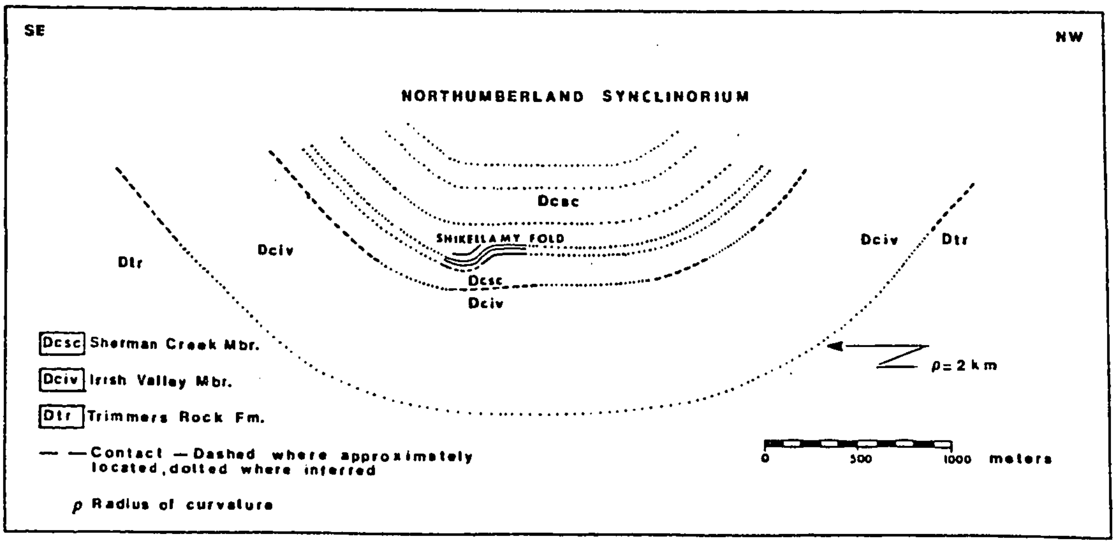
SE
NW
NORTHUMBERLAND SYNCLINORIUM
Dcsc
SHIKELLAMY FOLD
Dciv
Dtr
Dcsc Sherman Creek Mbr.
Dciv Irish Valley Mbr.
Dtr Trimmers Rock Fm.
Contact — Dashed where approximately located, dotted where inferred
ρ Radius of curvature
ρ = 2 km
0 500 1000 meters

B

FIGURE 5

The down-plunge structural cross section suggests that the Northumberland synclinorium has a flat-bottomed form in the study area. However, the width of the flat bottom decreases towards the top of the Sherman Creek Member (Dcsc),(Fig.5B). The flat-bottomed form of the Northumberland synclinorium suggests that, either the synclinorium is a kink-like fold or the synclinorium was underlain by a stiff medium during folding. Similar flatness was observed in the Berry-Buffalo and Cove synclines (Chapter I) and theoretical analysis of those fold forms suggest that the flat bottom is a reflection of a stiff underlying medium (Chapter II).

The Shikellamy fold is exposed near the southern hinge zone of the Northumberland synclinorium. The eastern extension of the fold is uncertain because it is covered by the Susquehanna River. The fold dies out about 1.2 km west of the river (Fig. 2).

A rockcut of an abandoned railroad along State Route 11, southwest of Northumberland, offers an opportunity to explore the Shikellamy fold (Fig. 6). The Shikellamy fold is asymmetric and has three limbs. The southern limb dips 15 to 25° towards the north, the central limb dips 30 to 40° towards the south, and the northern limb is nearly horizontal. The central limb is shorter than the other limbs (Fig. 5B). The northern and central limbs are nearly planar, except near the hinge zones. However, the southern limb is bent.

The interlimb angles are 140° at the anticlinal hinge and about 125° near the synclinal hinge. The anticlinal hinge is broad; its radius of curvature is about 90 m at the level of stratigraphic unit 70 (Fig. 6). The thicknesses of individual beds are constant throughout the cross section except near the hinge zones, where some of the beds show up to about 12 percent thickening (Fig. 6).

Dips of beds change angles from the central to the southern limbs of the fold along the railroad cut, and the variations of dips of beds can be shown by drawing dip isogons (Ramsay, 1967), which are lines on a cross section connecting points which have the same dip angle on adjacent surfaces (Fig. 7A).

Figure 6 - Cross sectional form of Shikellamy fold.

Below, detailed outcrop map of part of central limb, in section A-A', showing fault planes and slickenlines on average bedding planes.

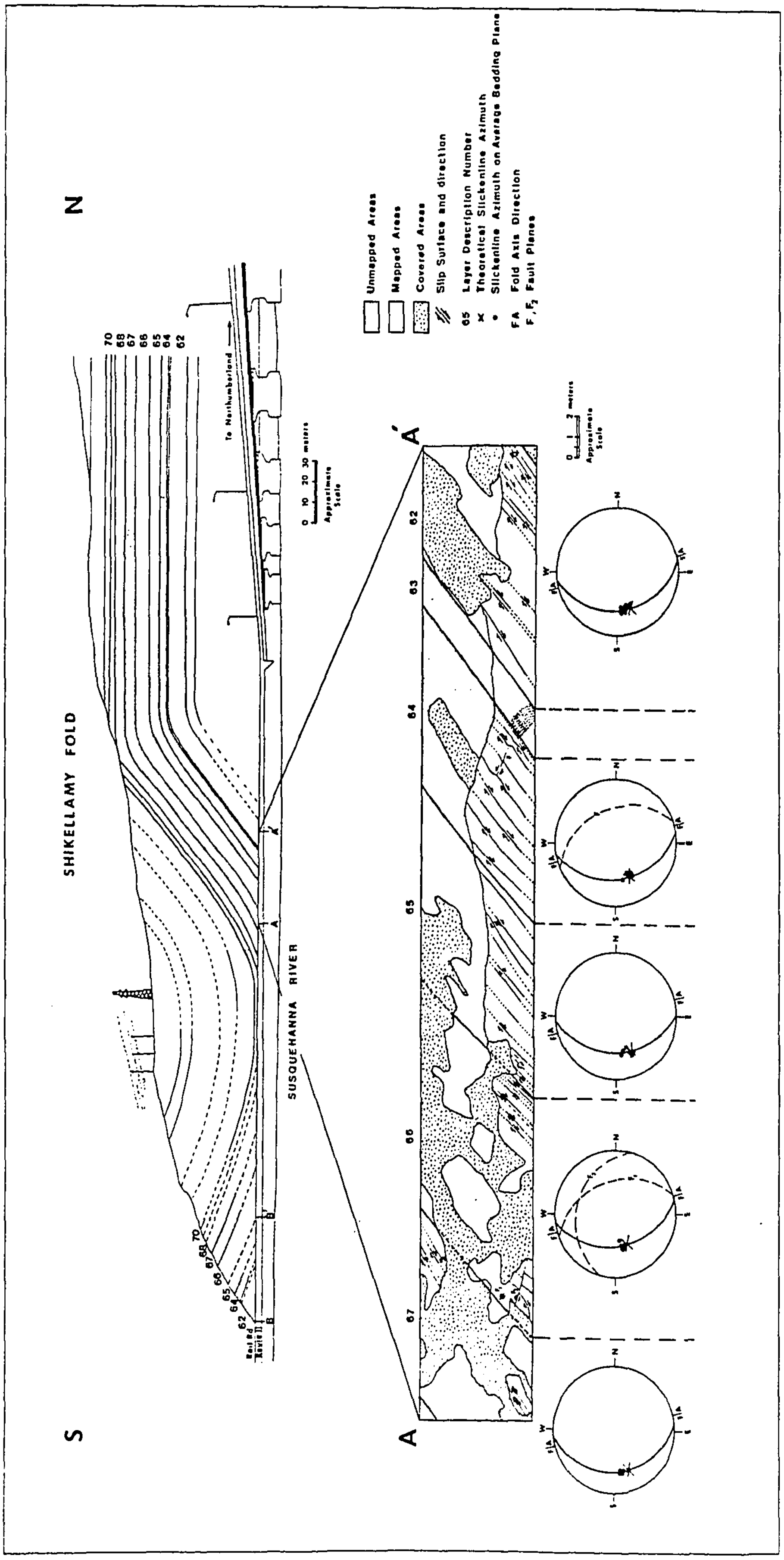
SHIKELLAMY FOLD
S
N
SUSQUEHANNA RIVER
To Northumberland
0 10 20 30 meters
Approximate Scale
Unmapped Areas
Mapped Areas
Covered Areas
Slip Surface and direction
65 Layer Description Number
x Theoretical Slickenline Azimuth
• Slickenline Azimuth on Average Bedding Plane
FA Fold Axis Direction
F, F2 Fault Planes
A
A′
62
63
64
65
66
67
68
70

FIGURE 6

Figure 7 - A .Isogon pattern of Shikellamy fold. The synclinal hinge of the fold has a roughly concentric form (type 1b), whereas the anticlinal hinge has a similar form (type 2).

B .Isogon pattern for five types of folds in the classification of folds (after Ramsay, 1967, fig. 7-24).

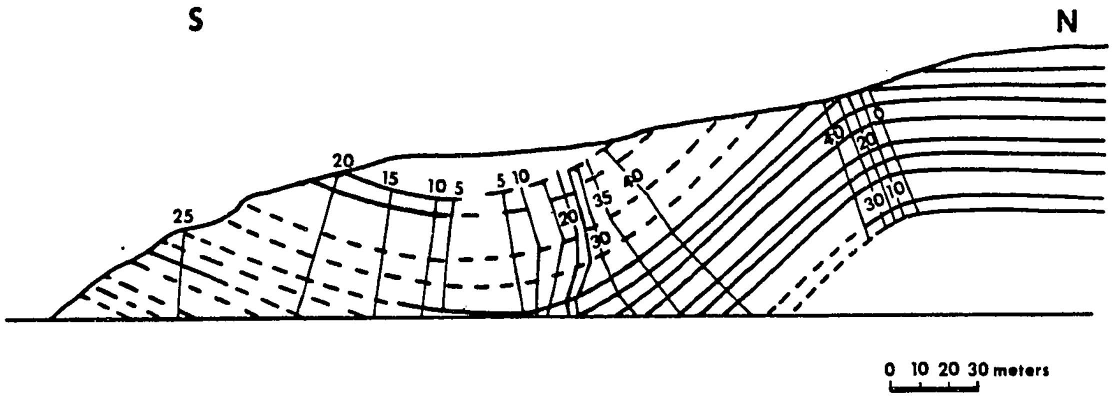
S
N
25
20
15
10
5
5
10
20
35
30
40
40
20
0
30
10
0 10 20 30 meters

A

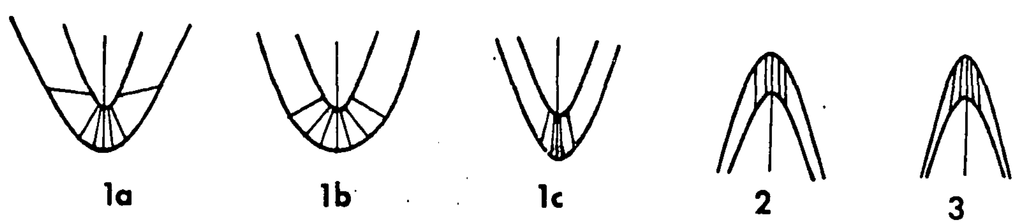
1a
1b
1c
2
3

B

FIGURE 7

Ramsay classified folds into three categories according to isogon patterns and the changes of curvature reflected by the patterns (Fig. 7B).

1) Isogons converge upward in synclinal bend. Curvature of the inner surface is greater than of the outer surface. This class is divided into three types: 1a, 1b, 1c - in which type 1b is concentric-like.

2) Parallel isogons. Curvature of the inner and outer surfaces are equal (similar fold).

3) Isogons converge upward in anticlinal bend. Curvature of the inner surface is smaller than that of the outer surface.

According to Ramsay's classification, the synclinal hinge of Shikellamy fold has a roughly concentric form (type 1b), whereas the anticlinal hinge has a similar form (type 2).

My best estimation of the overall form of Shikellamy fold is shown in Figure 8. It is estimated that 350 m of section of the lower units of the Sherman Creek Member (Dcsc) were involved in the folding. The fold dies out upward and downward and the rocks show 10-20% thickening towards cores of anticlinal and synclinal hinges.

Figure 8 - Probable form of Shikellamy fold. The rocks show 10-20 percent thickening towards cores of anticlinal and synclinal hinges.

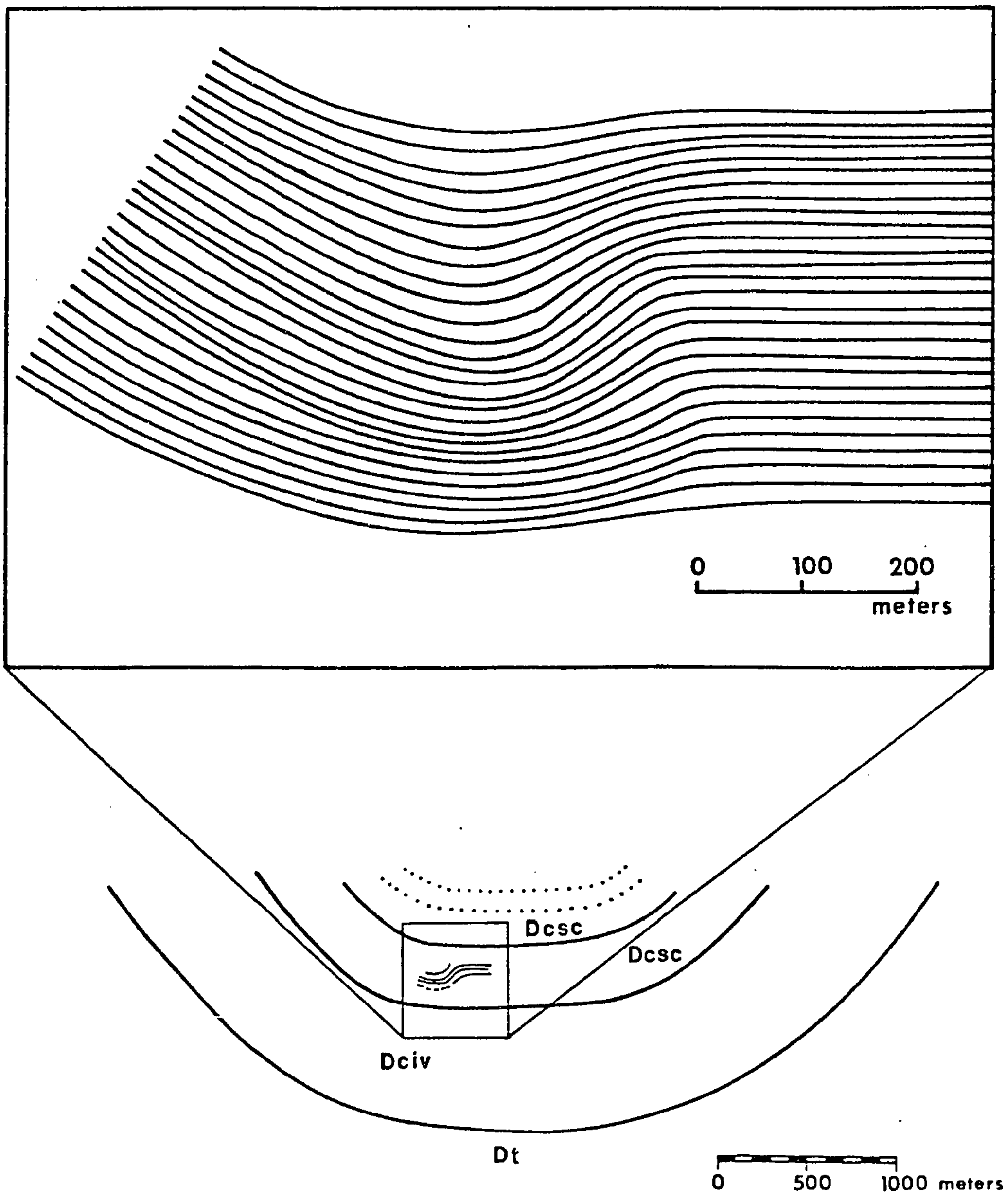

FIGURE 8

STRUCTURAL ANALYSIS OF THE SHIKELLAMY FOLD

Many small structures, including bedding-surface faults, reverse faults, low-angle faults and small asymmetric folds, occur within the Shikellamy fold. They are measured and grouped according to structural setting. The bedding-surface faults and the reverse faults seem to be good indicators of stress orientation during the growth of the Shikellamy fold.

The bedding-surface faults are very common in the steeply dipping layers of the central limb but they are sparse in the northern and southern limbs of the fold. The small and reverse faults occur in the central limb and the low-angle faults occur in the southern limb. The amplitudes of small folds are a few cm and the dip separation of reverse faults is 45 cm or less. The sense of shear of reverse faults is opposite to that of the bedding-surface faults; the sense of reverse faults is left-latral whereas that for bedding-surface faults is right-lateral as viewed in Figure 6.

Bedding-Surface Faults:

Three types of bedding-surface faults can be recognized within the Shikellamy fold; polished fault surfaces without slickenlines or with indistinct slickenlines, polished fault surfaces with distinct slickenlines, and unpolished fault surfaces with distinct fault steps and slickenlines. A total of 60 bedding-surface faults was measured in the three limbs of Shikellamy fold. Of these, 20 have distinct fault steps and 32 have distinct slickenlines. Typical fault steps are 2-10 cm apart, and the step widths range from 1 to 4 cm; 1 cm widths are most common. Step heights are 1 to 5 cm.

The traces of bedding-surface faults and other structures were mapped in detail in part of the central limb of the Shikellamy fold (Fig. 6) because the limb has many bedding-surface faults (80% of the total) and the rocks are well exposed. The spacings of bedding-surface faults define the thicknesses of the structural units, so I measured the spacing of bedding-surface faults and determined the types of faults occuring in the central limb. The results are summarized in Table I. In 32.5 m of the section, 48 bedding-surface faults were recognized in the section of A-A' (Fig. 6), so that the average thickness of structural units is about 0.7 m.

Most of the bedding surface faults contain slickenlines. The azimuths and plunges of the slickenlines, and the average bedding plane orientations for each rock unit in the central limb, are shown via stereonets in Figure 6. Also, a theoretical slickenline, defined as the direction within the bedding that is perpendicular to the fold axis, is shown with an "X" on each stereonet. Figure 6 shows that the actual slickenlines are clustered around the theoretical slickenlines, so that the slickenlines in the central limb of Shikellamy fold are essentially perpendicular to the synclinal axis. Slickenlines perpendicular to fold axes were reported by Nickelsen (1963), Faill (1969, 1973) and Faill and others (1973) for folds elsewhere in the central Appalachians. The sense of slip was deduced using the fault-steps of the bedding-surface faults. The sense of slip is consistently right-lateral as viewed in Figure 6.

Table I: Types and spacing of bedding-surface faults in the central limb of Shikellamy fold (between A-A', Fig. 6)

Unit No.	Rock type	Total thickness of unit (m)	Total number of faults	Average spacing of faults (m)	Maximum spacing of faults (m)	Minimum spacing of faults (m)	Occurrence of fault types		
							A	B	C
62	Siltstone	7.0	12	0.55	2.0	0.15	2	8	2
63	Mudshale	1.5	many tens or hundreds				many		
64	Sandstone	5.0	8	0.70	0.85	0.25		7	1
65	Siltstone	5.5	13	0.45	0.85	0.15	3	6	4
66	Sandstone	7.5	10	0.40	0.50	0.10	2	4	4
67	Sandstone	6.0	5	0.25	0.75	0.20	1	3	1
	TOTAL	32.50	48				8	28	12

Occurrence of fault types:

A) Polished fault surface without slickenlines or with indistinct slickenlines.

B) Polished fault surface with distinct slickenlines.

C) Unpolished fault surface with distinct fault steps and slickenlines.

Some bedding-surface faults were also observed in the northern and southern limbs of the Shikellamy fold. The average spacing of bedding-surface faults is about 2-4 m in the southern limb and about 25 m in the northern limb. Only two bedding-surface faults with fault steps and slickenlines were observed in the northern limb (Fig. 9); according to the steps, the direction of slip is right-lateral. Twelve bedding-surface faults were recognized in the southern limb. Six faults were observed in section B-B', along the railroad cut, but the direction of slickenlines could be determined for only four of the faults (Fig. 9, section B-B'). Six other faults were measured in an exposure 400 m west of the railroad cut, and their locations were projected onto the upper part of the section (Fig. 9). According to the fault steps, the direction of slip is left-lateral, as viewed in Figure 9, on the southern limb of the Shikellamy fold.

Thus, the measurements of bedding-surface faults indicate that the average spacing of the faults is about 2-4 m in the southern limb, 0.7 m in the central limb, and 25 m in the northern limb. The sense of slip is left-lateral in the southern limb and right-lateral in the central and northern limbs. The directions of slip are roughly normal to the fold axes of the Shikellamy fold.

Other Small Faults:

In the southern limb, there are two low-angle faults in siltstone, unit 62. Sense of shear could not be deduced from these faults because the fault surfaces have only slickenlines, not steps, and because the siltstone layers are cross-bedded, so that layering could not be

Figure 9 - Azimuth of slickenlines and direction of slip on average bedding planes within the Shikellamy fold.

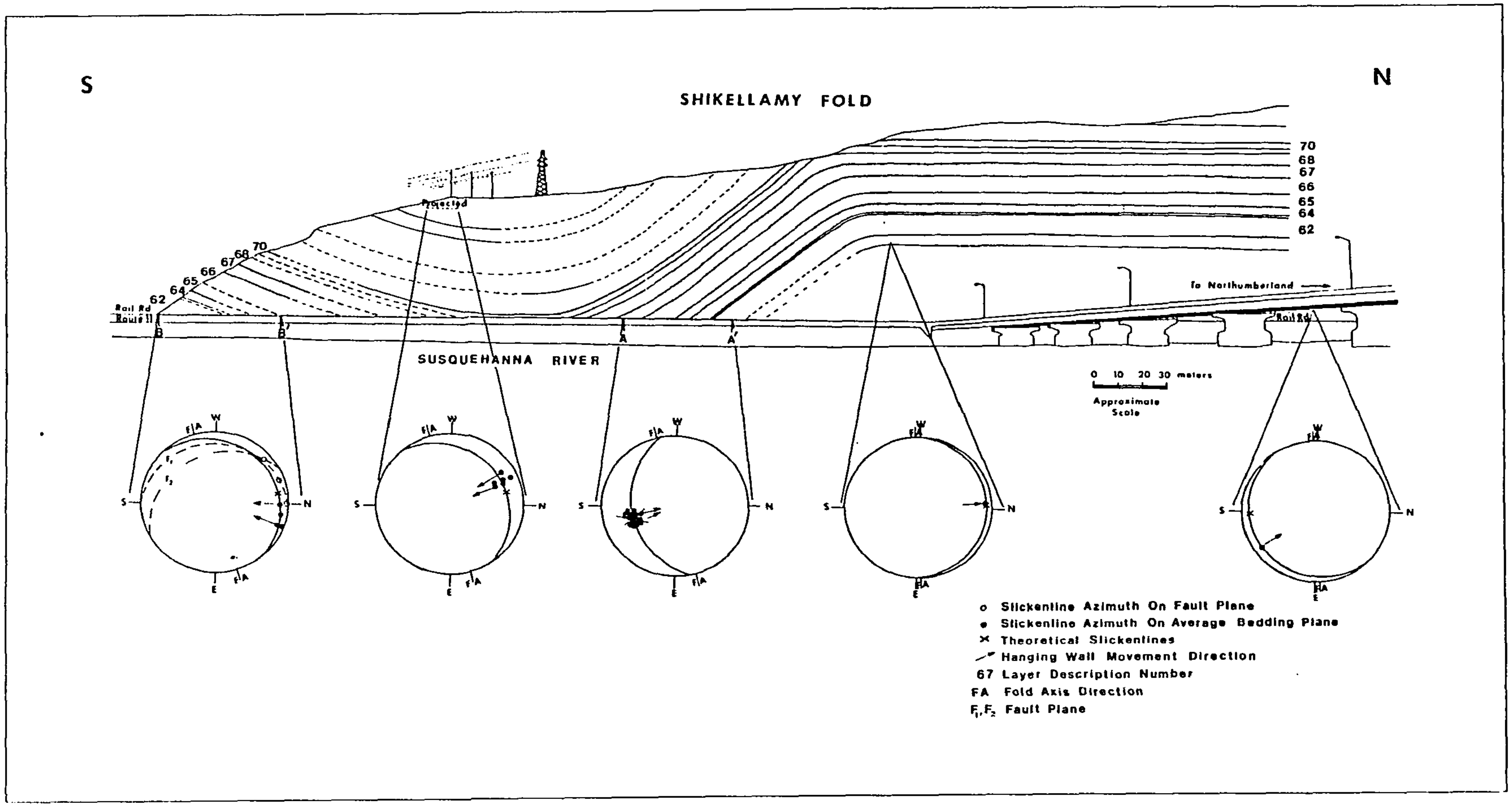
S
N
SHIKELLAMY FOLD
70
68
67
66
65
64
62
Projected
Rail Rd
Route 11
B
B'
A
A'
To Northumberland
Rail Rd
SUSQUEHANNA RIVER
0 10 20 30 meters
Approximate Scale
W
E
S
N
FA
o Slickenline Azimuth On Fault Plane
• Slickenline Azimuth On Average Bedding Plane
× Theoretical Slickenlines
Hanging Wall Movement Direction
67 Layer Description Number
FA Fold Axis Direction
F_1, F_2 Fault Plane

FIGURE 9

matched on either side of the faults. Figure 9, section B-B', shows stereoprojection of these faults. One fault is 14 m long, dips 16° towards the west and strikes N-S (Fig. 9, F1). The fault has two sets of slickenlines on its fault plane; the younger set has a N-S azimuth, and the older one a N 20°W azimuth. The younger set cuts across the older one , suggesting that the fault formed before the Shikellamy fold and that it was reactivated during the growth of the fold. The other fault, in section B-B', (Fig. 9, F2), dips 20° towards the west and strikes N 30° W. This fault has one set of slickenlines, with an azimuth of N 40° W.

Three reverse faults were observed in sandstone layers (units 64, 66) in the central limb of Shikellamy fold; none was observed in the other limbs. A fault in unit 64 (Fig. 6, F) is 1 m long and has 4.5 cm of dip separation. The fault is left-lateral and its attitude is N 68° E, 43°NW. The strike of this fault is subparallel to the Shikellamy synclinal axis. The acute angle between the fault and bedding surfaces is 86°. Two other reverse faults occur in unit 66. One fault (Fig. 6, F1) is 63 cm long and has 5 cm dip separation. Its attitude is N 70°E, 45°NW. The acute angle between the fault and bedding surfaces is 88°, and the strike of this fault is also subparallel to the Shikellamy synclinal axis. The other fault (Fig. 6, F2) is 2.3 m long, has 45 cm of dip separation and has an attitude of N 15° E, 32°NW. The acute angle between the fault and bedding surfaces is 72°. Both faults in unit 66 are left-lateral, as viewed in Figure 6.

The orientation of principal stress directions were estimated by stereoprojection of the three reverse faults and bedding-surface faults in the central limb of Shikellamy fold. The principal stresses are assumed to have been arranged so that the principal stress axes are related to fault planes as shown in Figure 10A. To determine the orientations of the principal stress axes, the attitudes of the reverse and bedding-surface faults and the sense of displacements are plotted on a stereonet as in Fig. 10B, C. and D. The intersection of the two faults is assumed to parallel the intermediate stress (σ_2). The directions of maximum compression (σ_1) and minimum compression (σ_3) are determined by inspection of the sense of displacement and by bisecting angles between the faults. The stereoprojection of one conjugate fault, in unit 64, suggests that the direction of maximum compression axis was 2°/166°, the intermediate compression axis was subhorizontal (8°/257°) and the minimum compression was subvertical (plunge 82°, Fig. 10B). The stereoprojection of the other conjugate faults (unit 66) indicate that σ_1 was 1°/137° and 10°/164°, that σ_2 was 5°/231° and 20°/254° and that σ_3 plunged 80 to 85° respectively (Fig. 10C and D).

Small folds:

Two small asymmetric folds were recognized in sandstone unit 64, in the central limb of Shikellamy fold. They occur along downward and upward projections of the reverse fault in that unit (Fig. 6, F), and the axes of these folds are roughly parallel to the Shikellamy synclinal axis. The axial surfaces of the small folds are inclined steeply towards the north, and their short limbs dip south. They

Figure 10 - A. Orientation of principal stress in idealized conjugate faults.

B. Conjugate faults and orientation of principal stresses in unit 64 in the central limb.

C. and D. Conjugate faults and orientation of principal stresses in unit 66 in the central limb.

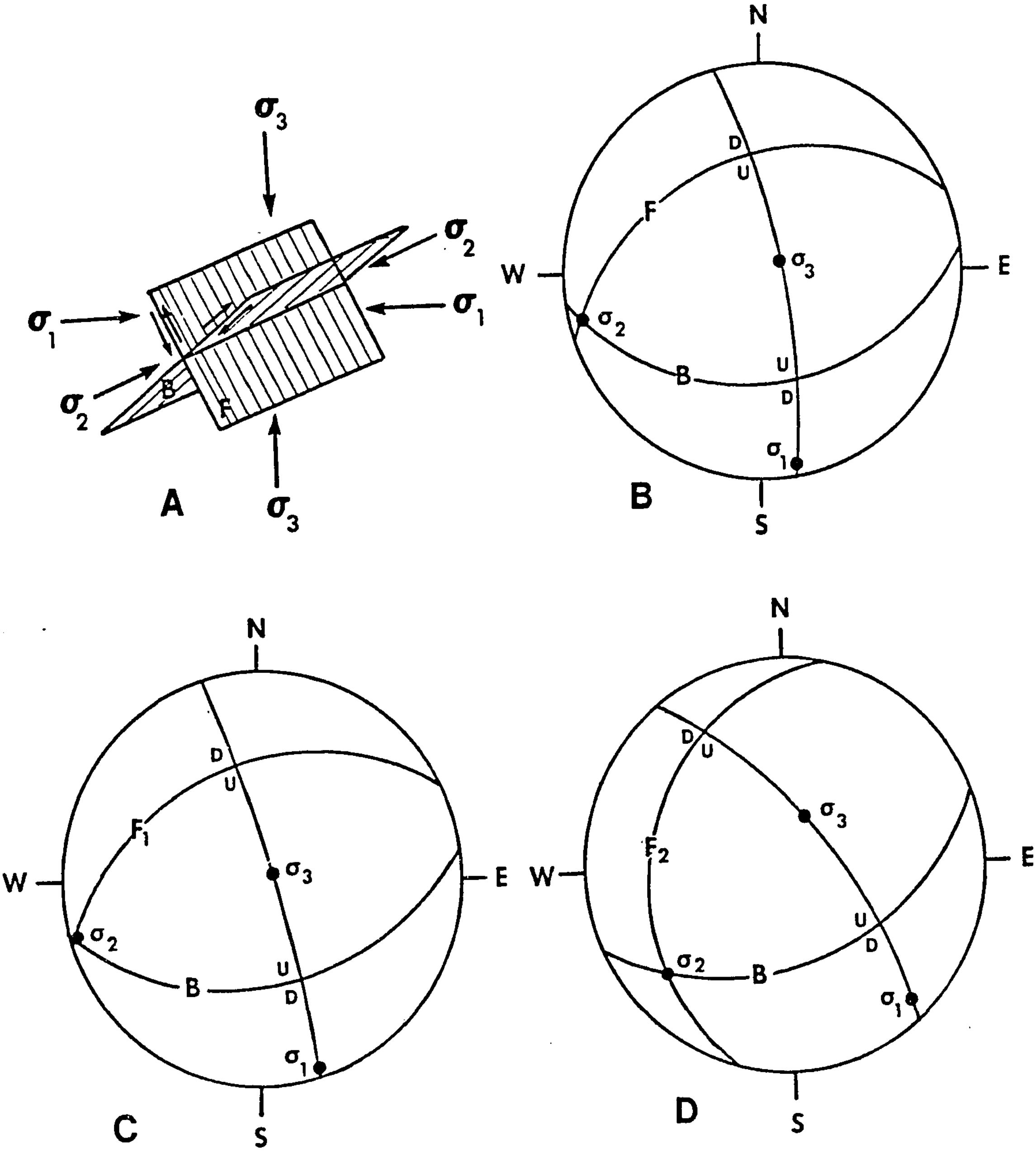

F,F1,F2 : Reverse Faults
B : Bedding-Surface Faults
U : Upthrown Fault Block
D : Downthrown Fault Block

σ_1: Maximum Stress
σ_2: Intermediate Stress
σ_3: Minimum Stress

FIGURE 10

range in amplitude from 2 to 7 cm. These folds resemble small-scale monoclinal kink bands.

SYNTHESIS OF STRUCTURAL INFORMATION AND CONCLUSION

Many asymmetric folds can be classified as either drag folds or kink bands, but the Shikellamy fold does not obviously fit either category. Some features of the fold closely resemble those of a monoclinal kink fold, but, nevertheless, the other features and the structural setting of the fold are atypical of those of minor monoclinal kink folds.

Theoretical, field and experimental studies of monoclinal-kink folding indicate that monoclinal kink bands form in an environment of a combination of layer-parallel shortening and shear, for example, as minor folds on the limb of a major fold, that monoclinal kink bands typically form in groups, and that axial planes of monoclinal kink bands form relative to axial planes of the major folds (Fig. 11). The Shikellamy fold occurs singly in the trough of the Northumberland synclinorium, and there apparently are two axial surfaces within the synclinorium, so the fold is atypical in these respects.

The overall shape of the part of the Shikellamy fold exposed in the railroad cut at Northumberland does resemble that of a kink band; there is a relatively straight, short limb (Fig. 9). Hinges of kink bands may be sharp or open (Honea and Johnson, 1976; Ramberg and Johnson, 1976); the anticlinal hinge of the Shikellamy fold is relatively sharp and similar whereas the synclinal hinge is open and concentric-like, as shown in the isogon pattern in Fig. 7A. Other features of the general shape, however, are atypical of those of kink bands. The structural cross section (Fig. 5A) indicates that the vertical extent of the

Figure 11 - Idealized pattern of asymmetric minor folds that have developed simultaneously on limbs or in hinge areas of major folds.

_a_: traces of axial planes of major folds

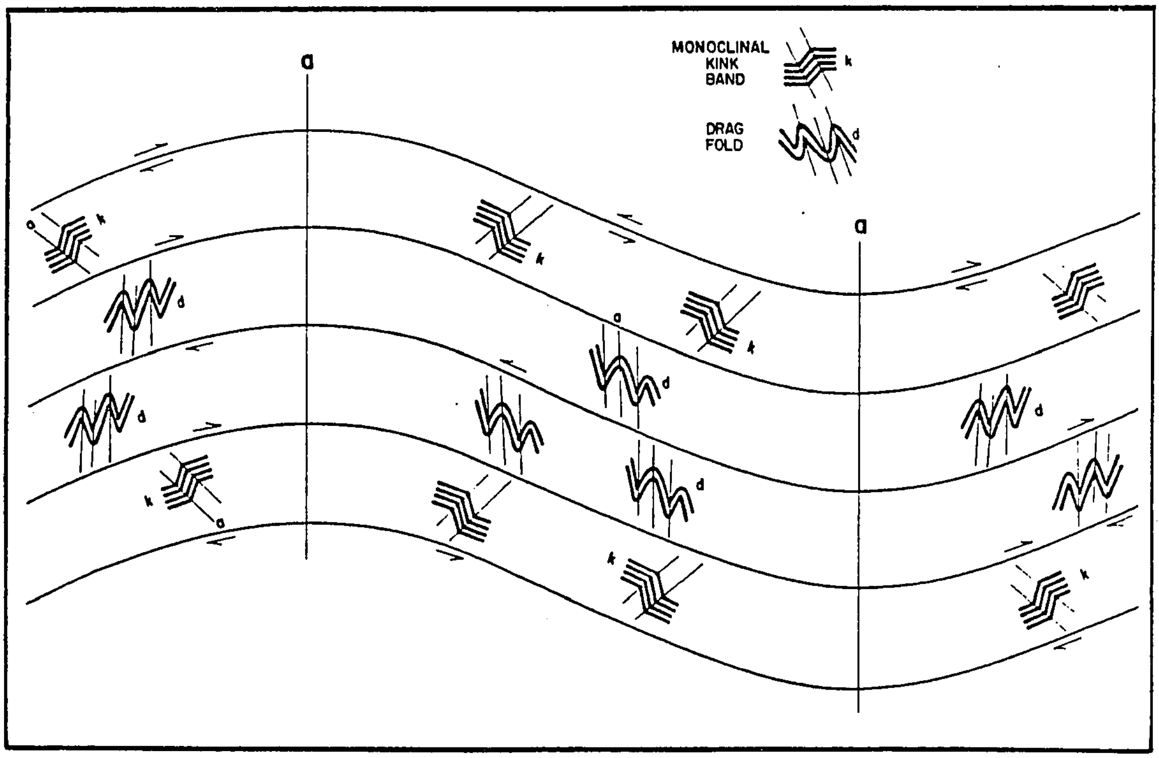

FIGURE 11

Shikellamy fold is relatively small as compared to the width of the fold, as shown in Fig. 8; this form is atypical of kink bands. Thus the overall form of the Shikellamy fold is merely suggestive of a monoclinal kink band; by no means is it conclusive, as indicated by Faill and others (1973, p. 132).

The position of the Shikellamy fold within the Northumberland synclinorium provides ambiguous information about the origin of the fold because the fold occurs in flat layers in the core of the synclinorium, immediately adjacent to the southern limb of the synclinorium. For example, it remains unclear whether the curved, southern limb of the Shikellamy fold reflects the formation of the fold or of the synclinorium (section C-C', Fig. 4; Fig. 5B). Thus the rules of thumb of asymmetric drag folds and monoclinal kink bands in the limbs of major folds (Fig. 11) are not readily applied to the Northumberland syncline and the Shikellamy fold.

The structural analysis provides further information about the type of fold. The interpretation of the structural data is based on mechanical analysis of conditions of kink folding (Honea and Johnson, 1976; Reches and Johnson, 1976; Collier, 1978) and of drag folding (Ramberg, 1963; Ramberg and Johnson, 1976). Drag folds are generally minor folds that have become asymmetric as a result of layer-parallel shear strain. They tend to be repetitious (Figs. 12A3 and 12B3). Further, if the sense of shear deformation relative to layering is right-lateral, the shorter limbs of drag folds face to the right (Fig. 12A3), so that the sense of asymmetry is related in an obvious way to the sense of shear deformation. Monoclinal kink folds, however, have the opposite sense of symmetry

Figure 12 - Relation between orientation of maximum compression, and sense of asymmetry for monoclinal kink bands and drag fold.

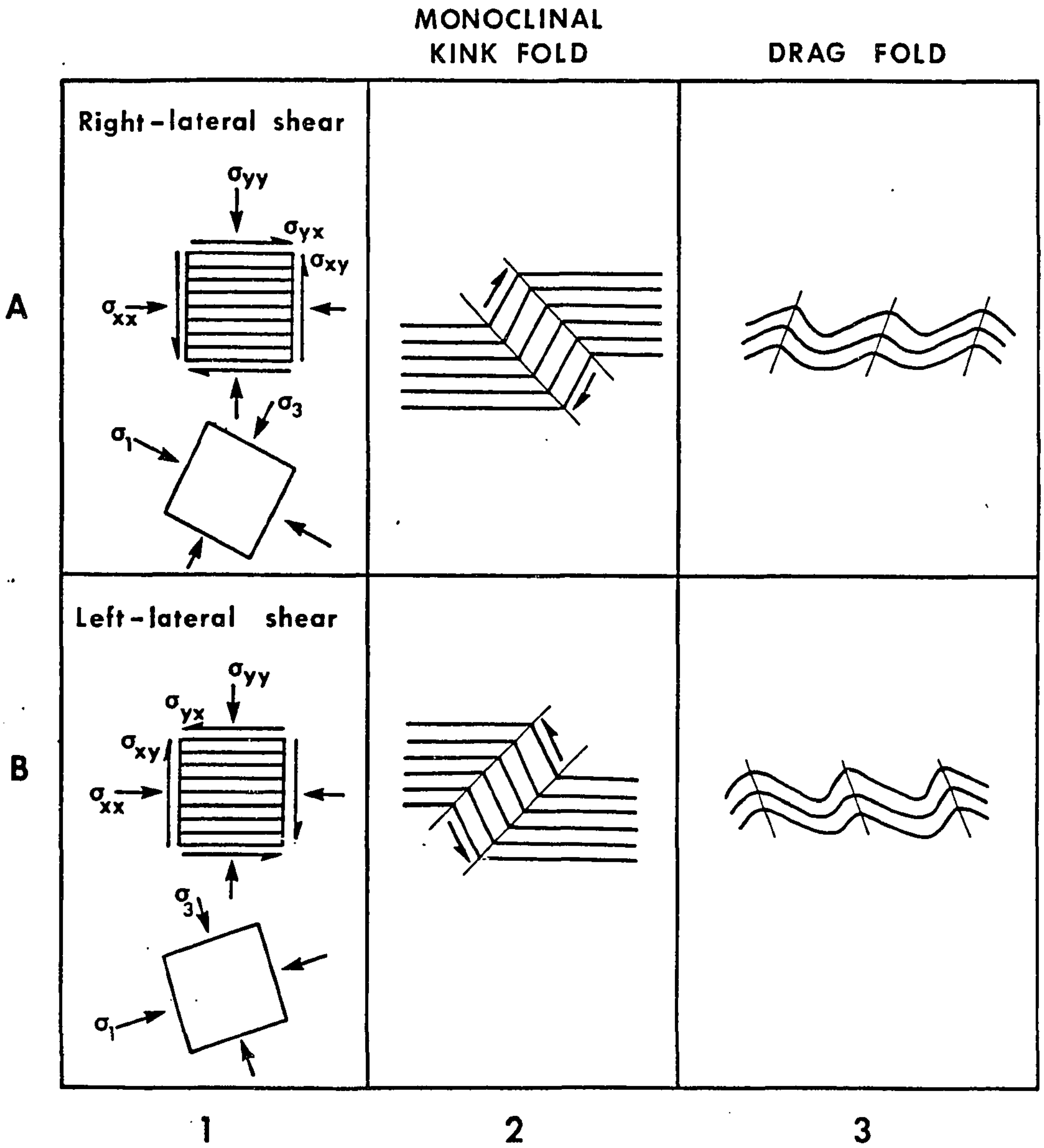
MONOCLINAL
KINK FOLD
DRAG FOLD
Right-lateral shear
σ_{yy}
σ_{yx}
σ_{xy}
σ_{xx}
σ_3
σ_1
A
Left-lateral shear
σ_{yy}
σ_{yx}
σ_{xy}
σ_{xx}
σ_3
σ_1
B
1
2
3

FIGURE 12

(Dewey, 1965; Reches and Johnson, 1976); if the sense of layer-parallel shear stress is right-lateral, the short limbs face left (Fig. 12A2). Monoclinal kink bands form, according to theoretical analysis of idealized multilayers, where there is significant layer-parallel shear stress as well as layer-parallel compression, and where there is significant yield strength of interbeds or of contacts between layers (Honea and Johnson, 1976) or the interbeds have highly nonlinear rheologic behaviors (Pfaff, in preparation). Furthermore, theoretical and experimental studies of kink folding indicate that slip between layers is largely restricted to the short limbs of kink bands (Reches and Johnson, 1976).

. The sense of slip on bedding-surface faults in the central and northern limbs of Shikellamy fold is consistent with the sense of shear stress indicated in Fig. 12A1, and the fold has the sense of asymmetry of the kink band shown in Fig. 12A2. The sense of slip on bedding-surface faults in the southern limb of the Shikellamy fold is opposite, but may well reflect folding of the southern limb of the Northumberland synclinorium rather than folding responsible for the Shikellamy fold.

Analysis of maximum compression directions using three sets of conjugate faults (Fig. 13) suggests that the maximum compression direction was roughly horizontal in the rocks in the central limb of Shikellamy fold. If the principal stresses rotated with the central limb during folding as is typical in multilayers with high contrasts in viscosities, the stress state reflected in the conjugate reverse faults, relative to layering in the central limb of the fold, would have the orientation indicated in Fig. 12A1: that is, would be consistent with

Figure 13 - Relationship among orientation of Shikellamy fold axis and orientation of principal stresses.

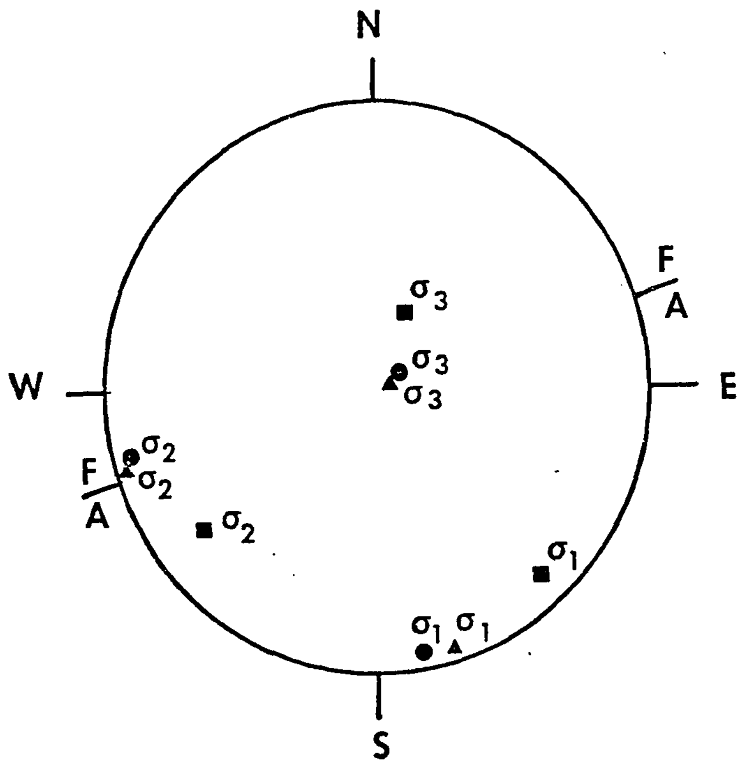

F/A : Synclinal Axis of the Shikellamy Fold

σ_1 : Maximum Stress

σ_2 : Intermediate Stress

σ_3 : Minimum Stress

● For Conjugate Faults in Unit 64

■ , ▲ For Conjugate Faults in Unit 66

FIGURE 13

a kink fold with the sense of symmetry shown in Fig. 12A2.

Thus, several lines of evidence - the monoclinal form, the concentration of slippage in the short central limb, the evidence of right-lateral slip on bedding-surface faults in the northern limb and the orientation of maximum compression directions relative to layering in the central limb - all suggest that the Shikellamy fold is a monoclinal, kink-like fold.

A reason that the origin of the Shikellamy fold has been difficult to interpret may well be related to the empirical observation that the Shikellamy fold is an unusually large kink-like fold for the central Appalachians. A rational explanation for the absence of large kink-like folds may suggest that the Shikellamy fold has a hybrid form, intermediate between those of idealized kink folds and asymmetric chevron folds.

REFERENCES CITED

Anderson, T. B., 1968, The geometry of a natural orthorombic system of kink bands. In: A. J. Baer and D. K. Norris (editors). Reg. in Tect. Geol. Sur. Can. Paper 68-52, p. 200-228.

Anderson, T. B., 1974, The relationship between kink-bands and shear fractures in the experimental deformation of slate. Geol. Soc. Lon., v. 130, p. 367-382.

Biot, M. A., 1965, Theory of similar folding of the first and second kind. Geol. Soc. Am. Bull., 76, p. 251-258.

Collier, M., 1978, Ultimate locking angles for conjugate and mono-clinal kink bands. Tectonophysics, v. 48, p. T1-T6.

Conlin, R. R. and Hoskins, D. M., 1962, Geology and mineral resources of the Mifflintown quadrangle. Penn. Top. and Geol. Sur. Atlas 126, 46 p.

Dewey, J. F., 1965, Nature and origin of kink-bands. Tectonophysics 1, p. 459-494.

Donath, F. A., 1968, Experimental study of kink-band development in Martinsburg slate. In: A. J. Baer and D. K. Norris (editors). Reg. in Tect. Geol. Sur. Can. Paper 68-52, p. 255-288.

Faill, R. T., 1969, Kink band structures in the Valley and Ridge Province, central Pennsylvania: Geol. Soc. Amer. Bull., v. 80, p. 2539-2550.

Faill, R. T., 1973, Kink band folding, Valley and Ridge Province, Pennsylvania: Geol. Soc. Am. Bull., v. 84, p. 1298-1314.

Faill, R. T., Wells, R. B., Nickelsen, R. R., and Hoskins, D. M., 1973, Structure and Silurian-Devonian stratigraphy of the Valley and Ridge province, central Pennsylvania, guide book for the 38th Annual Field conference of Pennsylvania Geologists. Penn. Top. and Geol. Sur., Oct. 5-6, 1973, 168 p.

Faill, R. T. and Wells, R. B., 1977, Bedrock geology and mineral resources of the Linden and Williamsport quadrangles, Lycoming County, Pennsylvania. Penn. Top. and Geol. Sur. Atlas 134ab, 66 p.

Faill, R. T., 1979, Geology and mineral resources of the Montourville South and Muncy quadrangles and part of the Hughesville quadrangle. Penn. Geol. Sur. Atlas 146ab, 114 p.

Gay, N. C. and Weiss, L. E., 1974, The relationship between principal stress directions and the geometry of kinks in foliated rocks. Tectonophysics, v. 21, p. 287-300.

Gray, C., Conlin, R. R., Hoskins, D. M., and Shepps, V. C., 1960, Geologic map of Pennsylvania, 1/250,000. Pennsylvania Topographic and Geologic Survey, 4th series.

Hoskins, D. M., 1976, Geology and mineral resources of the Millersburg 15-minute quadrangle. Penn. Geol. Sur. 4th series, Atlas 146, 38 p.

Honea, E. and Johnson, A. M., 1976, A theory of concentric, kink and sinusoidal folding and of monoclinal flexuring of compressible, elastic multilayers IV. Development of sinusoidal and kink folds in multilayers confined by rigid boundaries. Tectonophysics, v. 30, p. 197-239.

Johnson, A. M. and Pollard, D. D., 1973, Mechanism of growth of some laccolith intrusion in the Henry Mountains, Utah. Field observations, Gilbert's model, physical properties of flow of the magma. Tectonophysics, 18, p. 261-309.

Johnson, A. M. and Ellen, S. D., 1974, A theory of concentric kink and sinusoidal folding and of monoclinal flexuring of compressible, elastic multilayers. I. introduction. Tectonophysics, 21, p. 301-339.

Johnson, A. M. and Honea, E., 1975, A theory of concentric, kink and sinusoidal folding and of monoclinal flexuring of compressible, elastic multilayers. II. Initial stress and nonlinear equations of equilibrium. Tectonophysics, 25, p. 261-280.

Kock, F. G., Johnson, A. M. and Pollard, D. D., 1981, Monoclinal bending of strata over laccolithic intrusions, Tectonophysics, 74. p. T21-T31.

Mackin, J. H., 1950, The down structure method of viewing geologic maps. Jour. Geol. v. 58, p. 55-72.

Nickelsen, R. P., 1963, Fold patterns and continuous deformation mechanisms of the central Pennsylvania folded Appalachians. In: Guidebook to tectonics and Cambrian-Ordovician stratigraphy in the central Appalachians of Pennsylvania. Pittsburg Geol. Soc. and Appalachian Geol. Soc., p. 13-30.

Pfaff, V., Small scale kink-band near Montgomery Ferry along Juniata River in Pennsylvania (in preparation).

Patterson, M. S. and Weiss, L. E., 1966, Experimental deformation and folding in phyllite. Geol. Soc. Amer. Bull., v. 77, p. 343-374.

Ragan, D. M., 1973, Structural Geology, 2nd edition, John Wiley and Sons, N.Y., 208 p.

Ramberg, H., 1963, Evolution of drag folds. Geol. Mag. v. 100, p. 97-106.

Ramberg, I. B. and Johnson, A. M., 1976, A theory of concentric, kink, and sinusoidal folding and of monoclinal flexuring of compressible elastic multilayer. Part V., Asymmetric folding in interbedded chert and shale of the Franciscan Complex, San Francisco Bay area, California. Tectonophysics, v. 32, p. 295-320.

Ramsay, J. G., 1962, The geometry of conjugate fold system. Geol. Mag., v. 99, p. 517-526.

Ramsay, J. G., 1967, Folding and fracturing of rocks: New York, McGraw Hill Book Company, 568 p.

Reches, Z., and Johnson, A. M., 1976, A theory of concentric, kink, and sinusoidal folding and of monoclinal flexuring of compressible elastic multilayers. Part VI. Asymmetric folding and unidirectional kinking: Tectonophysics, v. 35, p. 295-334.

Reches, Z., 1977, The development of monoclines, Ph.D. Dissertation. Stanford University, 234 p.

Turner, F. J., 1964, Analysis of kinks in micas of an Innsbruck mica schist. Neues Jahrbuch fur mineralogie, 1964, p. 347-356.

Weiss, L. E., 1980, Nucleation of growth of kink bands. Tectonophysics, v. 65, p. 1-38.

APPENDIX I

SUMMARY OF FIRST AND SECOND-ORDER FOLDING THEORY AND ANALYSIS OF PREFERRED WAVELENGTHS.

INTRODUCTION

The purposes of this appendix are to summarize first- and second-order folding theories, to translate three computer programs (Appendix II, III and IV) from FOCAL to BASIC language, developed by Johnson (unpublished programs, 1981, 1982a and 1982b) for computing wavelengths and fold forms for complex multilayers, and to explain how the programs work.

The computer programs can be used on most microcomputers, with only minor modifications. The programs require about 16kb of memory available to BASIC language. The central goal of this appendix is to present programs in a form that will allow a structural geologist, with even minor experience in the use of microcomputers, to simulate the growth of folds in multilayers composed of layers with different viscosities and thicknesses, including the interaction caused by the simultaneous growth of folds with two different wavelengths. The objective is to make some of the powerful techniques of theoretical fold analysis available to structural geologists who wish to use the techniques but who are uninterested in becoming immersed in the complexities of folding theory.

The first program (Appendix II) computes amplitudes of waveforms to first-order accuracy (maximum slope angle of about 10 degrees), and the program is designed to determine one or more preferred wavelengths for complex viscous multilayers. The second program (Appendix III) computes amplitudes of waveforms to second-order accuracy (maximum slope angle of about 25 degrees). It is designed to determine forms of folds to finite, but small amplitudes, in multilayers for which thee is a single preferred wavelength. The third program (Appendix IV) is for determining fold forms where there are two preferred wavelengths growing simultaneously and interacting. This program assumes two wavelengths but four other waveforms grow spontaneously as a result of interaction of the first two waveforms.

FIRST-ORDER ANALYSIS OF PREFERED WAVELENGTHS

The computer program I will first discuss calculates the preferred wavelength for a multilayer, that is, the wavelength of the perturbation that becomes amplified the most during shortening of the multilayer. The preferred wavelength is a function of the amount of shortening, the number of layers and the viscosities and thicknesses of individual layers composing the multilayer. The computer program calculates the amplifications of perturbations in all the interfaces for each wavelength selected, and one can determine the preferred wavelength by plotting, the relation between amplification and wavelength.

In following paragraphs the essential equations of folding theory, accurate to first-order in the maximum slopes of interfaces, will be presented so that the equations used in the computer program can be understood. If one is interested solely in the program, one can turn immediately to page 141.

Summary of Theoretical Analysis

In the analysis of folding, the components of stress and velocity are separated into mean values and perturbed values. The mean values of stress and velocity are those that solve the problem describing the uniform deformation of a layer or stack of layers with planar interfaces. The mean values are exact. The perturbed stresses and velocities are the values that must be added to the mean values in order to describe stresses and velocities in a layer or stack of layers that have wavy interfaces. The perturbed values are exact only if the boundary conditions are satisfied exactly, and the order of approximation of a solution reflects the extent to which the boundary conditions are satisfied exactly. The mean values are uniform whereas the perturbed values are nonuniform--they vary from place to place and time to time within a layer. The components of velocity and stess for a point within a deforming layer are sums of the mean (bar over symbol) and perturbed (tilda over symbol) values:

$$v_x = \bar{v}_x + \tilde{v}_x \tag{1a}$$

$$v_z = \bar{v}_z + \tilde{v}_z \tag{1b}$$

$$\sigma_{xx} = \bar{\sigma}_{xx} + \tilde{\sigma}_{xx} \tag{1c}$$

$$\sigma_{zz} = \bar{\sigma}_{zz} + \tilde{\sigma}_{zz} \tag{1d}$$

$$\sigma_{xz} = \bar{\sigma}_{xz} + \tilde{\sigma}_{xz} \tag{1e}$$

The mean stresses and mean velocities are given by the relations

$$\bar{\sigma}_{xx} = 2\mu\bar{D}_{xx} - \bar{p} \tag{2a}$$

$$\bar{\sigma}_{zz} = 2\mu\bar{D}_{zz} - \bar{p} \tag{2b}$$

$$\bar{\sigma}_{xz} = 0 \tag{2c}$$

$$\bar{v}_x = \bar{D}_{xx}x \tag{2d}$$

$$v_z = \bar{D}_{zz} z \tag{2e}$$

$$\bar{p} = -(\bar{\sigma}_{xx} + \bar{\sigma}_{zz})/2 \tag{2f}$$

The mean shear stress is zero for the problems treated here. In these equations $\bar{p}$ is the mean pressure and μ is the coefficient of viscosity. We are dealing with plane strain.

For a layer, the perturbed velocities and stresses are (e.g., Johnson and Fletcher, 1982):

$$\tilde{v}_x = -[(a+b(\ell z)+d)S+(b+c+d(\ell z))C]\sin(\ell x) \tag{3a}$$

$$\tilde{v}_z = [(a+b(\ell z))C+(c+d(\ell z))S]\cos(\ell x) \tag{3b}$$

$$\tilde{\sigma}_{xx} = -2\mu\ell[(a+b(\ell z)+2d)S+(c+d(\ell z)+2b)C]\cos(\ell x)-\tilde{p}_o \tag{3c}$$

$$\tilde{\sigma}_{zz} = 2\mu\ell[(a+b(\ell z))S+(c+d(\ell z))C]\cos(\ell x)-\tilde{p}_o \tag{3d}$$

$$\tilde{\sigma}_{xz} = -2\mu\ell[(a+b(\ell z)+d)C+(c+b+d(\ell z))S]\sin(\ell x) \tag{3e}$$

where; $S=\sinh(\ell z)$; $C=\cosh(\ell z)$

In which $\underline{a}$, $\underline{b}$, $\underline{c}$ and $\underline{d}$ are arbitrary constants, ℓ is wave number, $\ell=2\pi/L$ and $\underline{L}$ is wavelength. Equations (3) are valid to first-order in the maximum slopes of interfaces. The meaning of first-order will become clear when we discuss boundary conditions, in following paragraphs.

The arbitrary constants are eliminated by means of boundary conditions at interfaces between layers. Fig.1 shows part of an interface and relations between normal, n and tangential, s components of velocity and the x- and z-components of velocity. The normal velocity is,

$$v_n = [v_z]_\zeta \cos\theta - [v_x]_\zeta \sin\theta \tag{4}$$

where ζ is the height of the interface. For a cosinusoidal interface,

$$\zeta_{t,b} = \pm T/2 + A_{t,b}\cos(\ell x) \tag{5}$$

in which T is thickness of a layer and t and b refer to top and bottom of a layer. Also,

$$\sin\theta = (\partial\zeta/\partial x)/[1+(\partial\zeta/\partial x)^2]^{1/2} \tag{6a}$$

$$\cos\theta = 1/[1+(\partial\zeta/\partial x)^2]^{1/2} \tag{6b}$$

The slope of an interface is,

$$(\partial\zeta/\partial x) = -A\ell\sin(\ell x)$$

which has a maximum value of $(A\ell)$. To first-order in the maximum slope eqs. (6) become,

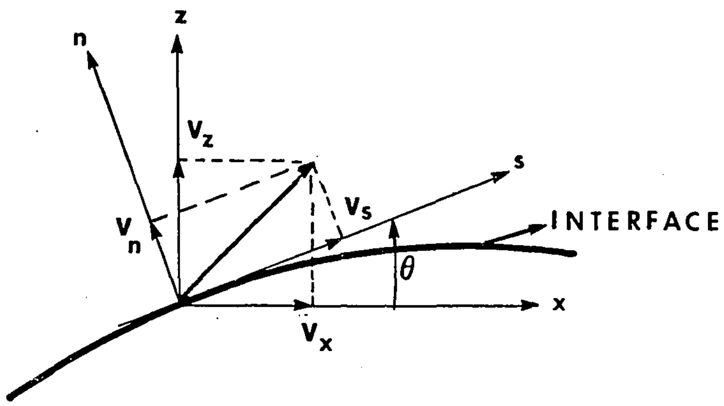

FIGURE 1

Boundary velocities at the contact between two layers with initial deflection. The slope angle of the interface is locally θ , the angle between the x-direction and the s-direction. The velocities acting on the surface can be expressed in terms of a horizontal velocity, $\underline{v}_s$, and a normal velocity, $\underline{v}_n$, which are parallel to local coordinates n and s.

$\cos\theta = 1$; $\sin\theta = (\partial\zeta/\partial x)$

so that the interface stresses and velocities become,

$$\sigma_{nn} = \bar{\sigma}_{zz} + [\tilde{\sigma}_{zz}]_\zeta \tag{7a}$$

$$\sigma_{ns} = (\bar{\sigma}_{zz} - \bar{\sigma}_{xx})(\partial\zeta/\partial x) + [\tilde{\sigma}_{xz}]_\zeta \tag{7b}$$

$$v_n = [\bar{v}_z + \tilde{v}_z]_\zeta - [\bar{v}_x]_\zeta(\partial\zeta/\partial x) \tag{7c}$$

$$v_n = [\bar{v}_z + \tilde{v}_z]_\zeta - [\bar{v}_x]_\zeta(\partial\zeta/\partial x)$$

$$v_s = [\bar{v}_x + \tilde{v}_x]_\zeta + [\bar{v}_z]_\zeta(\partial\zeta/\partial x) \tag{7d}$$

For folding problems where there is free slip between layers, one must match normal stress, σ_{nn}, and normal velocity, $\underline{v}_n$, across interfaces between adjacent layers. For such problems the shear stress, σ_{ns} , parallel to interface is zero. Furthermore, by using a method introduced by Johnson and Fletcher (1982), one can replace the four arbitrary constants, $\underline{a}$, $\underline{b}$, $\underline{c}$ and $\underline{d}$, with two new constants which markedly simplifies the solution for constants. By this method one expresses the normal stresses in terms of a constant (σ_0) value and a value that varies cosinusoidally with $\underline{x}$ with a constant coefficient σ :

$$(\sigma_{nn})_{t,b} = \sigma_0 + (\sigma_{t,b})\cos(\ell x) \tag{8}$$

Solving eqs. (3), (8), (7a) and (7b) for constants $\underline{a}$, $\underline{b}$, $\underline{c}$ and $\underline{d}$

in terms of σ_t and σ_b one derives (Johnson and Fletcher, 1982):

$$[v_x]_{\zeta_{t,b}} = -(1/2)[\{(\lambda_t-\lambda_b)C^2-(\Lambda_t+\Lambda_b)k\}/(SC+k)$$

$$\pm\{(\lambda_t+\lambda_b)S^2+(\Lambda_t-\Lambda_b)k\}/(SC-k)]\sin(\ell x)+\bar{D}_{xx}x \qquad (9a)$$

$$[v_z]_{\zeta_{t,b}} = (1/2)[\{(\Lambda_t-\Lambda_b)C^2+(\lambda_t+\lambda_b)k\}/(SC-k)$$

$$\pm\{(\Lambda_t+\Lambda_b)S^2-(\lambda_t-\lambda_b)k\}/(SC+k)]\cos(\ell x)$$

$$\pm\bar{D}_{xx}(T/2)-\bar{D}_{xx}A_{t,b}\cos(\ell x)+(\bar{v}_z)_o \qquad (9b)$$

in which $k=\pi T/L$; $S=\sinh(k)$; $C=\cosh(k)$

$(\bar{v}_z)_o$ is a constant mean velocity used to match boundary conditions between layers and

$$\Lambda_{t,b}=(\sigma_{t,b})/2\mu\ell \qquad (9c)$$

$$\lambda_{t,b}=-4\mu\bar{D}_{xx}(A_{t,b}\ell)/2\mu\ell \qquad (9d)$$

Thus the normal velocities at the two interfaces of a layer are:

$$(v_n)_{t,b}=(1/2)[\{(\Lambda_t-\Lambda_b)C^2+(\lambda_t+\lambda_b)k\}/(SC-k)\pm\{(\Lambda_t+\Lambda_b)S^2$$

$$-(\lambda_t-\lambda_b)k\}/(SC+k)]\cos(\ell x)\pm\bar{D}_{xx}(T/2)-\bar{D}_{xx}A_{t,b}\cos(\ell x)+(\bar{v}_z)_o$$

$$+\bar{D}_{xx}x\,A_{t,b}\ell\sin(\ell x) \qquad (10)$$

In solving for the constant, the normal velocities for adjacent layers are equated at each interface, and the coefficients of σ_t and σ_b form the matrix which is solved in the computer program. There are two constants for each layer, but one of the constants for a layer is equal to one of the constants for the overlying layer and the other constant for the layer is equal to one of the constants for the underlying layer. Therefore, one need solve for only $\underline{N}_c$ constants, where $N_c = N_L - 1$, and $\underline{N}_L$ is the number of layers in the multilayer stack. For example, $N_L=7$ for the multilayer shown in Fig.2, so that $N_c=6$.

The position of an interface as a function of time is determined by subsituting the expressions for the velocities into the interface equation (e.g., Fletcher, 1977). Maintaining terms to first-order in the maximum slope of an interface, the interface equation is

$$(\partial\zeta/\partial t) = [\bar{v}_z + \tilde{v}_z]_\zeta - [\bar{v}_x]_\zeta\ (\partial\zeta/\partial x) \tag{11}$$

Subsituting eqs. (5) and (9) into eq. (11), bearing in mind that $\underline{I}$, $\underline{L}$ and $\underline{A}$ are all functions of time, we derive,

$$\begin{aligned} dA_{t,b}/dt = {} & (1/2)[\{(\Lambda_t - \Lambda_b)C^2 + (\lambda_t + \lambda_b)k\}/(SC-k)] \\ & \pm(1/2)[\{(\Lambda_t+\Lambda_b)S^2-(\lambda_t-\lambda_b)k\}/(SC+k)] \end{aligned} \tag{12}$$

Thus, one uses eq. (10) to determine the constants σ_t and σ_b for each layer by solving a set of simultaneous equations and then uses these values in eq. (12) in order to incrementally integrate to obtain values

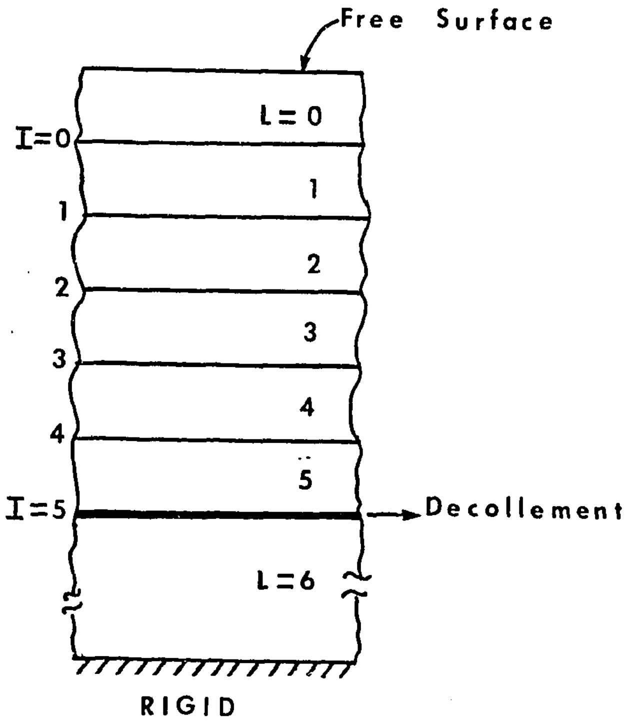

FIGURE 2

A sample multilayer used in computer programs, showing layers (L), interfaces (I) and a decollement.

for the amplitudes of cosinusoidal perturbations of interfaces. By repeating the approximate integrations for a series of time steps, one calculates the final amplitudes after a certain time, <u>t</u>. Instead of integrating with respect to time, the computer program integrates with respect to stretch, using the identity,

$$dA/(\bar{D}_{xx}dt) = \bar{S}_x(dA/d\bar{S}_x) \qquad (13)$$

where $\bar{S}_x$ is the mean horizontal stretch, which is related to the thickening, $\bar{S}_x = T_o/T = 1/\bar{S}_z$. T_o is original and T is final thickness.

<u>Computer Program for Calculating Preferred Wavelengths of Folds in Complex Multilayers</u>:

The computer program (Johnson, 1981, unpublished program) that calculates preferred wavelength of folds in complex multilayers is given in Appendix II. It is written in the Microsoft BASIC language so that it can operate on many microcomputers with moderate memory. The multilayer assumed by the program is shown in Fig.2. The multilayer contains two special layers and one special boundary. The layer at the top of the multilayer stack has a stree-free surface, and the surface remains undeflected. That surface simulates conditions where there is erosion and deposition that maintain a flat surface as the folds grow. The lowest layer in the multilayer stack stress free, so that its upper surface simulates a decollement. Its lower surface rest against a rigid boundary, so that the lower surface never deflects. There may be as many layers between special layers as one chooses and as one's computer can handle. Our Digital Corporation, Rainbow computer has about 19kb of memory free for BASIC programing, and it can handle at least 20 layers.

The special layers at the top and bottom of the multilayer stack do not seriously restrict the use of the program. For example, one can use the top layer to simulate a very thick medium merely by making that layer thick relative to the wavelength of folds considered. In general, the top layer behaves essentially as an infinitely thick medium if its thickness is greater than the wavelength of folding. Similarly, if one wishes to simulate a very thick substratum, one merely makes the next to last layer very thick; then the unstressed layer below the decollement plays no role in the folding.

A flow chart for the computer program is presented in Fig.3. Information about the thicknesses and viscosities of layers and the total number of layers are put into a subroutine within the program, so the data must be changed for each multilayer. However, it would be simple to change the program so that the computer asks the operator for this information, by using an INPUT statement. It should be noted that one enters the <u>final</u> thicknesses of layers, and that the computer calculates the initial thicknesses by using the value of stretch entered into the computer at an appropriate time. It should also be noted that all lengths are scaled by the computer. The scaling factor is the final thickness of layer 1. The viscosities of layers are scaled with the viscosity of layer 1.

The computer asks for the number of integration steps that are to be used in approximately integrating the equations for the amplitudes of interfaces. The larger the number of integration steps, the more accura-

Figure 3- Flow chart diagram for the first-order analysis of preferred wavelengths.

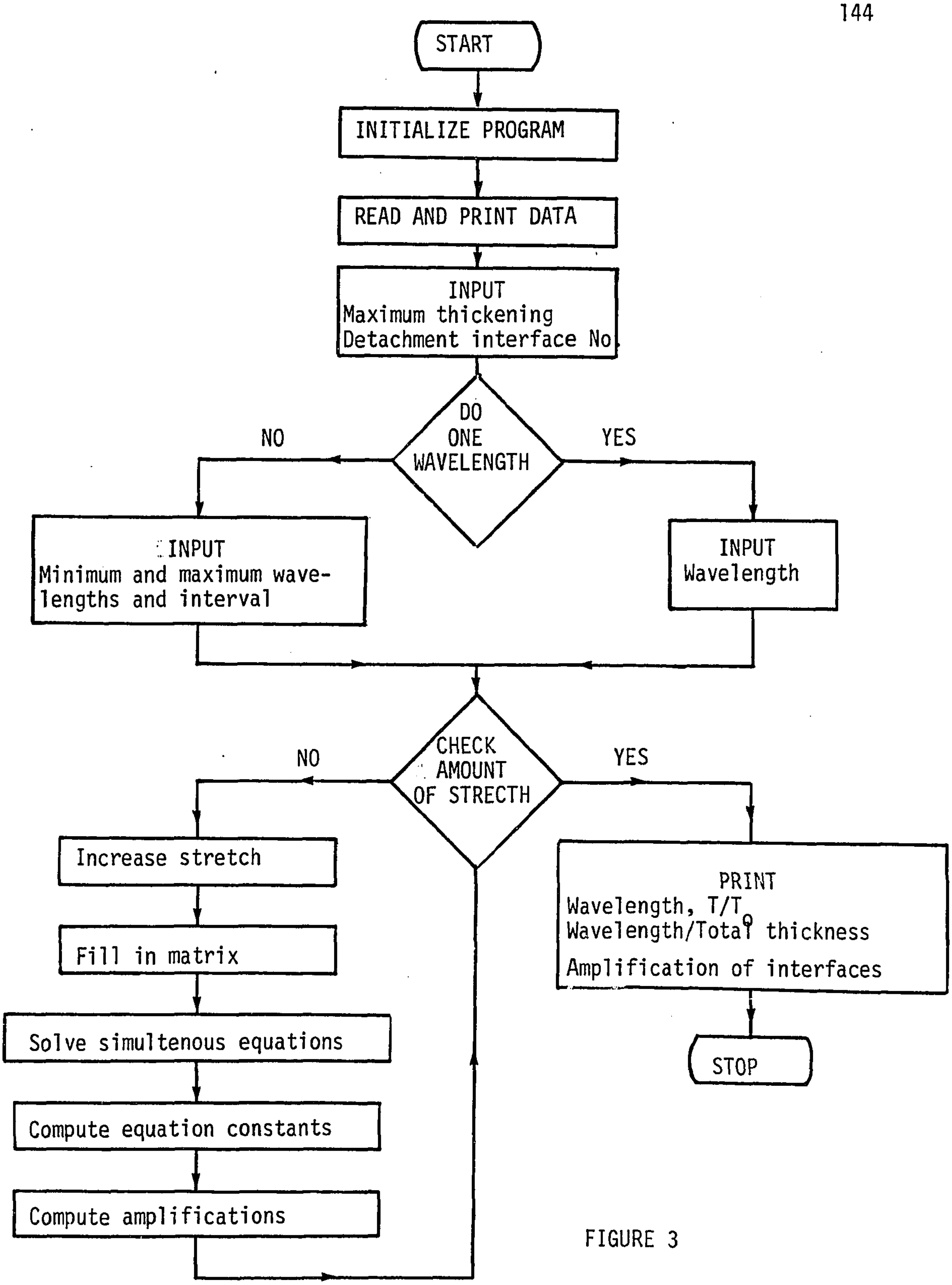
START
INITIALIZE PROGRAM
READ AND PRINT DATA
INPUT
Maximum thickening
Detachment interface No.
DO ONE WAVELENGTH
NO
YES
INPUT
Minimum and maximum wavelengths and interval
INPUT
Wavelength
CHECK AMOUNT OF STRECTH
NO
YES
Increase stretch
Fill in matrix
Solve simultenous equations
Compute equation constants
Compute amplifications
PRINT
Wavelength, T/T0
Wavelength/Total thickness
Amplification of interfaces
STOP

FIGURE 3

te will be the amplitudes; however, ten to twenty steps generally are sufficient.

A sample output of the computer program for a single multilayer is shown in Table I. The multilayer consists of five layers, one thin stiff layer and four, thick and soft layers. The layers were shortened 9.1 percent ($T/T_0=1.1$). The detachment surface was located at the interface 3. The shortening was accomplished in ten equal steps, the results of which are displayed on the computer monitor, but not on the printer. The printer displays only the final results, which are the amplification of first interface (l=0), between layers zero and one, was about 1.102 for a wavelength-to-thickness ratio of 0.2. The computations were done for seven different wavelength-to-thickness ratios, ranging from 0.2 to 0.8. The results show that the preferred wavelength is between 15.5 and 18.6 (in same units as the thickness of layers).

Application to Simple Multilayers:

Preferred wavelengths have been determined for single-layer folds of viscous (Fletcher, 1977; Johnson and Fletcher, 1982) and of power-law materials (Fletcher, 1974), but only dominant wavelengths have been determined previously for multilayers (Ramberg, 1962,1964; Biot, 1964). Thus I have used the computer program to solve a series of simple multilayers for preferred wavelengths. The examples are shown in Figs.4 through 9.

The first three (Fig. 4 to 6) are composed of identical layers, but the layers are confined by media with different viscosities. Figure 4 is for soft medium, Fig.5 is for medium-stiff media and Fig.6 is for very stiff media. The diagrams indicate that the amplifications of folds are

TABLE I

INTERFACE NO	LAY NO	MU(L)/MU(0)	T(L)/T(0)	T(L)
	0	1	1	10
0				
	1	1	1	10
1				
	2	100	0.1	1
2				
	3	1	1	10
3				
	4	1	1	10

DETACHMENT IS AT INTERFACE NO: 3

FINAL TOTAL THICKNESS OF MULTILAYER ABOVE THE DETACHMENT SURFACE IS: 31

WAVELENGTH 6.2

T/TO 1.1

WAVELENGTH/TOTAL THICKNESS 0.2

INTERFACE NO:	0	1	2	3
AMPLIFICATION:	1.102	3.052	3.052	1.002

WAVELENGTH 9.3

T/TO 1.1

WAVELENGTH/TOTAL THICKNESS 0.3

INTERFACE NO:	0	1	2	3
AMPLIFICATION:	1.174	6.166	6.166	1.071

WAVELENGTH 12.4

T/TO 1.1

WAVELENGTH/TOTAL THICKNESS 0.4

INTERFACE NO:	0	1	2	3
AMPLIFICATION:	1.058	8.883	8.883	1.392

TABLE I continued

WAVELENGTH	15.5			
T/TO	1.1			
WAVELENGTH/TOTAL THICKNESS	0.5			
INTERFACE NO:	0	1	2	3
AMPLIFICATION:	2.085	9.790	9.790	1.930

WAVELENGTH	18.6			
T/TO	1.1			
WAVELENGTH/TOTAL THICKNESS	0.6			
INTERFACE NO:	0	1	2	3
AMPLIFICATION:	2.709	9.554	9.554	2.460

WAVELENGTH	21.7			
T/TO	1.1			
WAVELENGTH/TOTAL THICKNESS	0.7			
INTERFACE NO:	0	1	2	3
AMPLIFICATION:	3.290	9.005	9.005	2.873

WAVELENGTH	24.8			
T/TO	1.1			
WAVELENGTH/TOTAL THICKNESS	0.8			
INTERFACE NO:	0	1	2	3
AMPLIFICATION:	3.818	8.483	8.483	3.168

Figure 4- Relations among ratio of wavelength-to-thickness, L/T, and amplification, A/A_o, of the fifth interface of a multilayer.

T: Total thickness of a multilayer

I: Interface number.

μ_L: Viscosity of layer.

μ_m: Viscosity of medium.

T/T_o: Final thickness-to-inital thickness.

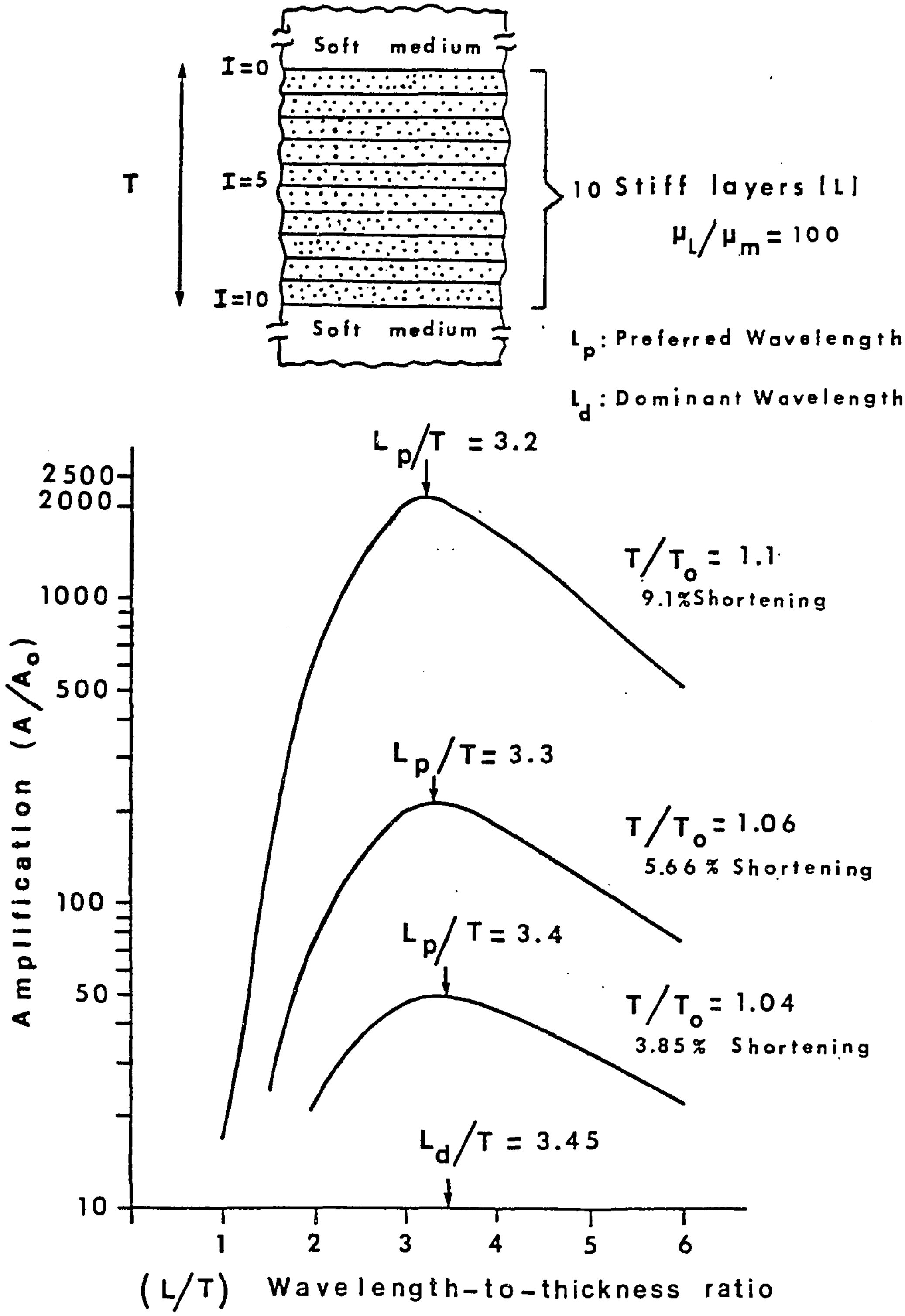
Soft medium
I=0
T
I=5
I=10
Soft medium
10 Stiff layers [L]
$\mu_L/\mu_m = 100$
L_p: Preferred Wavelength
L_d: Dominant Wavelength
$L_p/T = 3.2$
$T/T_o = 1.1$
9.1%Shortening
$L_p/T = 3.3$
$T/T_o = 1.06$
5.66 % Shortening
$L_p/T = 3.4$
$T/T_o = 1.04$
3.85 % Shortening
$L_d/T = 3.45$
2500
2000
1000
500
100
50
10
Amplification (A/A_o)
1
2
3
4
5
6
(L/T) Wavelength-to-thickness ratio

FIGURE 4

Figure 5- Relations among ratio of wavelength-to-thickness and amplification of the fifth interface of a soft layer confined by soft medium.

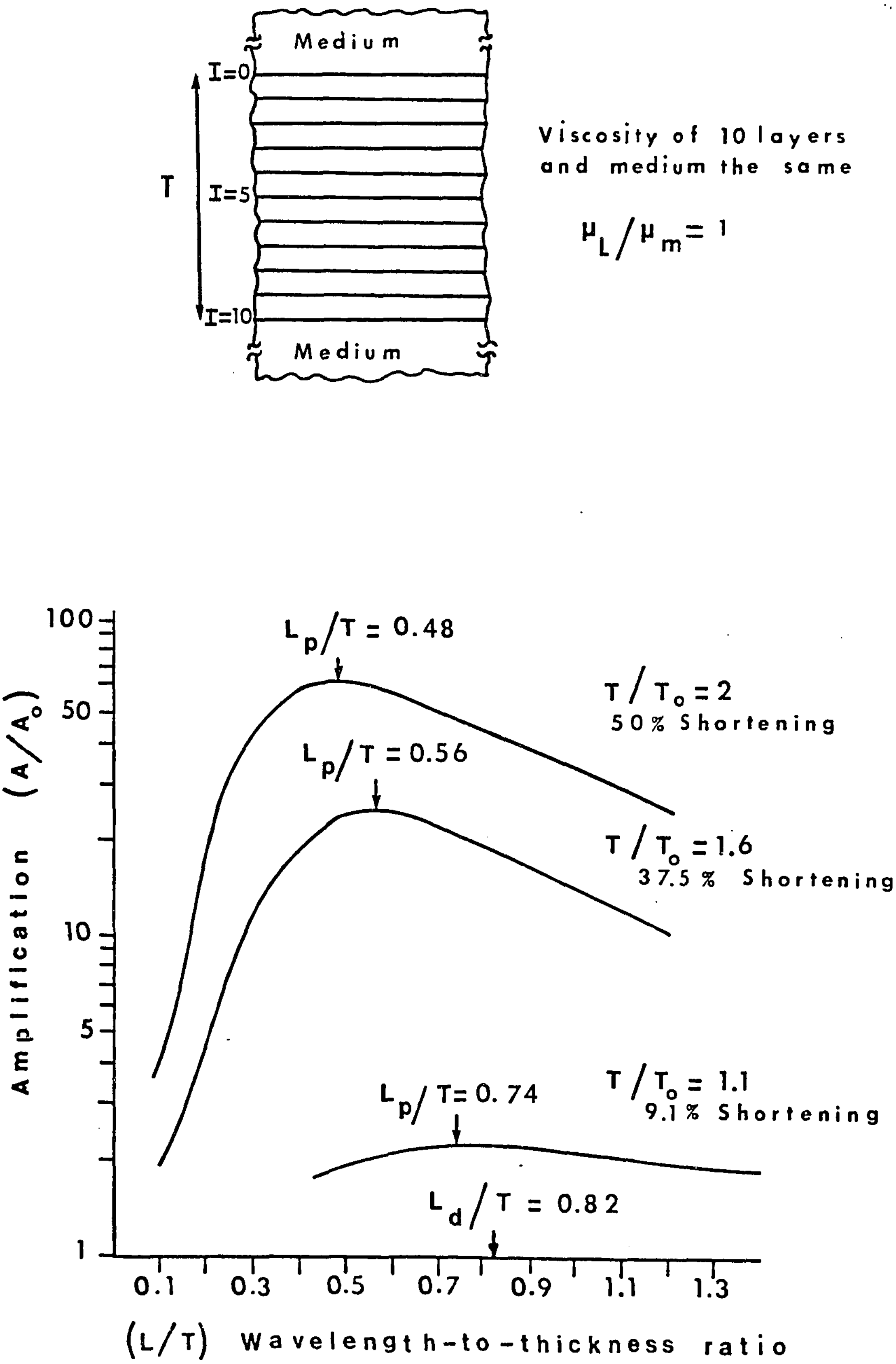
Medium
I=0
T
I=5
I=10
Medium
Viscosity of 10 layers and medium the same
$\mu_L/\mu_m = 1$
100
50
10
5
1
Amplification (A/A$_o$)
$L_p/T = 0.48$
$T/T_o = 2$
50% Shortening
$L_p/T = 0.56$
$T/T_o = 1.6$
37.5 % Shortening
$L_p/T = 0.74$
$T/T_o = 1.1$
9.1 % Shortening
$L_d/T = 0.82$
0.1
0.3
0.5
0.7
0.9
1.1
1.3
(L/T) Wavelength-to-thickness ratio

FIGURE 5

Figure 6- Relations among ratio of wavelength-to-thickness and amplification of the fifth interface where soft layers confined by stiff media.

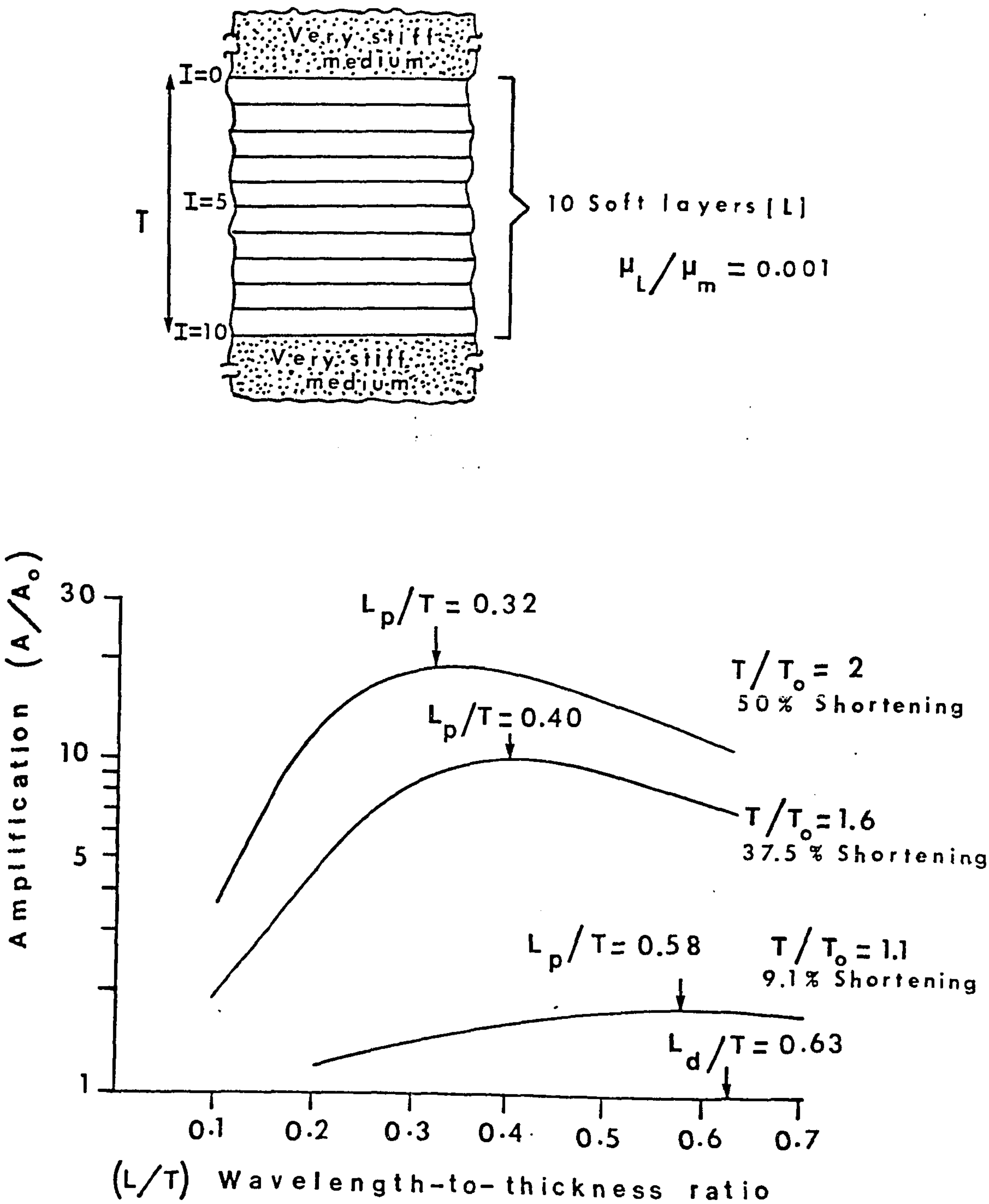

Very stiff medium
I=0
I=5
T
I=10
10 Soft layers [L]
$\mu_L / \mu_m = 0.001$
Very stiff medium
Amplification (A/A$_o$)
30
10
5
1
$L_p/T = 0.32$
$T/T_o = 2$
50% Shortening
$L_p/T = 0.40$
$T/T_o = 1.6$
37.5 % Shortening
$L_p/T = 0.58$
$T/T_o = 1.1$
9.1% Shortening
$L_d/T = 0.63$
0.1
0.2
0.3
0.4
0.5
0.6
0.7
(L/T) Wavelength-to-thickness ratio

FIGURE 6

much higher for soft (Fig.4) than for stiff (Figs. 5 or 6) media. The amplification for the interfaces at middepth (I=5) is about 2000 for soft media, and about 2 for medium stiff or very stiff media, if the multilayers is subjected to a shortening of 9.1 percent (thickening, T/T_0, of 1.1). Furthermore, the preferred wavelengths are much larger for soft than for stiff media. For a shortening of 9.1 percent (T/T_0= 1.1), the preferred wavelength ratio (L_p/T) is about 3.2 for soft media, 0.74 for medium-stiff media and 0.58 for very stiff media.

The multilayer shown in Fig.7 consists of interbedded stiff and soft layers and is confined by very stiff media. Comparison with Fig.6, which is for identical layers, indicates that the amplifications and wavelength ratios are much higher where there are interbedded stiff and soft layers.

Ramberg and Stromgard (1971) have shown that more than one dominant wavelength can develop in complex multilayers. Figures 8 and 9 show that two distinct peaks in the relation between amplification and wavelength ratio can occur in multilayer consisting of groups of thin and thick layers, so that, for such multilayers, there can be folds with two preferred wavelengths developing simultaneously. For example, where there are five thin, stiff layers below and two thick stiff layers above, separated by a thick, soft layer, a preferred wavelength ratio of L_p/T= 0.98 develops in interfaces between the thin layers and a preferred wavelength ratio of about 4.3 develops in all the interfaces (Fig.8). The top of the multilayer stack is a stress-free, flat surface whereas the multilayer is underlain by a thick, soft medium. Two distinct preferred wavelengths also develop in the multilayer shown in Fig.9, where the thin, stiff

Figure 7- Relation among ratio of wavelength-to-thickness and amplification of the interface of the interbedded stiff and soft layers confined by very stiff media.

μ_1: Viscosity of a stiff layer.

μ_2: Viscosity of a soft layer.

μ_m: Viscosity of a medium.

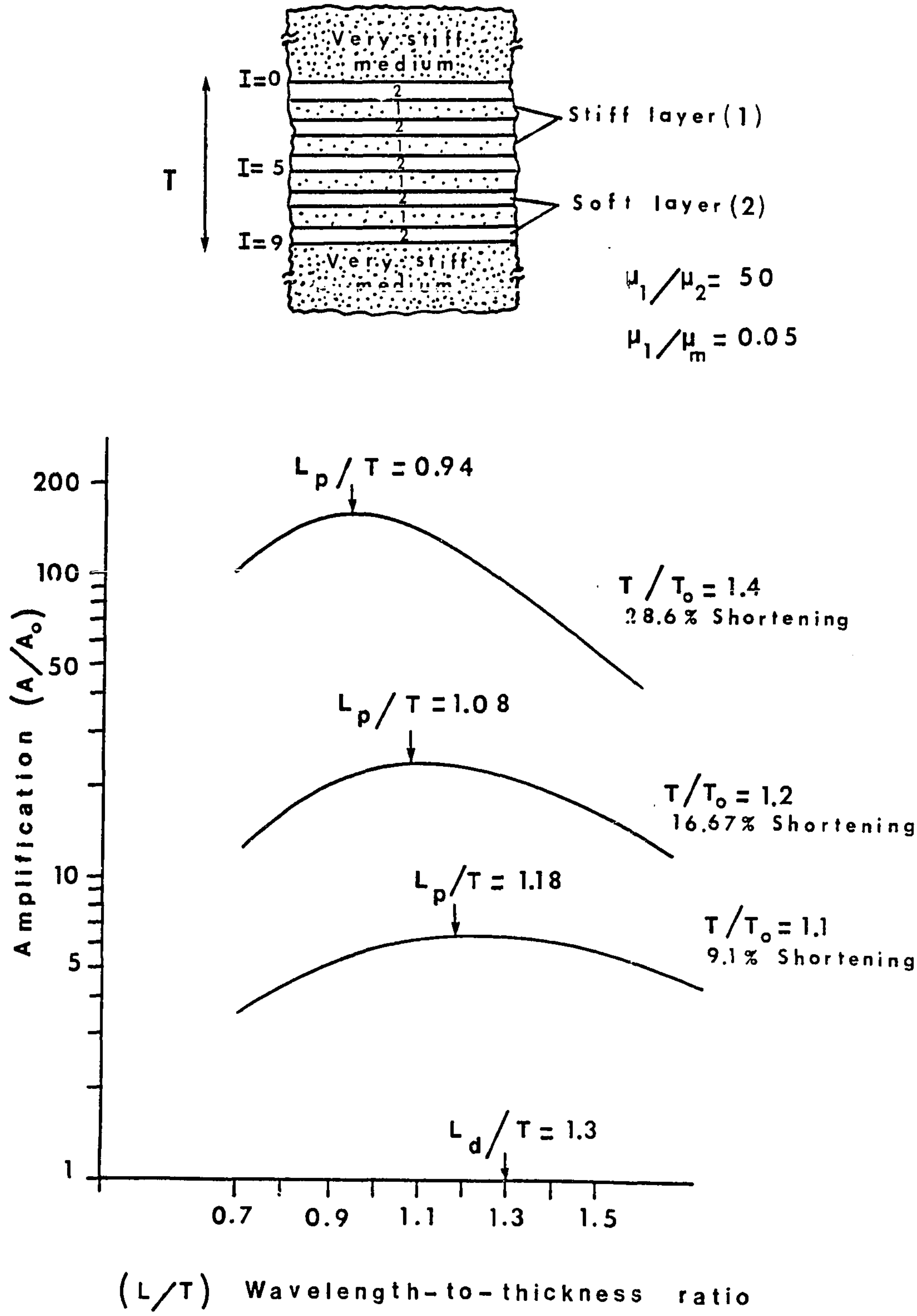
Very stiff medium
I=0
I= 5
I=9
T
Stiff layer(1)
Soft layer(2)
Very stiff medium
$\mu_1/\mu_2 = 50$
$\mu_1/\mu_m = 0.05$
$L_p/T = 0.94$
$T/T_o = 1.4$
28.6 % Shortening
$L_p/T = 1.08$
$T/T_o = 1.2$
16.67% Shortening
$L_p/T = 1.18$
$T/T_o = 1.1$
9.1 % Shortening
$L_d/T = 1.3$
Amplification (A/A_o)
200
100
50
10
5
1
0.7
0.9
1.1
1.3
1.5
(L/T) Wavelength-to-thickness ratio

FIGURE 7

Figure 8- Relations among ratio of wavelength-to-thickness and amplification of all interfaces within a multilayer.

I: Interface number.

μ: Viscosity.

t: Thickness of a thick layer.

t_1:Thickness of a thin layer.

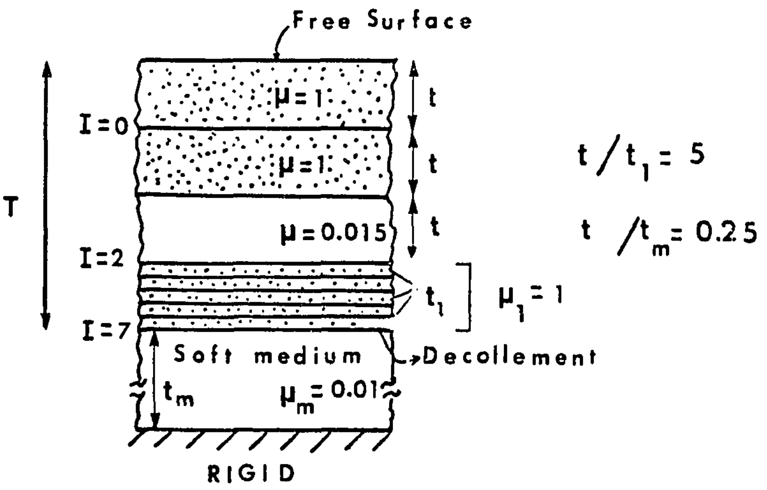
Free Surface
I=0
μ=1
μ=1
t
t
t
T
μ=0.015
I=2
I=7
t_1
μ_1 = 1
Soft medium
Decollement
t_m
μ_m = 0.01
RIGID
t/t_1 = 5
t/t_m = 0.25

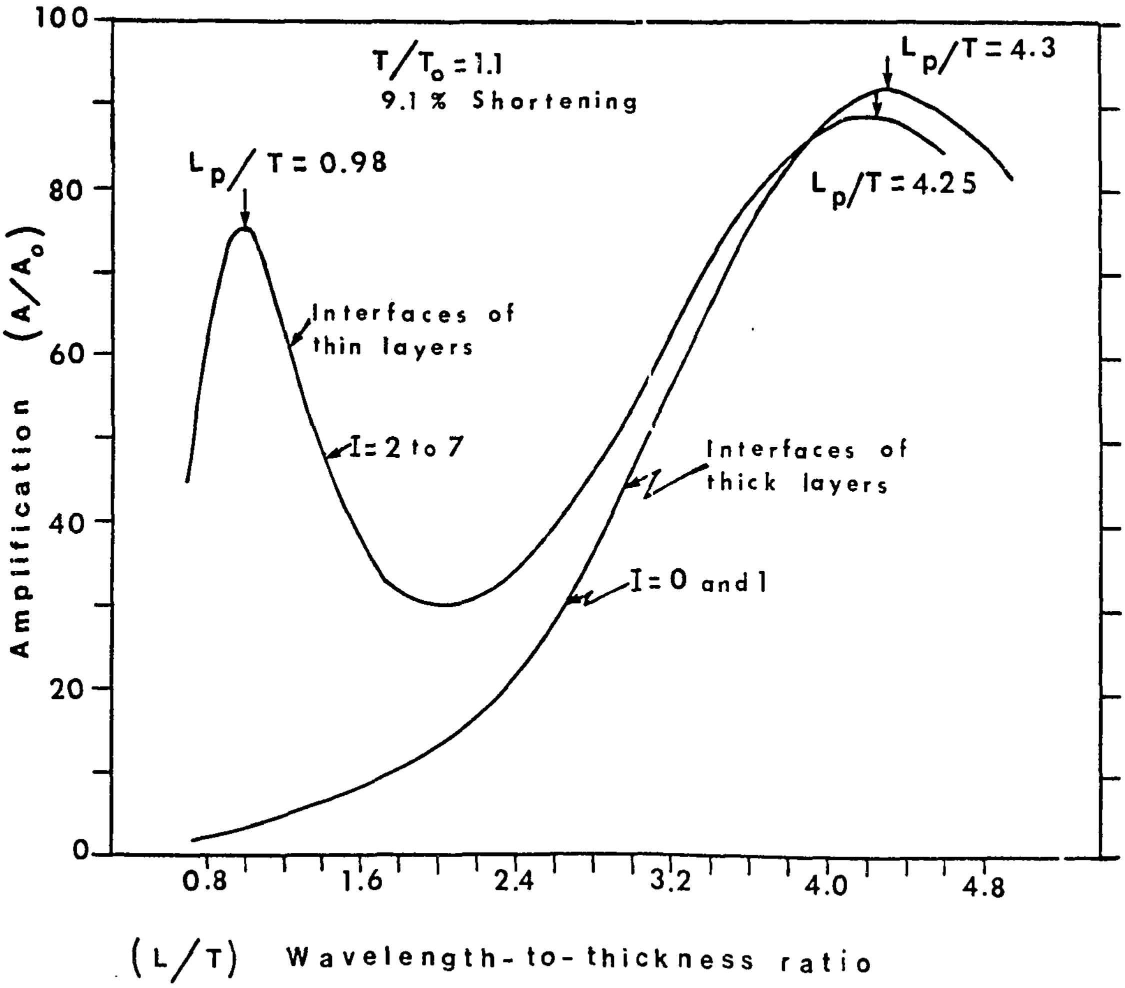
100
80
60
40
20
0
T/T_o = 1.1
9.1 % Shortening
L_p/T = 0.98
L_p/T = 4.3
L_p/T = 4.25
Interfaces of thin layers
I= 2 to 7
Interfaces of thick layers
I= 0 and 1
Amplification (A/A_o)
0.8
1.6
2.4
3.2
4.0
4.8
(L/T) Wavelength-to-thickness ratio

FIGURE 8

Figure 9- Relations among ratio of wavelength-to-thickness and amplification of all interfaces within a multilayer.

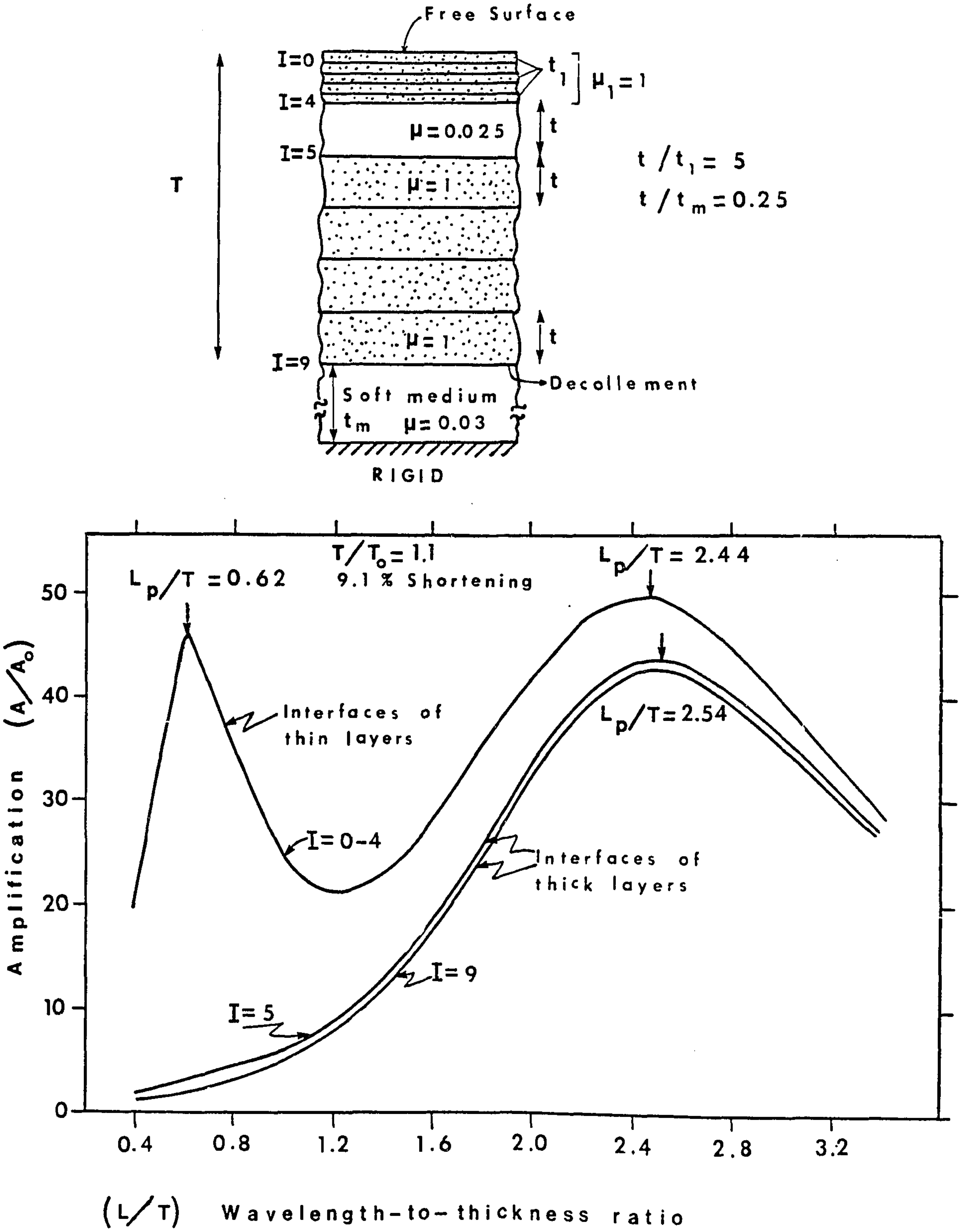
Free Surface
I=0
I=4
I=5
I=9
T
t_1
$\mu_1 = 1$
$\mu = 0.025$
t
$\mu = 1$
$t/t_1 = 5$
$t/t_m = 0.25$
Decollement
Soft medium
t_m $\mu = 0.03$
RIGID
$T/T_o = 1.1$
9.1 % Shortening
$L_p/T = 0.62$
$L_p/T = 2.44$
$L_p/T = 2.54$
Interfaces of thin layers
I= 0-4
Interfaces of thick layers
I= 9
I= 5
Amplification (A/A_o)
50
40
30
20
10
0
0.4
0.8
1.2
1.6
2.0
2.4
2.8
3.2
(L/T) Wavelength-to-thickness ratio

FIGURE 9

layers are below. Folds with a small preferred wavelength ratio of 6.2 form in interfaces between thin layers whereas folds with a greater preferred wavelength ratio of about 2.4 to 2.5 form in all the interfaces (Fig.9).

SECOND-ORDER ANALYSIS OF FOLD FORM (SINGLE WAVELENGTH)

The first-order analysis of folding used to compute preferred wavelengths is valid only for low slopes of interfaces and it provides only crude estimates of fold shapes. For example, according to the first-order analysis of the folding of a single layer in soft media, the interfaces are simple sine curves; the fold shape is similar. In multilayer, also, the shapes of interfaces are sinusoidal in a first-order analysis.

A method of analyzing folding for higher slopes was introduced by Fletcher (1979), who showed that, to second-order in the maximum slopes of interfaces, a single layer in soft media assumes a concentric-like form. Second-order analyses of multilayer folding have been performed by Johnson and Fletcher (1982) and third-order by Pfaff (in preperation).

Here I will present the basic equations for second-order analysis of multilayer folding (Johnson and Fletcher, 1982) and a computer program (Johnson, 1982a, unpublished program) that calculates the amplitudes of waveforms in interfaces as well as final shapes of interfaces.

Summary of Theoretical Analysis:

In the second-order analysis an interface, initially deflected in a cosinusoidal waveform, becomes deflected into a shape descibed by two cosinusoidal waveforms. If the wavelength of the initial perturbation is L, the wavelength of the second perturbation is $L/2$, and the second perturbation develops spontaneously. Thus the shape of the interface changes from that described in eq.(5) to the shape described by:

$$\zeta_{t,b} = \pm T/2 + A_{t,b}\cos(\ell x) + {}^2A_{t,b}\cos(2\ell x) \tag{14}$$

in which $\underline{A}$ is the amplitude of the first waveform and ${}^2\underline{A}$ is the amplitude of the second waveform.

To second-order in the maximum slopes of interfaces, the boundary stresses and the normal velocity are:

$$\sigma_{nn} = \bar{\sigma}_{zz} + [\tilde{\sigma}_{zz}]_\zeta - (\bar{\sigma}_{zz} - \bar{\sigma}_{xx})(\partial\zeta/\partial x)^2 - 2[\tilde{\sigma}_{xz}]_\zeta (\partial\zeta/\partial x)$$

$$\sigma_{nn} = \bar{\sigma}_{zz} + [\tilde{\sigma}_{zz}]_\zeta - (\bar{\sigma}_{zz} - \bar{\sigma}_{xx})(\partial\zeta/\partial x)^2 - 2[\tilde{\sigma}_{xz}]_\zeta (\partial\zeta/\partial x) \tag{15a}$$

$$\sigma_{ns} = [\tilde{\sigma}_{xz}]_\zeta + (\bar{\sigma}_{zz} - \bar{\sigma}_{xx})(\partial\zeta/\partial x) + [\tilde{\sigma}_{zz} - \tilde{\sigma}_{xx}]_\zeta (\partial\zeta/\partial x) \tag{15b}$$

$$v_n = [\bar{v}_z]_\zeta [1 - (\partial\zeta/\partial x)^2/2] - \bar{v}_x (\partial\zeta/\partial x) + [\tilde{v}_z]_\zeta - [\tilde{v}_x]_\zeta (\partial\zeta/\partial x) \tag{15c}$$

in the second-order analysis, quantities such as $(A\ell)$ and $(A\ell)^2$ are significant, but quantities such as $({}^2A\ell)^2$ and $(A\ell)({}^2A\ell)$ are insignificant, so that the analysis is valid to second-order in the maximum slope of the first waveform but to only first-order in the maximum slope of the second waveform.

As in the first-order analysis, one writes boundary normal stresses in terms of constants and trigonometric functions, and the constants are defined by the relation,

$$(\sigma_{nn})_{t,b} = \sigma_o + \sigma_{t,b}\cos(\ell x) + {}^2\sigma_{t,b}\cos(2\ell x) \tag{16}$$

For the second-order analysis, the equation for the normal velocities at layer interfaces is (Johnson and Fletcher, 1982)

$$[v_n]_{\zeta_{t,b}}=[\bar{v}_z]_\zeta[1-(\partial\zeta/\partial x)^2/2]-\bar{v}_x(\partial\zeta/\partial x)+(1/2)[\{(\Lambda_t-\Lambda_b)C^2$$
$$+(\lambda_t+\lambda_b)k\}/(SC-k)\pm\ \{(\Lambda_t+\Lambda_b)S^2-(\lambda_t-\lambda_b)k\}/(SC+k)]\cos(\ell x)$$
$$+(1/2)[\{((^2\Lambda_t)-(^2\Lambda_b))(^2C^2)+((^2\lambda_t)+(^2\lambda_b))2k\}/\{(^2S)(^2C)-2k\}$$
$$\pm((^2\Lambda_t)+(^2\Lambda_b))(^2S^2)-((^2\lambda_t)-(^2\lambda_b))2k\}/\{(^2S)(^2C)+2k\}]\cos(2\ell x)$$
$$+[(\pm a\pm d+kb)S+(c+b\pm kd)C](A_{t,b}\ell)\cos(2\ell x) \tag{17}$$

in which constants a, b, c and d are:

$$a=(1/2)[(\Lambda_t-\Lambda_b)(C+kS)+(\lambda_t+\lambda_b)kC]/(SC-k) \tag{18a}$$

$$b=-(1/2)[(\Lambda_t+\Lambda_b)S+(\lambda_t-\lambda_b)C]/(SC+k) \tag{18b}$$

$$c=(1/2)[(\Lambda_t+\Lambda_b)(S+kC)+(\lambda_t-\lambda_b)kS]/(SC+k) \tag{18c}$$

$$d=-(1/2)[(\Lambda_t-\Lambda_b)C+(\lambda_t+\lambda_b)S]/(SC-k) \tag{18d}$$

Constants Λ and λ are defined in eqs.(9c) and (9d) and constants $^2\Lambda$ and $^2\lambda$ are defined by

$$^2\Lambda_{t,b}=[^2\sigma_{t,b}+2\mu\bar{D}_{xx}(A_{t,b}\ell)^2-3\mu\ell\{(a+d\pm kb)C+(\pm c\pm b+kd)S\}(A_{t,b}\ell)]/4\mu\ell \tag{19a}$$

$$^2\lambda_{t,b}=[-8\mu\bar{D}_{xx}(^2A_{t,b}\ell)+\mu\ell\{(\pm 3a\pm 4d+3kb)S+(3c+4b\pm 3kd)C\}(A_{t,b}\ell)]/4\mu\ell \tag{19b}$$

One first equates the normal velocities at interfaces and solves for the first-order constants σ_t and σ_b. Then one uses the values of those constants to solve for the constants, ${}^2\sigma_t$ and ${}^2\sigma_b$, of the second waveform.

Finally, in order to compute amplitides of the first and second waveforms, one numerically integrate the following equations (Johnson and Fletcher, 1982),

$$dA_{t,b}/d\bar{S}_x=(1/\bar{S}_x)[(1/2)[\{(\Lambda_t-\Lambda_b)C^2+(\lambda_t+\lambda_b)k\}/(SC-k)$$

$$\pm\{(\Lambda_t+\Lambda_b)S^2-(\lambda_t-\lambda_b)k\}/(SC+k)]] \tag{20a}$$

$$d({}^2A_{t,b})/d\bar{S}_x=(1/\bar{S}_x)[(1/2)[\{(({}^2\Lambda_t)-({}^2\Lambda_b))({}^2C^2)+(({}^2\lambda_t)+({}^2\lambda_b))2k\}/$$

$$\{({}^2S)({}^2C)-2k\}\pm(({}^2\Lambda_t)+({}^2\Lambda_b))({}^2S^2)-(({}^2\lambda_t)-({}^2\lambda_b))2k\}/$$

$$\{({}^2S)({}^2C)+2k\}]] \tag{20b}$$

<u>Computer Program for Calculating Fold Forms</u>:

The computer program, written in Microsoft BASIC, is in Appendix III. The configuration of the multilayer and the boundary conditions are the same as those for the first-order analysis and are shown in Fig.2. A flow chart for the program is presented in Fig.10.

Figure 10- Flow chart diagram for the second-order analysis where there is one preferred wavelength.

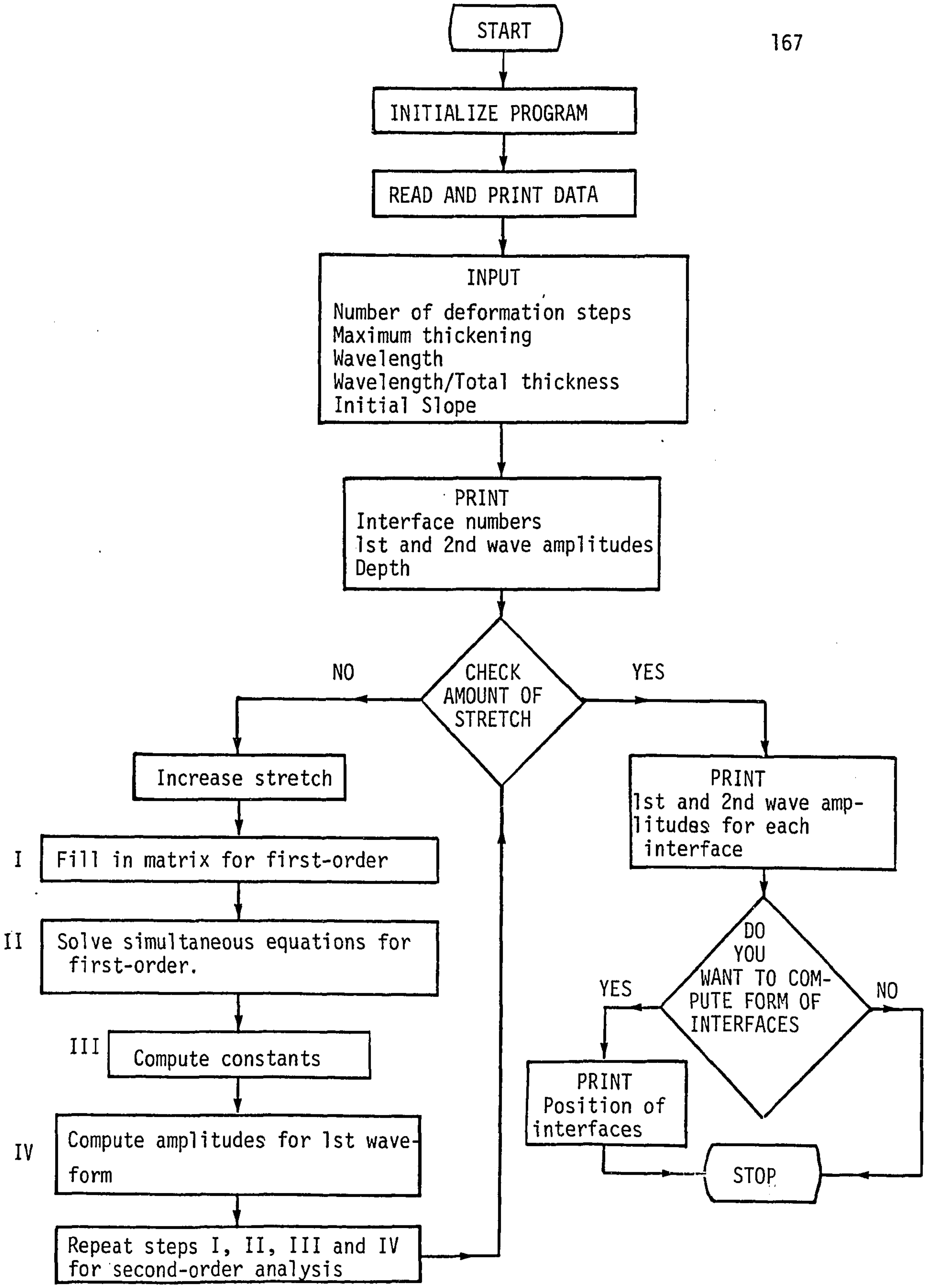
START
INITIALIZE PROGRAM
READ AND PRINT DATA
INPUT
Number of deformation steps
Maximum thickening
Wavelength
Wavelength/Total thickness
Initial Slope
PRINT
Interface numbers
1st and 2nd wave amplitudes
Depth
CHECK AMOUNT OF STRETCH
NO
YES
Increase stretch
I
Fill in matrix for first-order
II
Solve simultaneous equations for first-order.
III
Compute constants
IV
Compute amplitudes for 1st wave-form
Repeat steps I, II, III and IV for second-order analysis
PRINT
1st and 2nd wave amplitudes for each interface
DO YOU WANT TO COMPUTE FORM OF INTERFACES
YES
NO
PRINT
Position of interfaces
STOP

FIGURE 10

The program operates much like the program used to compute preferred wavelengths. The thicknesses and viscosities of layers are put into the subroutine starting at line 1620. The final wavelength of the first waveform and the maximum initial slope (tangent of slope angle) are entered by the operator when the computer asks for this information. The computer calculates the initial wavelength and the initial thicknesses of the layers. In general, the wavelength selected is the preferred wavelength for the multilayer, so that in general one runs the program that computes preferred wavelengths before running this program.

Table II shows an example of the output of the program for a simple multilayer consisting of four thick, soft, layers and one thin, stiff, layer. The layers were shortened by 9.1 percent (T/T_0=1/1)and the maximum initial slope was 0.003 (0.17 degree slope angle). The wavelength was 16 (in same unit as the thicknesses of layers). The shortening was accomplished in ten equal steps, the results of which are displayed on the computer monitor, but not on the printer. The printer displays only the final results, which are the amplifications of four interfaces for the first and second waves. Finally the position of points on the four interfaces are given interms of horizontal and vertical coordinates.

Application to Simple Multilayers:

Higher-order anayses have not been applied previously to multilayers, so I will present two examples. One is the form of a multilayer of identical stiff layers confined by soft media (shown in Fig.4)

TABLE II

MAXIMUM THICKENING (T/TO) 1.1

WAVELENGTH 16

WAVELENGTH/TOTAL THICKNESS 0.3902

CONDITIONS BEFORE FOLDING

MAXIMUM INITIAL SLOPE ANGLE (TANGENT) 0.003

AMPLITUDE OF INTERFACES

INTERFACE NO:	1ST WAVE	2ND WAVE	DEPTH
0	0	0	0
1	0.00763	0	0
2	0	0	0
3	0	0	0

CONDITIONS AFTER FOLDING

AMPLITUDES OF INTERFACES

INTERFACE NO	1ST WAVE	2ND WAVE	DEPTH
0	0.004117	-2.95×10^{-6}	-1
1	0.040847	-0.0001	-2
2	0.033199	-0.0004	-2.1
3	0.003943	2.06×10^{-6}	-3.1

LAYER NO:	MU(L)/MU(0)	T(L)/T(0)	THICKNESS
0	1	1	10
1	1	1	10
2	100	0.1	1
3	1	1	10
4	1	1	10

TABLE II continued

POSITION OF INTERFACES

INTERFACE NUMBER: 0

HORIZONTAL POSITION	VERTICAL POSITION
-4.000881	-9.999997
-3.200705	-9.998725
-2.400529	-9.997579
-1.600352	-9.996670
-0.800176	-9.996087
0	-9.995886
0.800177	-9.996087
1.600352	-9.996670
2.400529	-9.997579
3.200705	-9.008725
4.000881	-9.999997
4.801957	-10.00127
5.601233	-10.00242
6.401409	-10.00333
7.201585	-10.00392
8.001761	-10.00412
8.801937	-10.00392
9.602114	-10.00333
10.40229	-10.00242
11.20247	-10.00127
12.00264	-9.999997

INTERFACE NUMBER :1

HORIZONTAL POSITION	VERTICAL POSITION
-4.000881	-19.99986
-3.200705	-19.98726
-2.400529	-19.97595
-1.600352	-19.967
-0.800176	-19.96127
0	-19.9593
0.800176	-19.96127
1.600352	-19.967
2.400529	-19.97595
3.200705	-19.98726
4.000881	-19.99986
4.801057	-20.01251
5.601233	-20.02397
6.401409	-20.03309
7.201585	-20.03897
8.001761	-20.04099
8.801937	-20.03897
9.602114	-20.03309
10.40229	-20.02397
11.20247	-20.01251
12.00264	-19.99986

TABLE II continued

INTERFACE NUMBER: 2

HORIZONTAL POSITION	VERTICAL POSITION
-4.000881	-20.99996
-3.200705	-20.98971
-2.400529	-20.98047
-1.600352	-20.97316
-0.800176	-20.96846
0	-20.96684
0.800176	-20.96846
1.600352	-20.97316
2.400529	-20.98047
3.200705	-20.98971
4.000881	-20.99996
4.801057	-20.01023
5.601233	-21.0195
6.401409	-21.02687
7.201585	-21.03161
8.001761	-21.03324
8.801937	-21.03161
9.602114	-21.02687
10.40229	-21.0195
11.20247	-21.01023
12.00264	-20.99996

INTERFACE NUMBER: 3

HORIZONTAL POSITION	VERTICAL POSITION
-4.000881	-31
-3.200705	-30.99878
-2.400529	-30.99768
-1.600352	-30.99681
-0.800176	-30.99625
0	-30.99605
0.800176	-30.99625
1.600352	-30.99681
2.400529	-30.99768
3.200705	-30.99878
4.000881	-31
4.801057	-31.00122
5.601233	-31.00232
6.401409	-31.00319
7.201585	-31.00375
8.001761	-31.00394
8.801937	-31.00375
9.602114	-31.00319
10.40229	-31.00232
11.20247	-31.00122
12.00264	-31

and the other is the form of a multilayer of interbedded stiff and soft layers confined by very stiff media (shown in Fig.7). The wavelength in each example was selected to be roughly equal to the preferred wavelength, as shown in Figs. 4 or 7.

The first multilayer is composed of identical stiff layers (Fig.11). The layers were shortened 4.77 percent ($T/T_0=1.05$), the initial slope was 0.17 degree and the final wavelength was 30 times than the thickness of a stiff layer. Figure 11 shows the theoretical fold form. The interface at middepth in the multilayer is deflected as a pure cosine wave. Interfaces near the top of the stack of layers are flattened in crests of anticlines and sharpened in troughs of synclines, and interfaces near the bottom are sharpened in crests of anticlines and flattened in troughs of synclines. Thus the overall form of the fold is concentric-like.

The second multilayer is composed of alternating soft (2) and stiff (1) layers (Fig.12). The layers were shortened 28.6 percent ($T/T_0=1.4$), the initial slope was 0.17 degree and the final wavelength was 8.4 times than the thickness of a stiff layer. The amplitudes of folds are maximal at middepth and the shapes of interfaces are cosinusoidal. The stiff layers maintain roughly constant thicknesses whereas the soft interbeds distinctly thicken and thin. The correction in form due to the second waveform is very minor in such multilayers. The outer arcs of folds in layers, (L), 4 and 6 have slightly greater radii of curvature than inner arcs, so those two layers are bent into concentric-like forms.

Figure 11- Theoretical fold froms of stiff layers confined by very thick and soft media.

μ_L: Viscosity of a layer.

μ_m: Viscosity of medium.

Figure 12- Theoretical fold forms af a multilayer where interbedded stiff and soft layers confined by very stiff media.

L: Layer number

1: Stiff layer

2: Soft layer

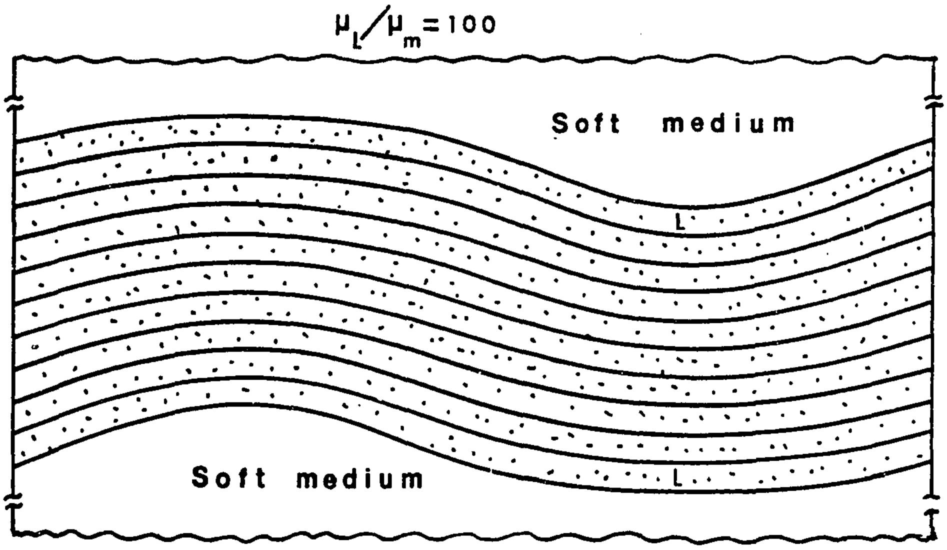

FIGURE 11

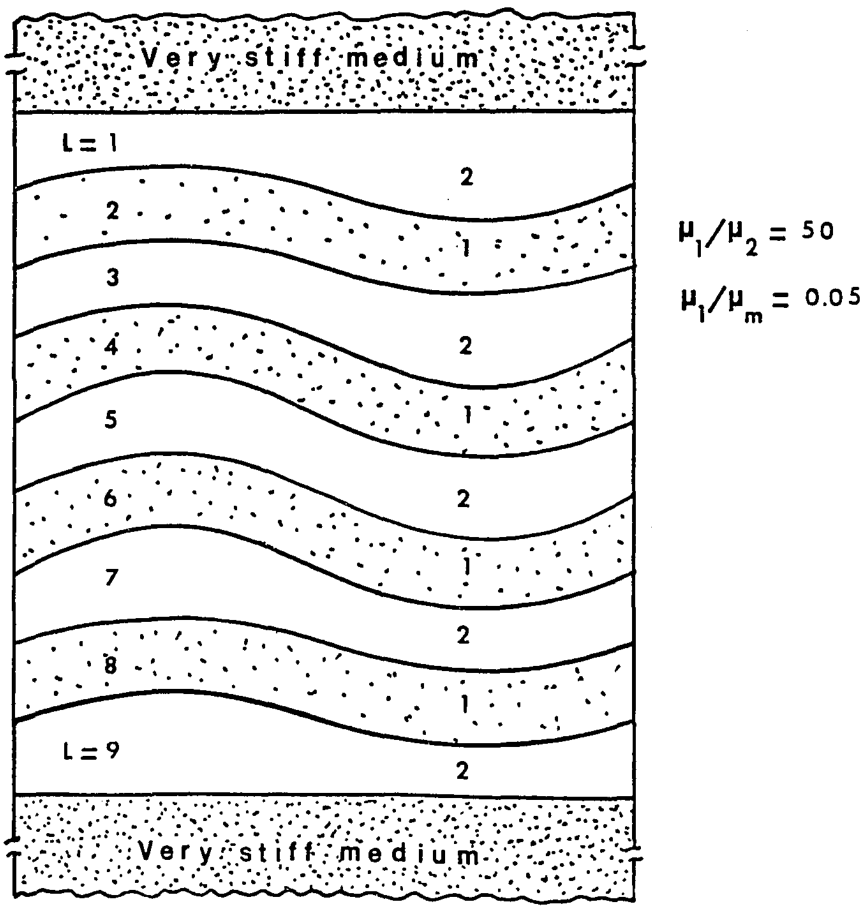

FIGURE 12

INTERACTION BETWEEN FOLDS OF DIFFERENT WAVELENGTHS (SECOND-ORDER ANALYSIS)

In several situations of interest in structural geology, folds with two different wavelengths grow simultaneously and interact with one another. An example is drag folds on the limbs of major folds (Ramberg, 1963). In the central Appalachians, the folds involving the entire rock sequence have wavelengths of about 18 km whereas folds involving the Ordovician rocks have wavelengths of about three km, and the two sizes of folds appear to have interacted as described in Chapter I. Here I will present the essential equations for the theory required to described interactions between folds of two sizes (Johnson, 1982c, unpublished notes) as well as a computer program that can be used to simulate the growth of such folds (Johnson, 1982b, unpublished notes).

Summary of Theoretical Analysis:

Suppose that there are waveforms with two distinct wavelengths, $\underline{L}_L$ and $\underline{L}_S$, growing simultaneously in a multilayer. I have shown in previous pages, Figs. 8 and 9, that a complex multilayer may have two preferred wavelengths. To first-order the two waveforms grow independently, but to second-order they interact. In the analysis we assume that the maximum slopes of both waveforms are significant to second-order, so that $(A\ell)^2, ({}^2A\ell_S)^2$, $(A\ell)({}^2A\ell_S)$ are significant quantities. Here $\underline{A}$ is the amplitude of the long waveform and ${}^2\underline{A}$ is the amplitude of the short waveform:

For this problem the position of an interface is described in terms of six waveforms (Johnson, 1982c),

$$\zeta_{t,b}=\pm T/2+A_{t,b}\cos[\ell_L x]+{}^2A_{t,b}\cos[\ell_S x]+{}^3A_{t,b}\cos[2\ell_L x]+{}^4A_{t,b}\cos[2\ell_S x]$$

$$+{}^5A_{t,b}\cos[(\ell_L-\ell_S)x]+{}^6A_{t,b}\cos[(\ell_L+\ell_S)x] \tag{21}$$

in which;

$\ell_L = 2\pi/L_L$; $\ell_S = 2\pi/L_S$

It is more convenient to write eq.(21) in the shorthand form,

$$\zeta_{t,b}=\pm T/2+\sum_{i=1}^{6} {}^iA_{t,b}\cos[{}^i\ell x] \tag{22}$$

Using this notation, the expression for the normal velocity at an interface is (Johnson, 1982c),

$$v_n=[\bar{v}_z]_\zeta[1-(\partial\zeta/\partial x)^2/2]-\bar{v}_x(\partial\zeta/\partial x)+\sum_{i=1}^{6}[\{{}^ia+{}^ib({}^ik)\}({}^iC)+\{{}^ic+{}^id({}^ik)\}({}^iS)]\cos({}^i\ell x)$$

$$+\sum_{i=1}^{2}({}^iA\,{}^i\ell)[\{{}^ia+{}^ib({}^ik)+{}^id\}({}^iS)+\{{}^ic+{}^id({}^ik)+{}^ib\}({}^iC)][\cos\{2({}^i\ell x)\}-1]$$

$$+(1/2)(\ell_S+\ell_L)A[\{{}^2a+{}^2b({}^2k)+{}^2d\}({}^2S)+\{{}^2c+{}^2d({}^2k)+{}^2b\}({}^2C)]\cos\{(\ell_S+\ell_L)x\}$$

$$+(1/2)(\ell_S+\ell_L)({}^2A)[(a+bk+d)S+(c+dk+b)C]\cos\{(\ell_S+\ell_L)x\}$$

$$+(1/2)(\ell_S-\ell_L)A[\{{}^2a+{}^2b({}^2k)+{}^2d\}({}^2S)+\{{}^2c+{}^2d({}^2k)+{}^2b\}({}^2C)]\cos\{(\ell_S-\ell_L)x\}$$

$$-(1/2)(\ell_S-\ell_L)({}^2A)[(a+bk+d)S+(c+dk+b)C]\cos\{(\ell_S-\ell_L)x\} \tag{23}$$

where

$${}^ia=(1/2)[({}^i\Lambda_t-{}^i\Lambda_b)\{{}^iC+{}^ik({}^iS)\}+({}^i\lambda_t+{}^i\lambda_b)({}^ik)({}^iC)]/[{}^iS({}^iC)-{}^ik] \tag{24a}$$

$${}^ib=-(1/2)[({}^i\Lambda_t+{}^i\Lambda_b)({}^iS)+({}^i\lambda_t+{}^i\lambda_b)({}^iC)]/[{}^iS({}^iC)-{}^ik] \tag{24b}$$

$${}^ic=(1/2)[({}^i\Lambda_t+{}^i\Lambda_b)({}^iS+{}^ik({}^iC)+({}^i\lambda_t-{}^i\lambda_b)({}^ik)({}^iS)]/[{}^iS({}^iC)+{}^ik] \tag{24c}$$

$${}^id=-(1/2)[({}^i\Lambda_t-{}^i\Lambda_b)({}^iC)+({}^i\lambda_t+{}^i\lambda_b)({}^iS)]/[{}^iS({}^iC)-{}^ik] \tag{24d}$$

$${}^iC=\cosh({}^ik); \quad {}^iS=\sinh({}^ik); \quad {}^ik={}^i\ell T/2$$

$${}^1\ell=\ell_L, \quad {}^2\ell=\ell_S, \quad {}^3\ell=2\ell_L \quad {}^4\ell=2\ell_S, \quad {}^5\ell=(\ell_S-\ell_L) \quad {}^6\ell=(\ell_L+\ell_S)$$

$${}^1\Lambda_{t,b}=(\sigma_{t,b})/2\mu\ell_L \tag{24e}$$

$${}^1\lambda_{t,b}=-4\mu\bar{D}_{xx}(A_{t,b}\ell_L)/2\mu\ell_L \tag{24f}$$

$${}^2\Lambda_{t,b}=({}^2\sigma_{t,b})/2\mu\ell_S \tag{24g}$$

$${}^2\lambda_{t,b}=-4\mu\bar{D}_{xx}({}^2A_{t,b}\ell_S)/2\mu\ell_S \tag{24h}$$

·for i=3 or 4 ; j=i-2

$$ {}^{i}\Lambda_{t,b}=[{}^{i}\sigma_{t,b}+2\mu\bar{D}_{xx}\{{}^{j}A_{t,b}({}^{j}\ell)\}^{2}-3\mu({}^{j}\ell)^{2}({}^{j}A_{t,b})[\{{}^{j}a+{}^{j}d\pm{}^{j}b({}^{j}k)\}({}^{i}C) $$

$$ +\{\pm{}^{j}c\pm{}^{j}b+{}^{j}d({}^{j}k)\}({}^{i}S)]]/\{2\mu({}^{j}\ell)\} \qquad (24i) $$

$$ {}^{i}\lambda_{t,b}=[-8\mu\bar{D}_{xx}({}^{i}A_{t,b})({}^{j}\ell)+\mu({}^{j}\ell)^{2}({}^{j}A_{t,b})[\{\pm3({}^{j}a)\pm4({}^{j}d)+3({}^{j}b)({}^{j}k)\}({}^{j}S) $$

$$ +\{3({}^{j}c)+4({}^{j}b)\pm3({}^{j}b)\}({}^{j}C)]]/\{2\mu({}^{j}\ell)\} \qquad (24j) $$

$$ {}^{5}\Lambda_{t,b}=[{}^{5}\sigma_{t,b}+4\mu\bar{D}_{xx}(A_{t,b})({}^{2}A_{t,b})(\ell_{S})(\ell_{L})-\mu(\ell_{S}-2\ell_{L})(\ell_{L})(A_{t,b})[\{{}^{2}a+{}^{2}d $$

$$ \pm{}^{2}b({}^{2}k)\}({}^{2}C)+\{\pm{}^{2}c\pm{}^{2}b+{}^{2}d({}^{2}k)\}({}^{2}S)]-\mu(\ell_{S}-2\ell_{L})(\ell_{S})({}^{2}A_{t,b})[\{a+d\pm bk\}C $$

$$ +\{\pm c\pm b+dk\}S]]/\{2\mu(\ell_{S}-\ell_{L})\} \qquad (24k) $$

$$ {}^{5}\lambda_{t,b}=[-4\mu\bar{D}_{xx}(A_{t,b})({}^{2}A_{t,b})(\ell_{S}-\ell_{L})+\mu(\ell_{S})(\ell_{L})(A_{t,b})[\{(\ell_{S}-2\ell_{L})({}^{2}c) $$

$$ +2(\ell_{S}-\ell_{L})({}^{2}b)\pm(\ell_{S}-2\ell_{L})({}^{2}d)({}^{2}k)\}\ ({}^{2}C)+\{\pm(\ell_{S}-2\ell_{L})({}^{2}a)\pm2(\ell_{S}-\ell_{L})({}^{2}d) $$

$$ +(\ell_{S}-2\ell_{L})({}^{2}b)({}^{2}k)\}({}^{2}S)]+\mu(\ell_{L})({}^{2}A_{t,b})[\{(\ell_{S}-2\ell_{L})c+2(\ell_{S}-\ell_{L})b $$

$$ \pm(\ell_{S}-2\ell_{L})dk\}C+\{\pm(\ell_{S}-2\ell_{L})a\pm2(\ell_{S}-\ell_{L})d+(\ell_{S}-2\ell_{L})bk\}S]]/\{2\mu(\ell_{S}-\ell_{L})\} \qquad (24\ell) $$

$$^{6}\Lambda_{t,b}=[^{6}\sigma_{t,b}+4\mu\bar{D}_{xx}(A_{t,b})(^{2}A_{t,b})(\ell_S)(\ell_L)-\mu(\ell_S+2\ell_L)(\ell_L)(A_{t,b})[\{^{2}a$$

$$+^{2}d\pm^{2}b(^{2}k)\}(^{2}C)+\{\pm^{2}c\pm^{2}b+^{2}d(^{2}k)\}(^{2}S)]-\mu(\ell_L+2\ell_S)(\ell_S)(^{2}A_{t,b})[\{a$$

$$+d\pm bk\}C+\{\pm c\pm b+dk\}S]]/\{2\mu(\ell_S+\ell_L)\} \tag{24m}$$

$$^{6}\lambda_{t,b}=[-4\mu\bar{D}_{xx}\ (A_{t,b})(^{2}A_{t,b})(\ell_S+\ell_L)+\mu A_{t,b}(\ell_S+\ell_L)[\{(\ell_S+2\ell_L)(^{2}c)$$

$$+2(\ell_S+\ell_L)(^{2}b)\pm(\ell_S+2\ell_L)(^{2}d)(^{2}k)\}(^{2}C)+\{\pm(\ell_S+2\ell_L)(^{2}a)$$

$$\pm2(\ell_S+\ell_L)(^{2}d)+(\ell_S+2\ell_L)(^{2}b)(^{2}k)\}(^{2}S)]+\mu(^{2}A_{t,b})(\ell_S+\ell_L)[\{(\ell_L$$

$$+2\ell_S)c+2(\ell_L+\ell_S)b\pm(\ell_L+2\ell_S)dk\}C+\{\pm(\ell_L+2\ell_S)a\pm2(\ell_L+\ell_S)d$$

$$+(\ell_L+2\ell_S)bk\}S]]/\{2\mu(\ell_L+\ell_S)\} \tag{24n}$$

and the equations that are to be solved for the amplitudes are (Johnson, 1982),

$$d(A_{t,b})/d\bar{S}_x=(1/\bar{S}_x)[(a\pm bk)C+(\pm c+dk)S \tag{25a}$$

$$d(^{2}A_{t,b})/d\bar{S}_x=(1/\bar{S}_x)[\{^{2}a\pm^{2}b(^{2}k)\}(^{2}C)+\{\pm^{2}c+^{2}d(^{2}k)\}(^{2}S)] \tag{25b}$$

$$d({}^3A_{t,b})/d\bar{S}_X=(1/\bar{S}_X)[\{{}^3a\pm{}^3b({}^3k)\}({}^3C)+\{\pm{}^3c+{}^3d({}^3k)\}({}^3S)]$$

$$+(1/\bar{S}_X)(A_{t,b}\ell_L)[(\pm a+bk\pm d)S+(c\pm dk+b)C] \qquad (25c)$$

$$d({}^4A_{t,b})/d\bar{S}_X=(1/\bar{S}_X)[\{{}^4a\pm{}^4b({}^4k)\}({}^4C)+\{\pm{}^4c+{}^4d({}^4k)\}({}^4S)]$$

$$+(1/\bar{S}_X)({}^2A_{t,b}\ell_S)[\{\pm{}^2a+{}^2b({}^2k)\pm{}^2d\}({}^2S)+\{{}^2c$$

$$\pm{}^2d({}^2k)+{}^2b\}({}^2C)] \qquad (25d)$$

$$d({}^5A_{t,b})/d\bar{S}_X=(1/\bar{S}_X)[\{{}^5a\pm{}^5b({}^5k)\}({}^5C)+\{\pm{}^5c+{}^5d({}^5k)\}({}^5S)]$$

$$+(1/\bar{S}_X)(1/2)(A_{t,b})(\ell_S-\ell_L)[\{\pm{}^2a+{}^2b({}^2k)\pm{}^2d\}({}^2S)$$

$$+\{{}^2c\pm{}^2d({}^2k)+{}^2b\}({}^2C)]-(1/\bar{S}_X)(1/2)({}^2A_{t,b})(\ell_S-\ell_L)[(\pm a$$

$$+bk\pm d)S+(c\pm dk+b)C] \qquad (25e)$$

$$d({}^6A_{t,b})/d\bar{S}_X=(1/\bar{S}_X)[\{{}^6a\pm{}^6b({}^6k)\}({}^6C)+\{\pm{}^6c+{}^6d({}^6k)\}({}^6S)]$$

$$+(1/\bar{S}_X)(1/2)(A_{t,b})(\ell_S+\ell_L)[\{\pm{}^2a+{}^2b({}^2k)\pm{}^2d\}({}^2S)+\{{}^2c\pm{}^2d({}^2k)$$

$$+{}^2b\}({}^2C)]+(1/\bar{S}_X)(1/2)({}^2A_{t,b})(\ell_S+\ell_L)[\pm a+bk\pm d)S+(c\pm dk+b)C] \qquad (25f)$$

Computer Program for Calculation Fold Forms:

The computer program is presented in Appendix IV and a flow chart for the program is shown in Fig.13. The input is very similar to that for program II (Appendix III), except two wavelengths are requested by the computer.

Table III shows an example of the output of the program for a simple multilayer consisting of four thick soft layers and one thin stiff layer. The layers were shortened by 28.6 percent (T/T_0= 1.4) and the maximum initial slope was 0.003 (0.17 degree slope angle). The long wavelength was 56 and short wavelength was 14 (in units of the thickness of first layer). Only one deformation step was used in the computation.

Application to Multilayers:

The forms of folds in two multilayers, composed of a stack of thin layers and a stack of thick layers separated by a soft layer, shown in Figs. 8 and 9, were determined with the computer program and the results are presented in Figs. 14 and 15. The wavelengths used in the computation were the preferred wavelengths shown in Figs. 8 and 9. The layers were shortened 9.1 percent (T/T_0=1/1) and the maximum initial slope of the layers were 0.1 and 0.2 degrees, respectively, for Figures 14 and 15.

In both examples one can recognized the folds with short wavelengths within the thin layers and the folds with long wavelengths

Figure 13- Flow chart diagram for the second-order analysis where there are two preferred wavelengths, including interaction.

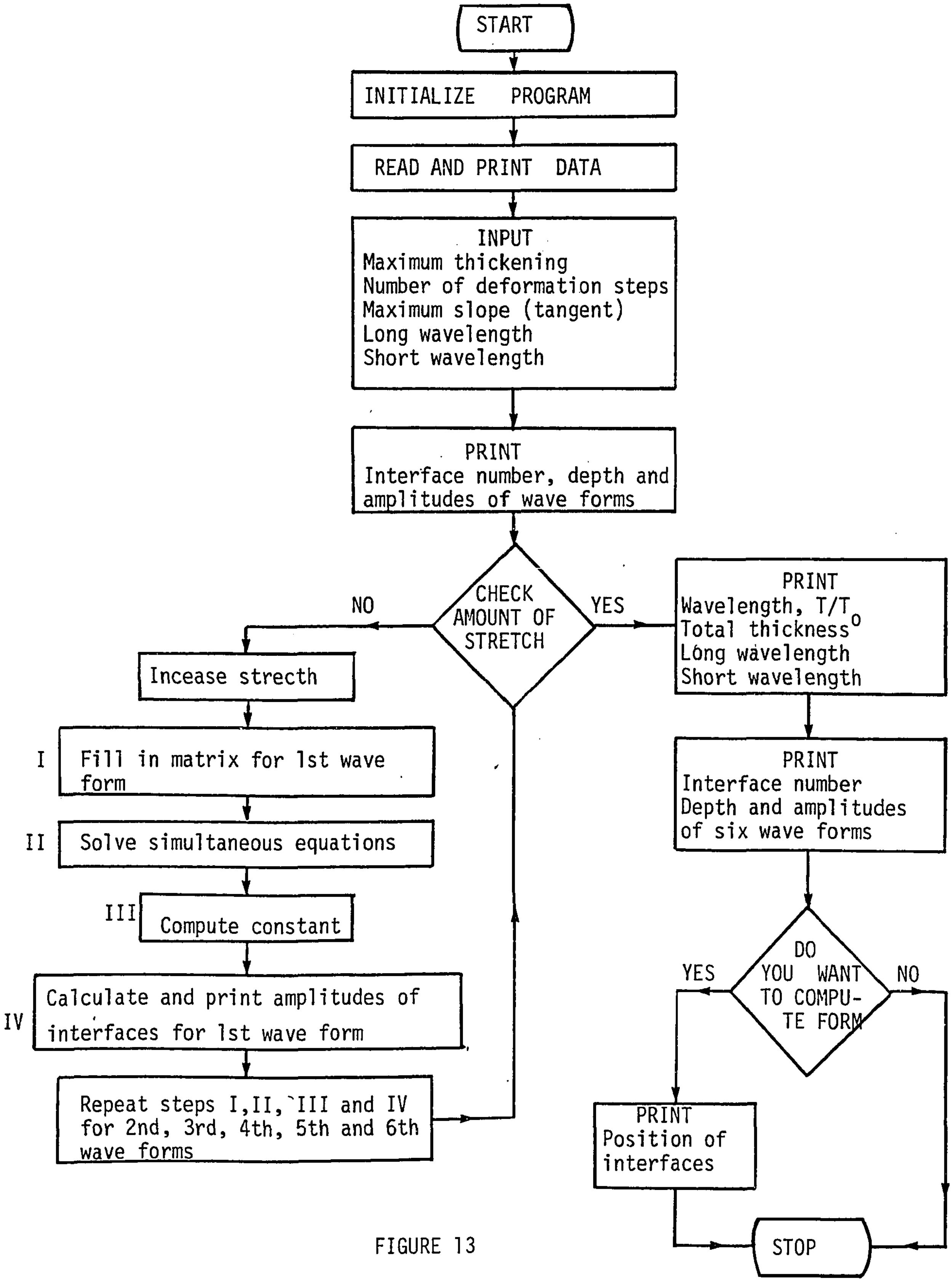
START
INITIALIZE PROGRAM
READ AND PRINT DATA
INPUT
Maximum thickening
Number of deformation steps
Maximum slope (tangent)
Long wavelength
Short wavelength
PRINT
Interface number, depth and amplitudes of wave forms
CHECK AMOUNT OF STRETCH
NO
YES
Incease strecth
I
Fill in matrix for 1st wave form
II
Solve simultaneous equations
III
Compute constant
IV
Calculate and print amplitudes of interfaces for 1st wave form
Repeat steps I,II,III and IV for 2nd, 3rd, 4th, 5th and 6th wave forms
PRINT
Wavelength, T/T$_0$
Total thickness
Long wavelength
Short wavelength
PRINT
Interface number
Depth and amplitudes of six wave forms
DO YOU WANT TO COMPUTE FORM
YES
NO
PRINT
Position of interfaces
STOP

FIGURE 13

TABLE III

LENGTH SCALE	10
MAXIMUM SLOPE (TANGENT)	0.003
TOTAL THICKNESS	32.1429
LONG WAVELENGTH	56
SHORT WAVELENGTH	14

CONDITIONS BEFORE FOLDING

INTERFACE NO:	DEPTH	AMPLITUDES OF WAVE FORMS					
		A1	A2	A3	A4	A5	A6
0	-7.1	0.027	0.007	0	0	0	0
1	-14.3	0.027	0.007	0	0	0	0
2	-15	0.027	0.007	0	0	0	0
3	-22.1	0.027	0.007	0	0	0	0

LAYER NO:	MU(L)/MU(0)	T(L)/SCALE	THICKNESS
0	1	0.7142	7.1421
1	1	0.7142	7.1421
2	100	0.0714	0.7142
3	1	0.7142	7.1421
4	1	1	10

CONDTIONS AFTER FOLDING

3 WAVE WAVELENGTH : 20.0028
4 WAVE WAVELENGTH : 5.0007
5 WAVE WAVELENGTH : 8.0011
6 WAVE WAVELENGTH : 13.3352

T/TO : 1.3998
TOTAL THICKNESS : 40.9956
LONG WAVELENGTH : 40.0056
SHORT WAVELENGTH : 10.0014

TABLE III continued

INTERFACE NO:	DEPTH	A1	A2	A3	A4	A5	A6
		AMPLITUDES OF WAVE FORMS					
0	-10	0.205	0.010	-0.019	-0.0	-0.001	-0.0
1	-20	0.275	0.062	-0.081	0.007	-0.027	-0.012
2	-21	0.275	0.062	0.084	-0.007	0.027	0.011
3	-31	0.142	0.010	0.018	0.0	0.001	0

LAYER NO	MU(L)/MU(O)	T(L)/SCALE	THICKNESS
0	1	0.9998	9.9986
1	1	0.9998	9.9986
2	100	0.0999	0.9999
3	1	0.9998	9.9986
4	1	1	10

POSITION OF INTERFACES

INTERFACE NUMBER: 0

HORIZONTAL POSITION	VERTICAL POSITION
-10.0014	-9.969425
-8.00112	-9.917017
-6.00084	-9.880261
-4.000559	-9.846483
-2.000279	-9.816441
5.96×10^{-7}	-9.803735
2.000281	-9.816441
4.000561	-9.846483
6.000841	-9.880261
8.001121	-9.917017
10.0014	-9.969425
12.00168	-10.04309
14.00196	-10.12157
16.00224	-10.17889
18.00252	-10.2053
20.0028	-10.2113
22.00308	-10.2053
24.00336	-10.17889
26.00364	-10.12157
28.00392	-10.04309
30.0042	9.969425

TABLE III continued

INTERFACE NUMBER: 1

HORIZONTAL POSITION	VERTICAL POSITION
-10.0014	-19.84731
-8.00112	-19.8505
-6.00084	-19.84716
-4.000559	-19.81738
-2.000279	-19.79536
5.9604×10^{-7}	-19.77388
2.000281	-19.79536
4.000561	-19.81738
6.000841	-19.84716
8.001121	-19.8505
10.0014	-19.84731
12.00168	-19.9858
14.00196	-20.19268
16.00224	-20.32274
18.00252	-20.3035
20.0028	-20.24528
22.00308	-20.3035
24.00336	-20.32274
26.00364	-20.19268
28.00392	-19.9858
30.0042	-19.84731

INTERFACE NUMBER: 2

HORIZONTAL POSITION	VERTICAL POSITION
-10.0014	-21.02598
-8.00112	-20.93691
-6.00084	-20.92431
-4.000559	-20.832
-2.000279	-20.63698
5.9604×10^{-7}	-20.54567
2.000281	-20.63698
4.000561	-20.832
6.000841	-20.92431
8.001121	-20.93691
10.0014	-21.02598
12.00168	-21.14308
14.00196	-21.22575
16.00224	-21.21466
18.00252	-21.17228
20.0028	-21.17166
22.00308	-21.17228
24.00336	-21.21466
26.00364	-21.22575
28.00392	-21.14308
30.0042	-21.02598

TABLE III continued

INTERFACE NUMBER :3

HORIZONTAL POSITION	VERTICAL POSITION
-10.0014	-31.00356
-8.00112	-30.96276
-6.00084	-30.92628
-4.000559	-30.88441
-2.000279	-30.84316
5.9604×10^{-7}	-30.82503
2.000281	-30.84316
4.000561	-30.88441
6.000841	-30.92628
8.001121	-30.96276
10.0014	-30.00356
12.00168	-31.0515
14.00196	-31.09259
16.00224	-31.11216
18.00252	-31.11272
20.0028	-31.10993
22.00308	-31.11272
24.00336	-31.11216
26.00364	-31.09259
28.00392	-31.0515
30.0042	-31.00356

Figure 14- Theoretical fold forms of a multilayer where thin layers are overlain by thick layers. The thin layers show second wave from (intermediate size) and the thick layers show first wave form (large size). The layers were shortened 9.1 percent.

Figure 15- Theoretical fold forms of a multilayer where thin layers are underlain by thick layers. The thick layers show first wave form and the thin layers show second wave form. The layers were shortened 9.1 percent.

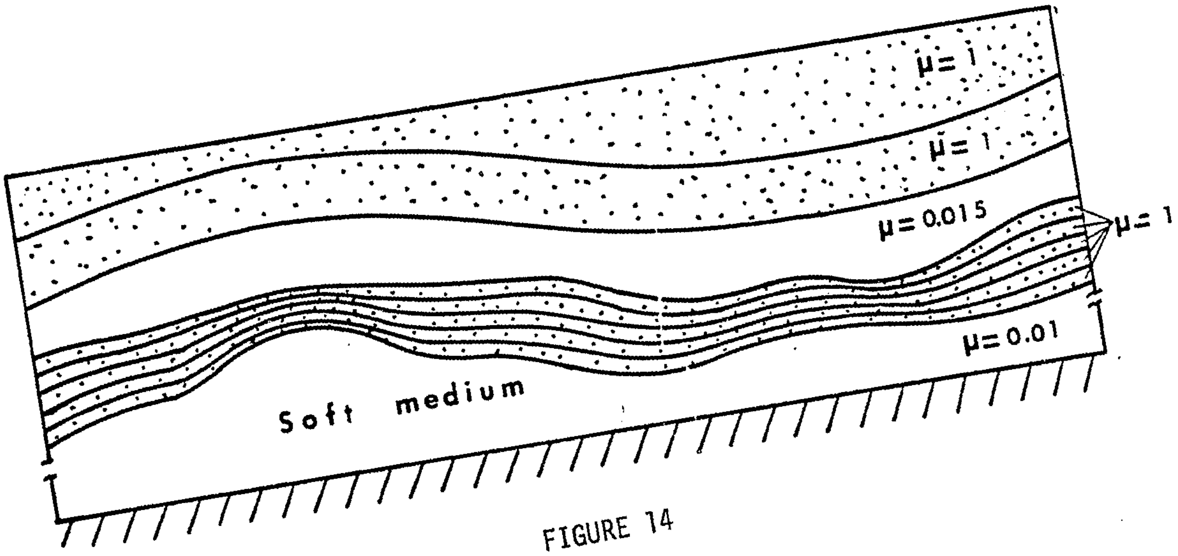

FIGURE 14

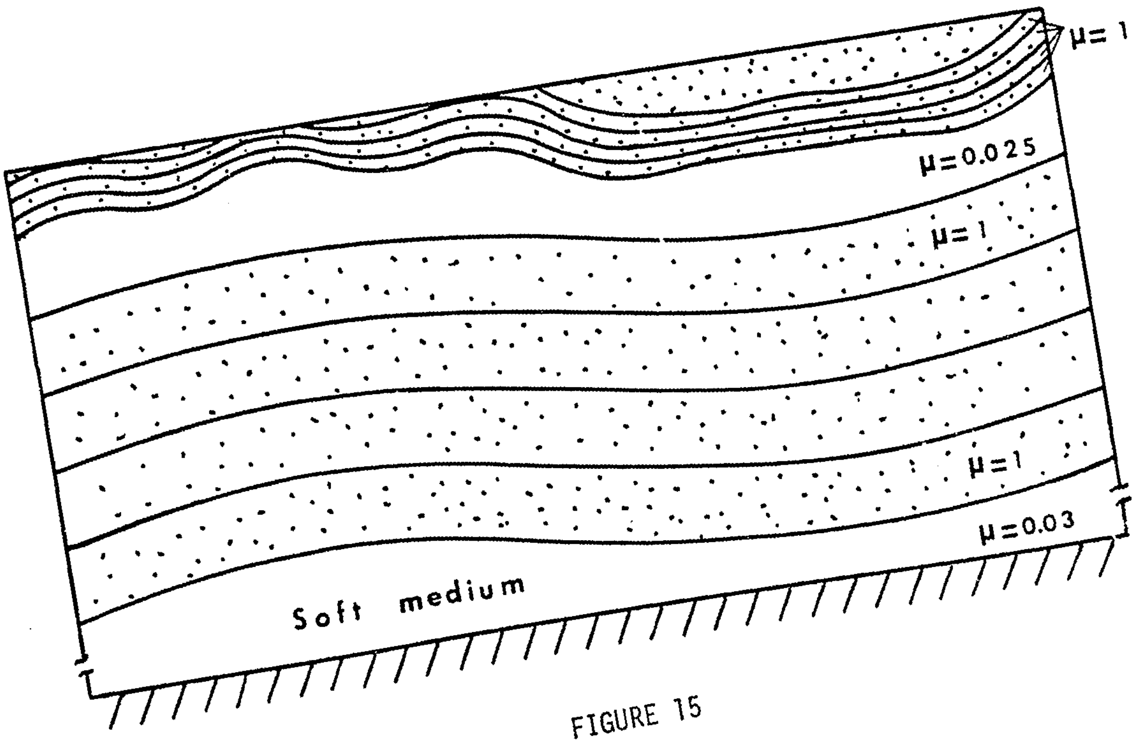

FIGURE 15

in all the layers. The origin of coordinates is the same for the long and short cosinusoidal waveforms so that the long and short waves are in phase in the anticline and out of phase in the syncline. This effect and effects of the other four waveforms result in a relatively complicated fold pattern in the thin layers. The layers are truncated at the upper surface of the multilayer bacuase the upper surface was assumed to remain flat (for example by erosion from highs and deposition in lows) during folding.

REFERENCES CITED

Biot, M.A., 1964. Theory of internal buckling on a confined multi-layered structure. Geol.Soc.Am.Bull., 75: 563-568.

Fletcher, R.C., 1974. Wavelength selection in the folding of a single layer with power-law rheology. Am.Jour.Sci., 274: 1029-1043.

Fletcher, R.C., 1977. Folding of single viscous layer: Exact infinitesimal amplitude solution. Tectonophysics,39: 593-606.

Fletcher, R.C., 1979. The shape of single-layer folds at small but finite amplitude. Tectonophysics, 60: 77-87.

Johnson, A.M., 1981. Computer program (FOCAL language) for determination of preferred wavelengths in a multilayer. Unpublished program, University of Cincinnati.

Johnson,A.M., 1982a. Computer program (FOCAL language) for determination of fold forms (second-order approximation). Unpublished program, University of Cincinnati.

Johnson, A.M., 1982b. Computer program (FOCAL langiage) for determination of fold forms for two waves, plus interaction (second-order approximation). Unpublished program, University of Cincinnati.

Johnson, A.M., 1982c. Solution to second-order for two waves plus interaction. Unpublished notes, University of Cincinnati

Johnson, A.M. and Fletcher, R.C., 1982. Final report to Earth Science Division, Geology Program of the National Science Foundation. Grant No: EAR 80-00053, Volume II.

Pfaff, V.(in preparation). Third-order folding theory and application to central Appalachians.

Ramberg, H., 1962. Contact strain and folding instability of a multilayered body under compression. Geol.Rudsch., 51: 409-439.

Ramberg, H., 1964. Selective buckling of composite layers with contrasted rheological properties, a theory for simultaneous formation of several order of folds. Tectonophysics, 1: 307-341.

Ramberg, H and Stromgard, K., 1971. Experimental test of modern buckling theory applied on multilayered media. Tectonophysics, 11: 461-472.

APPENDIX II

COMPUTER PROGRAM FOR FIRST-ORDER ANALYSIS OF PREFERRED WAVELENGTHS.

```
10 PRINT "STORED ON AMJ DISK UNDER <MULTI1.BAS>"
15 GOTO 200
20 REM
25 REM
100 REM ************SUBROUTINE**************
105 R=1/MU(L):T5=4*W1/R:K1=K(L)
110 EM=1/(E^K1):EP=E^K1:CH=(EP+EM)/2:SH=(EP-EM)/2
115 TM1=CH*SH-K1:TP1=CH*SH+K1:T1=(CH^2)/TM1:T2=K1/TM1
120 T3=(SH^2)/TP1:T4=K1/TP1
122 IF L>=LDET THEN DX=0 ELSE DX=1
125 RETURN
130 REM ************END SUB ****************
135 REM
140 REM
200 GOSUB 905
215 REM *********ONE WAVELENGTH*************
220 IF OO<0 THEN 235
225 REM *********MULTIPLE WAVELENGTHS******
230 WT=WT+WINT:IF WMAX+WINT/10-WT <0 THEN STOP
235 A(ILAST+1)=0:FOR I=0 TO ILAST:A(I)=.001:NEXT I
240 SX=1.0001:N=0
245 IF (SZ-.9990001/(SX+DS))<0 THEN 305 ELSE 405
250 REM
255 REM
300 REM *********FINISHED--PRINT RESULTS**
305 LPRINT "WAVELENGTH ",WT*TT*SCALE*SX^2
310 LPRINT "T/T0",1/SX:LPRINT "WAVELENGTH/TOTAL THICK",WT*
SX^2
315 PRINT "AMPLIFICATIONS":LPRINT "AMPLIFICATIONS OF INTER
FACES"
320 II=0:FOR I=0 TO ILAST
325 UA=A(I)/.001:PRINT UA;:LPRINT UA;
330 II=II+1:IF II=4 THEN PRINT:LPRINT:II=0
335 NEXT I
340 LPRINT:PRINT:IF OO<0 THEN 9999 ELSE 230
345 REM
350 REM
400 REM ********INCREASE AMOUNT OF STRETCH
405 SX=SX+DS:FOR L=0 TO LLAST:K(L)=PI*T(L)/(WT*TT*SX^2):NE
XT L
410 FOR I=0 TO ILAST:FOR J=0 TO 3:Y(I,J)=0:NEXT J:NEXT I
415 FOR L=1 TO LB:I=L-1:AP(L)=A(I)+A(I+1):AM(L)=A(I)-A(I+1
)
420 NEXT L:N=N+1
425 AP(0)=A(0):AM(0)=-A(0)
430 W1=2*PI*T(0)/(WT*TT*SX)
```

```
435 REM
440 REM
500 REM ********FILL-IN MATRIX***********
505 L=0:GOSUB 105
510 Y(0,1)=Y(0,1)-(T1+T3)*R
515 Y(0,3)=Y(0,3)+T5*R*(AP(0)*T2+AM(0)*T4)
520 L=LLAST:GOSUB 105
525 Y(ILAST,1)=Y(ILAST,1)-4*R*T1*T3/(T1+T3)
530 FOR L=1 TO LB:I=L-1
535 GOSUB 105
540 TP1=(T1+T3)*R:TM1=(T1-T3)*R
545 Y(I,1)=Y(I,1)-TP1:Y(I,2)=Y(I,2)+TM1
550 Y(I+1,0)=Y(I+1,0)+TM1:Y(I+1,1)=Y(I+1,1)-TP1
555 Y(I,3)=Y(I,3)-T5*R*(AP(L)*T2-AM(L)*T4)*DX
560 Y(I+1,3)=Y(I+1,3)+T5*R*(AP(L)*T2+AM(L)*T4)*DX
565 NEXT L
570 Y(0,0)=0:Y(ILAST,2)=0
575 REM
580 REM
600 REM ********START EQUATION SOLVER****
605 FOR I=0 TO ILAST:YY=1/Y(I,1):Y(I,1)=1
610 Y(I,2)=Y(I,2)*YY:Y(I,3)=Y(I,3)*YY
615 IF I=ILAST GOTO 640
620 J=I+1
625 Y(J,1)=Y(J,1)-Y(J,0)*Y(I,2)
630 Y(J,3)=Y(J,3)-Y(J,0)*Y(I,3)
635 Y(J,0)=0
640 NEXT I
645 FOR I=ILAST-1 TO 0 STEP -1
650 Y(I,3)=Y(I,3)-Y(I,2)*Y(I+1,3)
655 Y(I,2)=0
660 NEXT I
665 FOR I=0 TO ILAST:SIG(I)=Y(I,3):Y(I,3)=0:NEXT I
670 L=LLAST:GOSUB 105
675 SIG(LLAST)=SIG(ILAST)*(T1-T3)/(T1+T3)
680 REM ********END MATRIX SOLVER********
685 REM
690 REM
700 REM ********COMPUTE AMPLITUDES*******
705 FOR L=1 TO LLAST:I=L-1:CP(L)=SIG(I)+SIG(I+1):CM(L)=SIG
(I)-SIG(I+1)
710 NEXT L
715 FOR L=1 TO LB:I=L-1
720 GOSUB 105
725 T6=AP(L)*T2-AM(L)*T4:T7=CM(L)*T1+CP(L)*T3
730 Q(I)=(1/T5)*(T7-T5*T6*DX):NEXT L
735 L=LB:T6=-(AP(L)*T2+AM(L)*T4):T7=CM(L)*T1-CP(L)*T3
```

```
740 Q(ILAST)=(1/T5)*(T7+T5*T6*DX)
742 FOR I=0 TO ILAST:IF I>=LDET-1 THEN DX=0 ELSE DX=1
745 A(I)=A(I)-(DS/SX)*(A(I)*DX-Q(I)):NEXT I
750 PRINT:PRINT "AMPLITUDES":PRINT "DEFORM. STEP",N
755 II=0:FOR I=0 TO ILAST:PRINT A(I)/.001;
760  II=II+1:IF II=4 THEN PRINT:II=0
765 NEXT I
770 GOTO 245
775 REM ********END COMPUTATION**********
780 REM
785 REM
790 REM ********RETURN AND INCREASE STRETCH
795 REM
800 REM
900 REM *******INITIALIZE PROGRAM*******
905 PRINT "PROG. SOLVES COMPLEX MULTILAYERS OF VISC FLUIDS
 SEPARATED"
910 PRINT "BY FRICTIONLESS CONTACTS. WILL WORK FOR LONG WA
VELENGTHS"
915 PRINT "ONLY WITH DOUBLE PRECISION ARITHMETIC."
920 REM FIRST LAYER IS L=0;LAST IS LLAST;TOP LAYER (0) HAS
 FLAT TOP
925 REM FIRST INTERFACE, I=0, IS AT BASE OF TOP LAYER;LAST
 LAYER
930 REM ON RIGID SURFACE AND LAST LAYER IS UNSTRESSED. DEC
OLLEMENT IS
935 REM AT TOP OF LAST LAYER. LAST INTERFACE IS ILAST=LLAS
T-1. IN THE
940 REM SOL FOR CONSTANTS, THERE ARE ILAST+1 CONSTANTS (=L
LAST).
945 REM IN DIMENSION STATEMENTS, V(I), I=LLAST; V(I,J); I=
LLAST-1,
950 REM J=4.
955 DEFINT I,J,L:DEFDBL Y,W,T,E,K,C,S,R,A,P:DEFSNG U
960 READ LAYS:LLAST=LAYS-1:ILAST=LLAST-1
965 L=LLAST:DIM T(L),MU(L),A(L),K(L),SIG(L),Q(L),AP(L),AM(
L)
970 DIM CP(L),CM(L),Y(L-1,3)
975 REM T=THICK;MU=VISCOSITY RATIO;A=AMPLITUDE;K=DIM.WAVE
NO.
980 REM SIG=CONSTANT;Q=AMPLIF. FACTOR;Y=COEFF. IN MATRIX
985 PI=3.141592653589793#:E=2.718281828459045#:LB=LLAST-1
990 REM****************READ DATA************
995 GOSUB 1200
1000 REM ************COMPLETE INITIALIZATION*************
*
```

```
1005 TT=1:FOR L=1 TO LLAST:T(L)=T(L)/T(0):TT=TT+T(L):NEXT
L
1010 SCALE=T(0):T(0)=1
1015 FOR L=1 TO LLAST:MU(L)=MU(L)/MU(0):NEXT L
1020 MU(0)=1
1021 DATA 16 :REM **CHANGE THIS WHEN YOU CHANGE THE DATA *
***
1025 LPRINT: LPRINT "LAY NO","MU(L)/MU(0)","T(L)/T(0)","T(
L)"
1030 FOR L=0 TO LLAST:UM=MU(L):UT=T(L):UTT=UT*SCALE
1035 LPRINT L,UM,UT,UTT
1040 NEXT L
1042 INPUT "I.D. NO. OF LAYER BELOW DETACHMENT SURFACE";LD
ET
1043 LPRINT:LPRINT "DETACHMENT IS AT INTERFACE NO.";LDET-1
1044 TT=0:FOR L=0 TO LDET-1:TT=TT+T(L):NEXT L
1045 PRINT "NUMBER OF DEFORMATION STEPS(>10)";:INPUT NN
1050 PRINT "MAXIMUM THICKENING(SZ)";:INPUT SZ
1055 DS=(1/SZ-1)/NN
1060 PRINT "WT IS WAVELENGTH-TO-THICKNESS RATIO(FINAL)"
1062 LPRINT:LPRINT "FINAL TOTAL THICKNESS OF MULTILAYER AB
OVE DETACHMENT"
1063 LPRINT " SURFACE IS";TT*SCALE:LPRINT
1065 PRINT "DO ONE WAVELENGTH? IF YES, TYPE NEG. NO.";:INP
UT OO
1070 IF OO>0 THEN 1095
1075 PRINT "WAVELENGTH-TO-THICKNESS RATIO";:INPUT WT
1080 WT=WT*SZ^2:LPRINT:LPRINT
1085 LPRINT "SZZ",SZ:LPRINT "FINAL WAVELENGTH/THICKNESS",W
T
1090 RETURN
1095 PRINT "MINIMUM WAVELENGTH-TO-THICKNESS RATIO";:INPUT
WMIN
1100 PRINT "MAXIMUM";:INPUT WMAX:PRINT "INTERVAL";:INPUT W
INT
1105 WT=(WMIN-WINT)*SZ^2
1110 WMIN=WMIN*SZ^2:WMAX=WMAX*SZ^2:WINT=WINT*SZ^2:RETURN
1115 REM *******END SUBROUTINE***********
1120 REM
1125 REM
1200 REM *******PUT DATA HERE************
1201 REM ***THIS DATA FOR THE CENTRAL APPALACHIANS*****
1205 LLAST=15:T(0)=1:T(1)=.45:T(2)=.7:T(3)=.6:T(4)=1.5:T(5
)=.5:T(6)=1
1210 T(7)=.7:T(8)=.5:T(9)=.375:T(10)=.4:T(11)=.365:T(12)=.
2:T(13)=.25
```

```
1215 T(14)=1:T(15)=3
1230 MU(0)=1:MU(1)=100:MU(2)=5:MU(3)=5:MU(4)=100:MU(5)=25
1235 MU(6)=100:MU(7)=100:MU(8)=30:MU(9)=20:MU(10)=1:MU(11)
=1
1240 MU(12)=100:MU(13)=100:MU(14)=1:MU(15)=25
1245 RETURN
1248 REM ***THIS DATA FOR TEST RUN***********
1250 FOR L=0 TO 4:MU(L)=1:T(L)=10:NEXT:MU(2)=100:T(2)=1
1260 RETURN
1265 REM
1270 REM
1300 REM **********DEFINITIONS OF L AND I NUMBERS*********
1305 REM
1310 REM
1315 REM ----------------FLAT SURFACE---------------------
------
1320 REM                  L = 0
1325 REM --------I = 0 -----------------------------------
------
1330 REM                  L = 1
1335 REM --------I = 1 -----------------------------------
------
1340 REM                  L = 2
1345 REM --------I = 2 -----------------------------------
------
1350 REM                  L = 3     L = LB
1355 REM --------I = 3   I = ILAST---DECOLLEMENT-----------
-----
1360 REM                  L = 4     L = LLAST
1365 REM -------------------------------------------------
------
1370 REM ////////////////RIGID BASEMENT///////////////////
//////
1375 REM \\\\\\\\\\\\\\\\\\\\\\\\\\\\\\\\\\\\\\\\\\\\\\\\\
\\\\\\
1380 REM /////////////////////////////////////////////////
//////
9999 END
```

APPENDIX III

COMPUTER PROGRAM FOR SECOND-ORDER ANALYSIS WHERE THERE IS ONE PREFERRED WAVELENGTH

```
10 PRINT "STORED ON AMJ DISK UNDER <MULSEC.BAS>"
20 GOTO 405
22 REM
24 REM
100 REM ************SUBROUTINE**************
105 R=1/MU(L):WL=WF*W1:T5=4*WL/R:K1=WF*K(L)
110 EM=1/(E^K1):EP=E^K1:CH=(EP+EM)/2:SH=(EP-EM)/2
115 TM1=CH*SH-K1:TP1=CH*SH+K1:T1=(CH^2)/TM1:T2=K1/TM1
120 T3=(SH^2)/TP1:T4=K1/TP1
125 TP1=(T1+T3)/T5:TM1=(T1-T3)/T5
130 IF INT(WF+.1)=1 THEN APP=AP(L):AMM=AM(L):GOTO 140
135  APP=AP2(L):AMM=AM2(L)
140 RETURN
145 REM ************END SUB ****************
146 REM
147 REM
200 REM *************START SUBROUTINE***************
205 T1=CH*SH-K1:APP=AP(L):AMM=AM(L):T2=CH*SH+K1
210 AA=(CM(L)*(CH+K1*SH)-T5*DX*APP*K1*CH)/(T1*T5)
215 BB=-(CP(L)*SH-T5*DX*AMM*CH)/(T2*T5)
220 CC=(CP(L)*(SH+K1*CH)-T5*DX*AMM*K1*SH)/(T2*T5)
225 DD=-(CM(L)*CH-T5*DX*APP*SH)/(T1*T5)
230 YP=-.25*DX*WL*((APP^2)+AMM^2)
235 YM=-.5*DX*WL*APP*AMM
240 T1=(1/8)*WL*((3*CC+4*BB)*CH+3*K1*BB*SH)
245 T2=(1/8)*WL*((3*AA+4*DD)*SH+3*K1*DD*CH)
250 ZP=T1*APP+T2*AMM:ZM=T1*AMM+T2*APP
255 RETURN
260 REM ***********END SUBROUTINE******************
265 REM
270 REM
300 REM ***********BEGIN SUBROUTINE****************
305 WF=1:GOSUB 105:GOSUB 205
310 X=((APP+AMM)*(1+SN)/4+(APP-AMM)*(1-SN)/4)*WL
315 X=X*((SN*(AA+DD)+K1*BB)*SH+(CC+BB+SN*K1*DD)*CH)
320 WF=2:GOSUB 105
325 TZZ=X+YM*T1+ZP*T2+SN*(YP*T3-ZM*T4):WF=1
330 RETURN
335 REM ************END SUBROUTINE****************
340 REM
345 REM
400 REM ************MAIN PROGRAM*************
405 GOSUB 1405
410 AA=SLOPE*WL/(2*PI*SCALE):WT=WT*SZ^2
415 FOR I=0 TO ILAST+1:A(I)=0:A2(I)=0:NEXT
420 FOR I=1 TO ILAST-2:A(I)=AA:NEXT
```

```
425 SX=1.0001:N=0
430 GOSUB 540
435 IF (SZ-.9990001/(SX+DS))<0 THEN 505 ELSE 605
440 REM
445 REM
500 REM *********FINISHED--PRINT RESULTS**
505 UW=WT*TT*SCALE*SX^2:PRINT "WAVELENGTH",UW
510 UT=1/SX:UW=WT*SX^2
515 PRINT "T/T0",UT,"WAVELENGTH/TOTAL THICK",UW
518 LPRINT "CONDITIONS AFTER FOLDING"
520 GOSUB 530
525 GOTO 575
530 PRINT "AMPLITUDES":PRINT "INTERFACE","1ST WAVE","2N
D WAVE","DEPTH"
535 DP(0)=-T(0):FOR I=1 TO ILAST+1:DP(I)=DP(I-1)-T(I):N
EXT I
540 LPRINT "AMPLITUDES":LPRINT "INTERFACE","1ST WAVE","
2ND WAVE","DEPTH"
545 FOR I=0 TO ILAST:UA=A(I)*SCALE:U2A=A2(I)*SCALE:UD=D
P(I)
550 PRINT I,UA,U2A,UD:LPRINT I,UA,U2A,UD:NEXT I
555 LPRINT "LAYER","MU(L)/MU(0)","T(L)/T(0)","THICKNESS
"
560 FOR L=0 TO LLAST:UM=MU(L):UT=T(L):UTT=T(L)*SCALE
565 LPRINT L,UM,UT,UTT:NEXT L
570 RETURN
575 PRINT:PRINT "TO COMPUTE FORM, TYPE NEG NUMBER":INPU
T OO
580 IF OO<0 THEN 1700 ELSE 9999
585 REM
590 REM
600 REM ********INCREASE AMOUNT OF STRETCH*************
***
605 SX=SX+DS:FOR L=0 TO LLAST:K(L)=PI*T(L)/(WT*TT*SX^2)
:NEXT L
610 FOR I=0 TO ILAST:FOR J=0 TO 3:Y(I,J)=0:NEXT J:NEXT
I
615 FOR L=1 TO LLAST:I=L-1:AP(L)=A(I)+A(I+1):AM(L)=A(I)
-A(I+1)
620 AP2(L)=A2(I)+A2(I+1):AM2(L)=A2(I)-A2(I+1):NEXT L:N=
N+1
625 AP(0)=A(0):AM(0)=-A(0):AP2(0)=A2(0):AM2(0)=-A2(0)
630 W1=2*PI*T(0)/(WT*TT*SX)
635 REM
700 REM
705 REM ********FILL-IN MATRIX***********
```

```
710 L=0:DX=1:WF=1:GOSUB 105
715 Y(0,1)=Y(0,1)-TP1
720 Y(0,3)=Y(0,3)-(APP*T2+AMM*T4)*DX
725 DX=0:Y(ILAST,3)=Y(ILAST,3)+(APP*T2-AMM*T4)*DX:DX=1
730 Y(ILAST,1)=Y(ILAST,1)-4*T1*T3/(T5*(T1+T3)):DX=1
735 GOSUB 805
740 GOTO 995
745 REM
750 REM
800 REM *************START SUBROUTINE******************
**
805 FOR L=1 TO LB:I=L-1:J=L
810 GOSUB 105
815 Y(I,1)=Y(I,1)-TP1:Y(I,2)=Y(I,2)+TM1
820 Y(J,0)=Y(J,0)+TM1:Y(J,1)=Y(J,1)-TP1
825 Y(I,3)=Y(I,3)+DX*(APP*T2-AMM*T4)
830 Y(J,3)=Y(J,3)-DX*(APP*T2+AMM*T4)
835 NEXT L
840 Y(0,0)=0:Y(ILAST,2)=0
845 REM
850 REM
900 REM ********START MATRIX SOLVER****
905 FOR I=0 TO ILAST:YY=1/Y(I,1):Y(I,1)=1
910 Y(I,2)=Y(I,2)*YY:Y(I,3)=Y(I,3)*YY
915 IF I=ILAST GOTO 940
920 J=I+1
925 Y(J,1)=Y(J,1)-Y(J,0)*Y(I,2)
930 Y(J,3)=Y(J,3)-Y(J,0)*Y(I,3)
935 Y(J,0)=0
940 NEXT I
945 FOR I=ILAST-1 TO 0 STEP -1
950 Y(I,3)=Y(I,3)-Y(I,2)*Y(I+1,3)
955 Y(I,2)=0
960 NEXT I
965 FOR I=0 TO ILAST:SIG(I)=-Y(I,3):Y(I,3)=0:NEXT I
970 RETURN
975 REM ***********END MATRIX SOLVER***************
980 REM ***********END SUBROUTINE ****************
985 REM
990 REM
995 L=LLAST:GOSUB 105
1000 SIG(LLAST)=SIG(ILAST)*(T1-T3)/(T1+T3)
1100 REM ********COMPUTE AMPLITUDES*******
1105 FOR L=1 TO LLAST:I=L-1:CP(L)=SIG(I)+SIG(I+1):CM(L)
=SIG(I)-SIG(I+1)
1110 NEXT L
```

```
1115 CP(0)=SIG(0):CM(0)=-SIG(0)
1120 FOR L=1 TO LB:I=L-1
1125 GOSUB 105
1130 T6=AP(L)*T2-AM(L)*T4:T7=CM(L)*T1+CP(L)*T3
1135 Q(I)=(1/T5)*(T7-T5*T6):NEXT L
1140 L=LB:T6=-(AP(L)*T2+AM(L)*T4):T7=CM(L)*T1-CP(L)*T3
1145 Q(ILAST)=(1/T5)*(T7+T5*T6)
1150 FOR I=0 TO ILAST:A(I)=A(I)-(DS/SX)*(A(I)-Q(I)):NEX
T I
1155 PRINT:PRINT "AMPLITUDES":PRINT "DEFORM. STEP",N
1160 FOR I=0 TO ILAST:UA=A(I)*SCALE:PRINT UA;:NEXT I
1165 FOR L=1 TO LLAST:I=L-1:AP(L)=A(I)+A(I+1):AM(L)=A(I
)-A(I+1)
1170 NEXT L:AP(0)=A(0):AM(0)=-A(0)
1175 REM
1180 REM
1200 REM ****************FILL IN MATRIX 2ND ORDER *****
************
1205 FOR I=0 TO ILAST:FOR J=0 TO 3:Y(I,J)=0:NEXT J:NEXT
 I
1210 L=0:DX=1:WF=2:GOSUB 105
1215 Y(0,1)=Y(0,1)-TP1:Y(0,3)=Y(0,3)-DX*(APP*T2+AMM*T4)
1220 SN=-1:GOSUB 300:Y(0,3)=Y(0,3)-TZZ
1225 L=LLAST:SN=-1:GOSUB 300
1230 Y(ILAST,1)=Y(ILAST,1)-(4*T1*T3/T5+TZZ*(T3-T1))/(T1
+T3)
1235 DX=0:Y(ILAST,3)=Y(ILAST,3)+(APP*T2-SN*AMM*T4)*DX
1240 SN=1:GOSUB 300
1245 Y(ILAST,3)=Y(ILAST,3)+TZZ:TZ(LLAST)=TZZ:DX=1
1250 FOR L=1 TO LB:I=L-1:SN=1:GOSUB 300
1255 Y(I,3)=Y(I,3)+TZZ:TZ(L)=TZZ:SN=-1:GOSUB 300
1260 Y(I+1,3)=Y(I+1,3)-TZZ
1265 NEXT L
1270 TQ(LB)=TZZ
1275 WF=2:DX=1:GOSUB 805
1280 REM
1285 REM
1300 REM**************COMPUTE AMPLITUDES OF 2ND WAVEFORM
S*********
1305 WF=2:SN=1:FOR LL=1 TO LLAST:I=LL-1:J=I
1310 IF LL=LLAST THEN L=LB:I=L-1:SN=-1:TZZ=TQ(LB):GOTO
1320
1315 L=LL:TZZ=TZ(L):GOSUB 105
1320 SP=SIG(I)+SIG(I+1):SM=SIG(I)-SIG(I+1)
1325 Q1=(SM*T1+SN*SP*T3)/T5:Q1=Q1-AP2(L)*T2+AM2(L)*T4*S
N
```

```
1330 Q(J)=TZZ-Q1
1335 A2(J)=A2(J)-(DS/SX)*(A2(J)-Q(J)):NEXT LL
1340 PRINT:PRINT "AMPLITUDES 2ND WAVEFORM"
1345 II=0:FOR I=0 TO ILAST:UA=A2(I)*SCALE:PRINT UA;
1350 II=II+1:IF II=4 THEN PRINT:II=0
1355 NEXT I
1360 GOTO 435
1365 REM ********END COMPUTATION**********
1370 REM ********RETURN AND INCREASE STRETCH
1375 REM
1380 REM
1400 REM *******INITIALIZE PROGRAM*******
1405 PRINT "PROG. SOLVES COMPLEX MULTILAYERS OF VISC FL
UIDS SEPARATED"
1410 PRINT "BY FRICTIONLESS CONTACTS. WILL WORK FOR LON
G WAVELENGTHS"
1415 PRINT "ONLY WITH DOUBLE PRECISION ARITHMETIC."
1420 REM FIRST LAYER IS L=0;LAST IS LLAST;TOP LAYER (0)
 HAS FLAT TOP
1425 REM FIRST INTERFACE, I=0, IS AT BASE OF TOP LAYER;
LAST LAYER
1430 REM ON RIGID SURFACE AND LAST LAYER IS UNSTRESSED.
 DECOLLEMENT IS
1435 REM AT TOP OF LAST LAYER. LAST INTERFACE IS ILAST=
LLAST-1. IN THE
1440 REM SOL FOR CONSTANTS, THERE ARE ILAST+1 CONSTANTS
 (=LLAST).
1445 REM IN DIMENSION STATEMENTS, V(I), I=LLAST; V(I,J)
; I=LLAST-1,
1450 REM J=4.
1455 DEFINT I,N,J,L:DEFDBL Y,W,T,E,K,C,S,R,A,P:DEFSNG U
:PRINT
1460 READ LAYS:LLAST=LAYS-1:ILAST=LLAST-1
1465 L=LLAST:DIM T(L),MU(L),A(L),K(L),SIG(L),Q(L),AP(L)
,AM(L)
1470 DIM CP(L),AP2(L),AM2(L),A2(L),CM(L),Y(L-1,3),DP(L)
,TZ(L),TQ(L)
1475 REM T=THICK;MU=VISCOSITY RATIO;A=AMPLITUDE;K=DIM.W
AVE NO.
1480 REM SIG=CONSTANT;Q=AMPLIF. FACTOR;Y=COEFF. IN MATR
IX
1485 PI=3.141592653589793#:E=2.718281828459045#:LB=LLAS
T-1
1490 GOSUB 1605
1495 TT=1:FOR L=1 TO LLAST:T(L)=T(L)/T(0):TT=TT+T(L):NE
XT L
```

```
1500 SCALE=T(0):T(0)=1
1505 FOR L=1 TO LLAST:MU(L)=MU(L)/MU(0):NEXT L
1510 MU(0)=1
1515 LPRINT: LPRINT "LAY NO","MU(L)/MU(0)","T(L)/T(0)",
"T(L)"
1520 FOR L=0 TO LLAST:UM=MU(L):UT=T(L):UTT=T(L)*SCALE
1525 LPRINT L,UM,UT,UTT
1530 NEXT L
1535 PRINT:PRINT "NUMBER OF DEFORMATION STEPS(>10)";:IN
PUT NN
1540 PRINT "MAXIMUM THICKENING(SZ)";:INPUT SZ
1545 LPRINT "MAXIMUM THICKENING (T/TO)",SZ
1550 DS=(1/SZ-1)/NN
1555 PRINT "WAVELENGTH (METERS)";:INPUT WL
1560 WT=WL/(SCALE*TT)
1565 LPRINT "WAVELENGTH",WL," WAVE-LGTH/TOT THICK",WT
1570 PRINT "MAXIMUM INITIAL SLOPE";:INPUT SLOPE
1572 LPRINT "CONDITIONS  BEFORE FOLDING"
1575 LPRINT "MAXIMUM INITIAL SLOPE ANGLE (TANGENT)",SLO
PE
1580 RETURN
1585 REM *******END SUBROUTINE***********
1590 REM
1595 REM
1600 REM *******PUT DATA HERE************
1605 DATA 13:FOR L=0 TO 12:MU(L)=1000:T(L)=10:NEXT
1610 FOR L=1 TO 10:T(L)=1:MU(L)=1:NEXT
1615 RETURN
1620 LLAST=18:T(0)=1:T(1)=.45:T(2)=.7:T(3)=.6:T(4)=2
1625 T(5)=1:T(6)=.7:T(7)=.2:T(8)=.3:T(9)=.175:T(10)=.2
1630 T(11)=.25:T(12)=.15:T(13)=6.500001E-02:T(14)=.3:T(
15)=.2
1635 T(16)=.175:T(17)=.075:T(18)=1
1640 FOR L=0 TO LLAST:MU(L)=1:NEXT L
1645 MU(1)=100:MU(2)=5:MU(3)=100:MU(4)=75:MU(5)=100:MU(
6)=100
1650 MU(7)=5:MU(8)=100:MU(9)=5:MU(10)=23:MU(15)=100:MU(
16)=100
1655 MU(17)=100
1660 RETURN
1665 REM ***************END DATA***********************
1670 REM
1675 REM
1700 REM************INTERFACE FORM SUBROUTINE***********
*****
1705 LPRINT:LPRINT "POSITIONS OF INTERFACES"
```

```
1710 WL=WT*SCALE*TT*SX^2:XI=WL/20
1715 FOR I=0 TO ILAST:X=-WL/4-XI
1720 LPRINT "INTERFACE NUMBER",I
1725 LPRINT "HORIZ. POS.","VERT. POS."
1730 X = X+XI:IF 3*WL/4+XI/20-X<0 THEN 1755
1735 Z=DP(I)+A(I)*COS(2*PI*X/WL)+A2(I)*COS(4*PI*X/WL)
1740 UX=X:UZ=Z*SCALE
1745 LPRINT UX,UZ
1750 GOTO 1730
1755 NEXT I
1760 REM
1765 REM
1800 REM **********DEFINITIONS OF L AND I NUMBERS******
**
1805 REM
1810 REM
1815 REM -----------------FLAT SURFACE-----------------
---------
1820 REM                    L = 0
1825 REM --------I = 0 --------------------------------
---------
1830 REM                    L = 1
1835 REM --------I = 1 --------------------------------
---------
1840 REM                    L = 2
1845 REM --------I = 2 --------------------------------
---------
1850 REM                    L = 3     L = LB
1855 REM --------I = 3   I = ILAST---DECOLLEMENT-------
--------
1860 REM                    L = 4     L = LLAST
1865 REM ----------------------------------------------
---------
1870 REM /////////////////RIGID BASEMENT////////////////
/////////
1875 REM \\\\\\\\\\\\\\\\\\\\\\\\\\\\\\\\\\\\\\\\\\\\\\\
\\\\\\\\\
1880 REM ///////////////////////////////////////////////
/////////
9999 END
```

APPENDIX IV

COMPUTER PROGRAM FOR SECOND-ORDER ANALYSIS WHERE THERE ARE TWO PREFERRED WAVELENGTHS, INCLUDING INTERACTION.

```
1 PRINT "STORED ON AMJ DISK UNDER <APPALN.BAS>"
10 GOTO 1210
15 REM
20 REM
100 REM ************SUBROUTINE***************
105 R=1/MU(L):T5=4*WN*WF/R:KK=WF*K(L)
110 EM=1/(E^KK):EP=E^KK:CH=(EP+EM)/2:SH=(EP-EM)/2
115 TM1=CH*SH-KK:TP1=CH*SH+KK:T1=(CH^2)/TM1:T2=KK/TM1
120 T3=(SH^2)/TP1:T4=KK/TP1
125 TP1=(T1+T3)/T5:TM1=(T1-T3)/T5
130 RETURN
135 REM ************END SUB ****************
140 REM
145 REM
200 REM *************START SUBROUTINE**************
205 T1=CH*SH-KK:T2=CH*SH+KK:GOSUB 305
210 GOSUB 405
215 AA=(CM(L)*(CH+KK*SH)-T5*DX*AP*KK*CH)/(T1*T5)
220 BB=-(CP(L)*SH-T5*DX*AM*CH)/(T2*T5)
225 CC=(CP(L)*(SH+KK*CH)-T5*DX*AM*KK*SH)/(T2*T5)
230 DD=-(CM(L)*CH-T5*DX*AP*SH)/(T1*T5)
235 Q1=WN*U*(U+2*SG*V)/(4*(U+SG*V)):S1=-Q1*((AA+DD)*CH+
DD*KK*SH)
240 S2=-Q1*((CC+BB)*SH+BB*KK*CH):Q2=2*(U+SG*V)/(U+2*SG*
V):Q1=Q1*V
245 S3=Q1*((CC+Q2*BB)*CH+BB*KK*SH):S4=Q1*((AA+Q2*DD)*SH
+DD*KK*CH)
250 RETURN
255 REM ***********END SUBROUTINE******************
260 REM
265 REM
300 REM **************BEGIN SUBROUTINE****************
**
305 I=L-1:IF I<0 THEN 315
310 CP(L)=SIG(I,IW)+SIG(I+1,IW):CM(L)=SIG(I,IW)-SIG(I+1
,IW):RETURN
315 CP(0)=SIG(0,IW):CM(0)=-SIG(0,IW):RETURN
320 REM
325 REM
400 REM ******************START SUB******************
405 IF I<0 THEN AM=-A(0,IW):AP=A(0,IW):RETURN
410 IF IW3<3 THEN AM=AMM(L,IW3):AP=APP(L,IW3):RETURN
415 AM=A(I,IW)-A(I+1,IW):AP=A(I,IW)+A(I+1,IW):RETURN
420 REM ******************END SUB********************
425 REM
430 REM
```

```
500 REM **********************START SUBPROGRAM ********
****************
505 IW=IW3:WF=U1+SG*U2:SN=1
510 FOR L=1 TO LB:I=L-1:GOSUB 105:GOSUB 605:Q(I)=TZZ(I)
-Q1-Q2:NEXT L
515 L=LB:SN=-1:GOSUB 605:Q(ILAST)=TQ-Q1-Q2
520 FOR I=0 TO ILAST:A(I,IW3)=A(I,IW3)-(DS/SX)*(A(I,IW3
)-Q(I)):NEXT I
525 IF N=NN THEN LPRINT:LPRINT IW3,"=WAVE","WAVELENGTH=
",WL*SCALE*SX/WF
530 PRINT:PRINT IW3,"=WAVE","L/TTOT",WL*SX/(WF*TT)
535 PRINT "AMPLITUDES":FOR I=0 TO ILAST:UA=A(I,IW3)*SCA
LE:PRINT UA;
540 NEXT I
545 ON (IW3-2) GOTO 1810,1815,1820,1235
550 REM ********************END SUB********************
*********
555 REM
560 REM
600 REM **********************START SUB****************
605 SM = SIGMA(I)-SIGMA(I+1):SP=SIGMA(I)+SIGMA(I+1)
610 Q1=(SM*T1+SN*SP*T3)/T5:GOSUB 405:Q2=SN*AM*T4-AP*T2
615 RETURN
620 IF I<0 THEN TP=(1-SN)*A(0,IW)/2:RETURN
625 TP=((1+SN)*A(I,IW)+(1-SN)*A(I+1,IW))/2:RETURN
630 REM ******************END SUB**********************
****
635 REM
640 REM
700 REM*********************START SUBROUTINE**************
**********
705 I=L-1:GOSUB 405:YM=S1*AM+S2*AP+YM:ZM=SGN(U+SG*V)*(S
3*AM+S4*AP)+ZM
710 YP=YP+S1*AP+S2*AM:ZP=SGN(U+SG*V)*(S3*AP+S4*AM)+ZP
715 RETURN
720 REM *******************END SUB********************
***********
725 REM
730 REM
800 REM *******************START SUBROUTINE************
***********
805 YM=0:YP=0:ZM=0:ZP=0
810 U=U1:WF=U:GOSUB 105:V=U2:IW=IW1:GOSUB 205:IW=IW2:GO
SUB 705
815 U=U2:WF=U:GOSUB 105:V=U1:IW=IW2:GOSUB 205:IW=IW1:GO
SUB 705
820 U=U1:V=U2:SN=1:GOSUB 905:YM=YM+TP
```

```
825 SN=-1:GOSUB 905:YP=YP+TP
830 RETURN
835 REM ****************END SUB*************************
*************
840 REM
845 REM
900 REM ****************START SUBROUTINE***************
*************
905 IF I>-1 THEN TP=A(I,IW1)*A(I,IW2)-SN*A(I+1,IW1)*A(I
+1,IW2)
910 IF I<0 THEN TP=-SN*A(0,IW1)*A(0,IW2)
915 TP=(TP*(U*V/(U+SG*V))*WN*DX)*SG
920 RETURN
925 REM *****************END SUB************************
*************
930 REM
935 REM
1000 REM ***************START SUBROUTINE***************
********
1005 U=U1:V=U2:IW=IW2:GOSUB 620
1010 IW=IW1:WF=U:GOSUB 105:GOSUB 205:TP=TP*(U+SG*V)*WN/
2
1015 T1=(SN*(AA+DD)+KK*BB)*SH+(CC+BB+SN*KK*DD)*CH:TP=TP
*T1:TZ=TP
1020 U=U2:V=U1:IW=IW1:GOSUB 620
1025 IW=IW2:WF=U:GOSUB 105:GOSUB 205:TP=TP*(U+SG*V)*WN/
2
1030 T1=(SN*(AA+DD)+KK*BB)*SH+(CC+BB+SN*KK*DD)*CH:TP=TP
*T1:TZ=TZ+TP
1035 WF=U1+SG*U2:GOSUB 105:TZ=(TZ+YM*T1+ZP*T2+SN*(YP*T3
-ZM*T4))/DV
1040 RETURN
1045 REM ****************END SUB************************
***************
1050 REM
1055 REM
1100 REM********************START SUBPROG**************
********
1105 FOR I=0 TO ILAST:FOR J=0 TO 3: Y(I,J)=0:NEXT J:NEX
T I
1110 L=0:I=L-1:DX=1:GOSUB 805:SN=-1:GOSUB 1005
1115 Y(0,3)=Y(0,3)-TZ:WF=U1+SG*U2:IW=IW3:GOSUB 105:GOSU
B 405
1120 Y(0,1)=Y(0,1)-TP1:Y(0,3)=Y(0,3)-(AP*T2+AM*T4)*DX
1125 L=LLAST:DX=0:SN=-1:GOSUB 105:I=L-1:GOSUB 405
```

```
1130 Y(ILAST,3)=Y(ILAST,3)+(AP*T2-AM*T4)*DX:DX=1:GOSUB
805
1135 SN=1:GOSUB 1005:TZZ(I)=TZ:Y(ILAST,3)=Y(ILAST,3)+TZ
:SN=-1
1140 GOSUB 1005:Y(ILAST,1)=Y(ILAST,1)-(4*T1*T3/T5+TZ*(T
3-T1))/(T1+T3)
1145 DX=1:WF=U1+SG*U2:IW=IW3:FOR L=1 TO LB:I=L-1
1150 GOSUB 805:SN=1:GOSUB 1005:TZZ(I)=TZ
1155 Y(I,3)=Y(I,3)+TZ:SN=-1:GOSUB 1005:Y(I+1,3)=Y(I+1,3
)-TZ
1160 TQ=TZ:NEXT L:WF=U1+SG*U2:IW=IW3:GOTO 1610
1165 REM********************END SUBPROG*****************
*********
1170 REM
1175 REM
1200 REM*******************START MAIN PROGRAM***********
*********
1205 REM********************INITIALIZE AND READ DATA****
***
1210 GOSUB 2005
1215 WT=WL*SX/TT
1220 SX=1.0001:N=0
1225 GOSUB 1305
1230 LPRINT:LPRINT:LPRINT:LPRINT "CONDITIONS AFTER FOLD
ING"
1235 IF (SZ-1/(SX+DS))<0 THEN 1245 ELSE 1505
1240 REM *********FINISHED--PRINT RESULTS**
1245 UW=WL*SCALE*SX:PRINT "WAVELENGTH",UW
1250 UT=1/SX:UW=WL*SX/TT:UTT=TT*SCALE
1255 LPRINT "T/TO THICKENING",UT:LPRINT "TOTAL THICK",U
TT
1260 UW=WL*SX*SCALE:US=UW/WW:LPRINT "LONG WAVE",UW," SH
ORT WAVE",US
1265 GOSUB 1305
1270 GOTO 1405
1275 REM
1280 REM
1300 REM **********************SUBROUTINE**************
************
1305 PRINT "AMPLITUDES":PRINT "INTERFACE A1,A2,A3,A4,A5
,A6"
1310 DP(0)=-T(0)/SX:FOR I=1 TO ILAST:DP(I)=DP(I-1)-T(I)
/SX:NEXT I
1315 DP(LLAST)=DP(ILAST)-T(LLAST):LPRINT
1320 LPRINT "INTERFACE  DEPTH  AMPLITUDES  A1,A2,A3,A4,
A5,A6"
```

```
1325 FOR I=0 TO ILAST:UD=DP(I)*SCALE:PRINT I,UD:
1330 LPRINT USING "+###.#  ";I,UD;
1335 FOR IW=1 TO 6:UA=A(I,IW)*SCALE:PRINT UA;
1340 LPRINT USING "+##.###  ";UA;:NEXT IW
1345 LPRINT:PRINT:NEXT I
1350 LPRINT:LPRINT "LAYER","MU(L)/MU(0)","T(L)/SCALE","
THICKNESS"
1355 FOR L=0 TO LLAST:UM=MU(L):UT=T(L)/SX:UTT=T(L)*SCAL
E/SX
1360 IF L=LLAST THEN UT=T(L):UTT=UT*SCALE
1365 LPRINT L,UM,UT,UTT:NEXT L
1370 RETURN
1375 REM ************************END SUB****************
************
1380 REM
1385 REM
1400 REM **************COMPUTE FORM********************
1405 PRINT:PRINT "TO COMPUTE FORM, TYPE NEG NUMBER":INP
UT OO
1410 IF OO<0 THEN 2300 ELSE 9999
1415 REM***************END OF PROGRAM*******************
1420 REM
1425 REM
1430 REM
1500 REM*********************INCREASE AMOUNT OF STRETCH*
*************
1505 TT=0:SX=SX+DS:FOR L=0 TO LB:K(L)=PI*T(L)/(WL*SX^2)
:TT=TT+T(L)/SX
1510 NEXT L:K(LLAST)=PI*T(LLAST)/(WL*SX):TT=TT+T(LLAST)
1515 PRINT:PRINT:PRINT "  T/TO",1/SX
1520 WF=1:IW=1:IW3=1:N=N+1
1525 WN=2*PI/(WL*SX)
1530 REM ********FILL-IN MATRIX***********
1535 FOR I=0 TO ILAST:FOR J=0 TO 3:Y(I,J)=0:NEXT J:NEXT
 I
1540 FOR L=1 TO LLAST:I=L-1:APP(L,IW3)=A(I,IW3)+A(I+1,I
W3)
1545 AMM(L,IW3)=A(I,IW3)-A(I+1,IW3):NEXT L:APP(0,IW3)=A
(0,IW3)
1550 AMM(0,IW3)=-A(0,IW3)
1555 L=0:I=L-1:DX=1:GOSUB 105:GOSUB 405
1560 Y(0,1)=Y(0,1)-TP1
1565 Y(0,3)=Y(0,3)-(AP*T2+AM*T4)*DX
1570 L=LLAST:GOSUB 105:I=L-1:GOSUB 405
1575 DX=0:Y(ILAST,3)=Y(ILAST,3)+(AP*T2-AM*T4)*DX:DX=1
1580 Y(ILAST,1)=Y(ILAST,1)-4*T1*T3/(T5*(T1+T3))
1585 REM
```

```
1600 REM
1605 REM *************START SUBPROGRAM*****************
***
1610 FOR L=1 TO LB:I=L-1:J=L
1615 GOSUB 105:GOSUB 405
1620 Y(I,1)=Y(I,1)-TP1:Y(I,2)=Y(I,2)+TM1
1625 Y(J,0)=Y(J,0)+TM1:Y(J,1)=Y(J,1)-TP1
1630 Y(I,3)=Y(I,3)+DX*(AP*T2-AM*T4)
1635 Y(J,3)=Y(J,3)-DX*(AP*T2+AM*T4)
1640 NEXT L
1645 Y(0,0)=0:Y(ILAST,2)=0
1700 REM ********START MATRIX SOLVER****
1705 FOR I=0 TO ILAST:YY=1/Y(I,1):Y(I,1)=1
1710 Y(I,2)=Y(I,2)*YY:Y(I,3)=Y(I,3)*YY
1715 IF I=ILAST GOTO 1740
1720 J=I+1
1725 Y(J,1)=Y(J,1)-Y(J,0)*Y(I,2)
1730 Y(J,3)=Y(J,3)-Y(J,0)*Y(I,3)
1735 Y(J,0)=0
1740 NEXT I
1745 FOR I=ILAST-1 TO 0 STEP -1
1750 Y(I,3)=Y(I,3)-Y(I,2)*Y(I+1,3)
1755 Y(I,2)=0
1760 NEXT I
1765 FOR I=0 TO ILAST:SIGMA(I)=-Y(I,3):Y(I,3)=0:NEXT I
1770 L=LLAST:GOSUB 105
1775 SIGMA(LLAST)=SIGMA(ILAST)*(T1-T3)/(T1+T3)
1780 REM ******************END SUBPROGRAM**************
*************
1785 REM
1790 REM
1795 IF IW3<3 THEN FOR I=0 TO ILAST+1:SIG(I,IW3)=SIGMA(
I):NEXT I:GOTO 1905
1800 GOTO 505
1805 IW3=3:IW=3:U1=1:U2=1:IW1=1:IW2=1:SG=1:DV=2:GOTO 11
05
1810 IW3=4:IW=4:U1=WW:U2=WW:IW1=2:IW2=2:SG=1:DV=2:GOTO
1105
1815 IW3=5:IW=5:U1=WW:U2=1:IW1=2:IW2=1:SG=1:DV=1:GOTO 1
105
1820 IW3=6:IW=6:SG=-1:GOTO 1105
1825 REM *********************END SUB*****************
1830 REM
1835 REM
1900 REM ********COMPUTE AMPLITUDES*******
```

```
1905 IW=IW3:FOR L=0 TO LLAST:I=L-1:GOSUB 305:NEXT L
1910 FOR L=1 TO LB:I=L-1
1915 GOSUB 105:GOSUB 405
1920 T6=AP*T2-AM*T4:T7=CM(L)*T1+CP(L)*T3
1925 Q(I)=(1/T5)*(T7-T5*T6):NEXT L
1930 L=LB:T6=-(AP*T2+AM*T4):T7=CM(L)*T1-CP(L)*T3
1935 Q(ILAST)=(1/T5)*(T7+T5*T6)
1940 FOR I=0 TO ILAST:A(I,IW)=A(I,IW)-(DS/SX)*(A(I,IW)-
Q(I)):NEXT I
1945 PRINT:PRINT:PRINT "DEFORM. STEP",N
1950 IF IW=1 THEN PRINT:PRINT "LONG WAVE":GOTO 1960
1955 PRINT:PRINT "SHORT WAVE"
1960 PRINT "L/TTOT",WL*SX/(WF*TT)
1965 FOR I=0 TO ILAST:UA=A(I,IW)*SCALE:PRINT UA;:NEXT I
1970 IF IW=2 THEN 1805
1975 WF=WW:IW=2:IW3=2:GOTO 1535
1980 REM
1985 REM
2000 REM *******INITIALIZE PROGRAM*******
2005 PRINT "PROG. SOLVES COMPLEX MULTILAYERS OF VISC FL
UIDS SEPARATED"
2010 PRINT "BY FRICTIONLESS CONTACTS. WILL WORK FOR LON
G WAVELENGTHS"
2015 PRINT "ONLY WITH DOUBLE PRECISION ARITHMETIC.":REM
 TOP LAYER (L=0)
2020 REM IS FLAT. PROGRAM TREATS A LONG AND A SHORT WAV
E TO 2ND ORDER,
    INCLUDING INTERACTIONS.  THUS THERE ARE SIX WAVES:
2025 REM WL,WS,WL/2,WS/2,WL/(WL/WS+1),WL/(WL/WS-1)
2030 REM LAST LAYER (LLAST) RESTS ON FRICTIONLESS, RIGI
D SURFACE.
THUS, DECOLLEMENT IS AT TOP OF LAST LAYER, AS SHOWN IN
DIAGRAM
BELOW.
2035 REM IN DIMENSION STATEMENTS, V(I), I=LLAST; V(I,J)
; I=LLAST-1,
2040 REM J=4.
2045 DEFINT I,N,J,L:DEFDBL Y,W,T,E,K,C,S,R,A,P:DEFSNG U
:PRINT
2050 INPUT "NUMBER OF LAYERS";LAYS
2055 LLAST=LAYS-1:ILAST=LLAST-1
2060 L=LLAST:DIM T(L),MU(L),A(L,6),K(L),SIGMA(L),Q(L),A
PP(L,2),AMM(L,2)
2065 DIM CP(L),CM(L),Y(L-1,3),DP(L),TZZ(L)
2070 DIM SIG(L,2)
2075 REM T=THICK;MU=VISCOSITY RATIO;A=AMPLITUDE;K=DIM.W
AVE NO.
```

```
2080 REM SIG=CONSTANT;Q=AMPLIF. FACTOR;Y=COEFF. IN MATR
IX
2085 PI=3.14159265358979#:E=2.71828182845904#:LB=LLAS
T-1
2090 GOSUB 2225:REM**************READ DATA*************
*****
2095 INPUT "MAXIMUM THCKENING(SZ)";SZ
2100 SCALE=T(0):FOR L=0 TO LB:T(L)=T(L)/SZ:NEXT L
2105 TT=0:FOR L=0 TO LLAST:T(L)=T(L)/SCALE:TT=TT+T(L):N
EXT L
2110 FOR L=1 TO LLAST:MU(L)=MU(L)/MU(0):NEXT L
2115 MU(0)=1
2120 INPUT "NUMBER OF DEFORMATION STEPS(>10)";NN
2125 DS=(1/SZ-1)/NN
2130 LPRINT:LPRINT "CONDITIONS BEFORE FOLDING":LPRINT
2135 INPUT "LONG WAVELENGTH(M)";WL:LPRINT "LENGTH SCALE
",SCALE
2140 INPUT "SHORT WAVELENGTH";WS:WW=WL/WS:WL=WL*SZ/SCAL
E:WT=WL/TT
2145 FOR I= 0 TO LLAST:FOR IW=1 TO 6:A(I,IW)=0:NEXT IW:
NEXT I
2150 INPUT "MAXIMUM INITIAL SLOPE";SLOPE
2155 B=SLOPE*WL/(2*PI):FOR I=0 TO ILAST:A(I,1)=B
2160 A(I,2)=(B/WW):NEXT I
2165 LPRINT "MAXIMUM SLOPE",SLOPE
2170 LPRINT "TOTAL THICKNESS",TT*SCALE:PRINT "TTOT",TT*
SCALE
2175 LPRINT "LONG WAVE",WL*SCALE:LPRINT "SHORT WAVE",WL
*SCALE/WW
2180 RETURN
2185 REM *******END SUBROUTINE***********
2190 REM
2195 REM
2200 REM *******PUT DATA HERE************
2205 REM************T(L) IS FINAL THICKNESS************
****
2210 LLAST=4:FOR L=0 TO LLAST:T(L)=100:MU(L)=1:NEXT L
2215 T(2)=20:MU(2)=100
2220 RETURN
2225 LLAST=18:T(0)=1:T(1)=.45:T(2)=.7:T(3)=.6:T(4)=2
2230 T(5)=1:T(6)=.7:T(7)=.2:T(8)=.3:T(9)=.175:T(10)=.2
2235 T(11)=.25:T(12)=.15:T(13)=6.500001E-02:T(14)=.3:T(
15)=.2
2240 T(16)=.175:T(17)=.075:T(18)=1
2245 FOR L=0 TO LLAST:MU(L)=1:NEXT L
2250 MU(1)=100:MU(2)=5:MU(3)=100:MU(4)=75:MU(5)=100:MU(
```

```
6)=100
2255 MU(7)=5:MU(8)=100:MU(9)=5:MU(10)=23:MU(15)=100:MU(
16)=100
2260 MU(17)=100
2265 RETURN
2270 REM *******************END OF DATA****************
*******
2275 REM
2280 REM
2300 REM***********INTERFACE FORM SUBROUTINE***********
*****
2305 LPRINT:LPRINT "POSITIONS OF INTERFACES"
2310 WL=WL*SX:XI=WL/20
2315 FOR I=0 TO ILAST:X=-WL/4-XI
2320 LPRINT "INTERFACE NUMBER",I
2325 LPRINT "HORIZ. POS.","VERT. POS."
2330 X = X+XI:IF 3*WL/4+XI/20-X<0 THEN 2365
2335 Z=DP(I)+A(I,1)*COS(2*PI*X/WL)+A(I,2)*COS(2*PI*WW*X
/WL)
2340 Z=Z+A(I,3)*COS(4*PI*X/WL)+A(I,4)*COS(4*PI*WW*X/WL)
2345 Z=Z+A(I,5)*COS(2*PI*(WW+1)*X/WL)+A(I,6)*COS(2*PI*(
WW-1)*X/WL)
2350 UX=X*SCALE:UZ=Z*SCALE
2355 LPRINT UX,UZ
2360 GOTO 2330
2365 NEXT I
2370 REM *********************END PLOTTING*************
******
2375 REM
2380 REM
2400 REM **********DEFINITIONS OF L AND I NUMBERS******
**
2405 REM
2410 REM
2415 REM -----------------FLAT SURFACE-----------------
---------
2420 REM                     L = 0
2425 REM --------I = 0 --------------------------------
---------
2430 REM                     L = 1
2435 REM --------I = 1 --------------------------------
---------
2440 REM                     L = 2
2445 REM --------I = 2 --------------------------------
---------
2450 REM                     L = 3      L = LB
2455 REM --------I = 3   I = ILAST---DECOLLEMENT-------
```

```
--------
2460 REM                         L = 4      L = LLAST
2465 REM ---------------------------------------------
---------
2470 REM //////////////////RIGID BASEMENT////////////////
//////////
2475 REM \\\\\\\\\\\\\\\\\\\\\\\\\\\\\\\\\\\\\\\\\\\\\\\\
\\\\\\\\\
2480 REM /////////////////////////////////////////////
//////////
2485 REM
2490 REM
2495 REM ***************FORM OF MATRIX**********
2500 REM***NORMAL FORM OF MATRIX IS:
2505 REM    YP    Y     0     0     0     0     Y     I=
0
2510 REM    Y     YP    Y     0     0     0     Y     I=
1
2515 REM    0     Y     YP    Y     0     0     Y     I=
2
2520 REM    0     0     Y     YP    Y     0     Y     I=
3
2525 REM    0     0     0     Y     YP    Y     Y     I=
4
2530 REM    0     0     0     0     Y     YP    Y     I=
5
2535 REM  J=0   J=1   J=2    J=3   J=4   J=5  J=6
2540 REM *****HERE YP IS PIVOT NUMBER******************
****
2545 REM
2550 REM
2555 REM **********COMPRESSED FORM USED IN THIS PROGRAM
:
2560 REM    NULL  YP    Y     Y     I=0
2565 REM    Y     YP    Y     Y     I=1
2570 REM    Y     YP    Y     Y     I=2
2575 REM    Y     YP    Y     Y     I=3
2580 REM    Y     YP    Y     Y     I=4
2585 REM    Y     YP    NULL  Y     I=5
2590 REM  J=0    J=1   J=2   J=3
2595 REM *****BEWARE! MATRIX SOLVER IS WRITTEN ACCORDIN
GLY!****
9999 END
```

APPENDIX V

MEASURED STRATIGRAPHIC SECTIONS ALONG ABONDONED RAILROAD, NORTHUMBERLAND, PENNSYLVANIA.

MEASURED STRATIGRAPHIC SECTION DESCRIPTIONS ALONG AN ABANDONED RAILROAD, NEAR NORTHUMBERLAND, PENNSYLVANIA

	Layer Thickness (in meters)	Cumulative Thickness
TRIMMERS ROCK FORMATION (Dtr)		
1 - Siltstone; olive gray (5Y 3/2) to dusky yellowish brown (10YR 2/2), resistant to non-resistant, blocky to brittle fractures, medium laminated (1.5-2.5 mm) to thin bedded (4-10 cm). At 2 and 6 meters from the bottom two fossil horizons, (Ambocoelia, Chonetia) 5 cm thick, are present. Fossils are preserved molds and casts, shells are leached.	19	19
2 - Siltstone; olive gray (5Y 3/2), non-resistant to resistant, brittle to blocky fractures, medium laminated (1-3 mm) to thick bedded (30-40 cm). Bedding normal. Joints are well developed in thick bedded layers.	6	25
3 - Siltstone; lower 20 cm is dark yellowish brown (10YR 4/2); the rest is olive gray (5Y 3/2), resistant, blocky fractures, thin bedded (10-20 cm) and slabby parting. Bedding normal. Joints are well developed in lower one meter.	9	34
4 - Mudshale; moderate yellowish brown (10YR 5/4) to olive gray (5Y 3/2), non-resistant, splintery fractures, mica abundant, medium laminated (1-3 mm) and fissile parting.	2	36
5 - Siltstone; light olive gray (5Y 3/2) to dark yellowish brown (10YR 4/2), resistant, blocky fractures, thin bedded (5-15 cm), mica abun-		

	Layer Thickness (in meters)	Cumulative Thickness
dant, some beds are lenticular, slabby parting.	4	10
6 - Mudshale; moderate yellowish brown (10YR 5/4) to olive gray (5Y 3/2), non-resistant, splintery fractures, mica abundant, medium laminated (1-3 mm), platy parting, between 1.5 to 2.5 meters from lower contact. One meter thick bedded siltstone; olive gray (5Y 5/2), resistant, blocky fractures, thin bedded (10-15 cm); some beds are lenticular.	5	45
7 - Covered	50	95
8 - Siltstone; olive gray (5Y 3/2), resistant, blocky fractures, thin bedded (10-20 cm). Bedding normal. Joints are well developed; some beds are lenticular.	3	98
9 - Siltstone; olive gray (5Y 3/2), resistant, brittle fractures, thick lamination (5-10 mm), mica abundant; fissile parting; bedding normal. Joints are well developed.	24	122
10 - Siltstone; olive gray (5Y 3/2), resistant, blocky to concoidal fractures, very thin (1-3 cm) to thick bedded (3-20 cm), slabby parting, 2 meters from the bottom 5 cm thick fossil horizon present.	7	129
11 - Siltstone; olive gray (5Y 3/2), blocky fractures, thin bedded (3-10 cm), slabby parting, 16, 17 and 50 meters from the bottom three fossil horizons are present (brachiopoda). Fossils are preserved molds and casts, shells are leached.	56	185

	Layer Thickness (in meters)	Cumulative Thickness
12 - Siltstone; olive gray (5Y 3/2), resistant, blocky fractures, thickly laminated (5-10 mm) to thick bedded (20-50 cm). 60 meters from bottom 10 cm thick fossil horizon present (brachiopoda).	106	291
13 - Siltstone; olive gray (5Y 3/2), resistant, blocky fractures, thin (3-10 cm) to very thick bedded (30-50 cm). Bedding normal. Joints are well developed; two fossil horizons (5 cm thick) present at 20 and 30 meters from the bottom.	45	336
14 - Siltstone; olive gray (5Y 3/2), resistant to non-resistant, thinly laminated (0.5-1 mm) to thin bedded (10-20 cm), fissile parting.	48	384
15 - Siltstone; olive gray (5Y 3/2), non-resistant to resistant, brittle fractures, medium laminated (1-3 mm)	15	399
16 - Sandstone; olive gray (5Y 3/2), resistant, concoidal fractures, very fine grained, well rounded and well sorted, cemented with silica, thin bedded (10-20 cm), upper parts thick to very thick bedded (50-100 cm).	14	413
17 - Siltstone; olive gray (5Y 3/2), non-resistant to resistant, brittle fractures, medium laminated (1-3 mm) to very thin bedded (2-5 cm). Two fossil horizons present (17 cm thick) at 2 and 4 meters from the bottom; fossils are preserved molds and casts.	6	419
18 - Interbedded siltstone and sandstone; olive gray (5Y 3/2) to dark gray (N3), resistant,		

	Layer Thickness (in meters)	Cumulative Thickness
blocky fractures, thin bedded (5-10 cm). Sandstone is fine grained, well rounded, well sorted and cemented with silica.	10	429
19 - Siltstone; olive gray (5Y 3/2), resistant, blocky fractures, lower 3 meters medium laminated (1-3 mm), upper 9 meters very thin bedded (1-3 cm).	12	441
20 - Interbedded mudshale and siltstone; mudshale olive gray (5Y 3/2), brittle fractures, non-resistant, medium laminated (1-3 mm). Siltstone is olive gray (5Y 3/2), non-resistant, brittle fractures, thin to medium laminated (o.5.2 mm).	28	469
21 - Mudshale; olive gray (5Y 3/2), non-resistant, splintery fractures, thin to medium laminated (0.5-2 mm), weathers fissile.	21	490
22 - Siltstone; olive gray (5Y 3/2), resistant, brittle fractures, medium to thickly laminated (3-5 mm), platy parting.	7	497

CATSKILL FORMATION

IRISH VALLEY MEMBER (Dciv)

23 - Siltstone; grayish brown (5YR 3/2), resistant, very thick bedded (120 cm), lower contact shows sole marks.	6	503
24 - Mudshale; grayish brown (5YR 3/2), non-resistant, brittle fractures, medium to thick lamination (3-7 mm), weathers platy and fissile.	3	506

	Layer Thickness (in meters)	Cumulative Thickness
25 - Siltstone; olive gray (5Y 3/2) to grayish brown (5YR 3/2), resistant, blocky fractures, thin bedded (5-25 cm) and has abundant fossils. Fossils are preserved molds and casts; shells are leached (Rhynchonellid, Leiorhnchus, Tropidoleptus).	4	510
26 - Mudshale; grayish brown (5YR 3/2) to olive gray (5Y 3/2), non-resistant, brittle fractures, thick to medium lamination (1-8 mm), platy and fissile parting, fossils are abundant.	7	517
27 - Sandstone; light gray (N7), resistant, blocky fractures, thin to thick bedded (30 - 100 cm), very fine grained, well rounded, and cemented with silica.	3	520
28 - Mudshale; dark gray (N3), resistant, brittle fractures, medium laminated, fissile parting.	1	521
29 - Siltstone; olive gray (5Y 3/2) to dusky yellowish brown (10YR 3/2), thick laminated (3-6 mm), lower 35 cm is very fine grained bedded sandstone.	49	570
30 - Siltstone; blackish red (5R 2/2) to dusky yellowish brown (10YR 2/2), resistant, thickly laminated (3-7 mm) to thick bedded (40-100 cm), mica abundant.	12	582
31 - Sandstone; medium light gray (N6), blocky fractures, very fine grained, well sorted, well rounded, thin bedded (5-30 cm), cemented with silica.	3	585

	Layer Thickness (in meters)	Cumulative Thickness
32 - Siltstone; olive gray (5Y 3/2), non-resistant, brittle fractures, medium laminated (1-3 mm), fissile parting.	15	600
33 - Sandstone; greenish black (5G 2/1), resistant, very fine grained, mica abundant, thick bedded (70-100 cm), cemented with silica.	4	604
34 - Siltstone; olive gray (5Y 3/2), non-resistant, thickly laminated (5-10 mm), at 12 meters from the bottom big nodules present (50 cm diameter).	15	619
35 - Covered	35	654
36 - Sandstone; dusky yellowish brown (10YR 2/2), resistant, blocky fractures, thin bedded (5-25 cm) and cemented with silica.	8	662
37 - Siltstone; olive gray (5Y 3/2), resistant, brittle fractures, thickly laminated (5-10 mm), platy parting.	7	669
38 - Sandstone; dusky yellowish brown (10 YR 2/2), resistant, blocky fractures, fine grained, well sorted, well rounded, thin bedded (5-25 cm) and cemented with silica.	15	684
39 - Siltstone; olive gray (5Y 3/2), non-resistant, brittle, medium laminated (2-4 mm), fissile parting.	10	694
40 - Covered	120	814

	Layer Thickness (in meters)	Cumulative Thickness
41 - Sandstone; olive gray (5Y 3/2), resistant, blocky fractures, thin bedded (5-25 cm), fine grained, well sorted and well rounded, cemented with silica	17	831
42 - Covered	48	879
43 - Siltstone; grayish brown (5YR 3/2), non-resistant, brittle to splintery fractures, medium laminated (2-4 mm)	8	887
44 - Covered	70	957
45 - Sandstone; very dusky red (10R 2/2), resistant, hackly fractures, very fine grained, well sorted, well rounded, thin bedded (2-25 cm) and cemented with silica	10	967
46 - Siltstone; olive gray (5Y 3/2), non-resistant, brittle fractures, medium laminated (1-3 mm), platy parting	4	971
47 - Sandstone; olive gray (5Y 3/2) to very dusky red (10R 2/2), resistant, blocky fractures, very fine grained, well sorted, well rounded, thin bedded (10-20 cm) and cemented with silica	3	974
48 - Interbedded siltstone and sandstone; olive gray (5Y 3/2), non-resistant, brittle fractures. Siltstone; thickly laminated (0.5-1 mm). Sandstone; thin bedded (2-5 cm), mica abundant, and cemented with silica	6	980
49 - Sandstone; very dusky red (10R 2/2), resistant, blocky fractures, well rounded, well sorted, thin bedded (5-15 cm), cemented with silica	1	981

	Layer Thickness (in meters)	Cumulative Thickness
50 - Siltstone; olive gray (5Y 3/2), non-resistant, brittle fractures, thickly laminated (0.5-1 mm), cemented with silica	7	988
51 - Sandstone; olive gray (5Y 3/2), resistant, blocky fractures, very fine grained, well sorted, well rounded, thin bedded (4-6 cm), cemented with silica	1	989
52 - Covered	211	1200

SHERMAN CREEK MEMBER (Dcsc)

53 - Siltstone; very dusky red (10R 2/2), non-resistant, brittle fractures, thickly laminated (5-8 mm), platy weathers	2	1202
54 - Sandstone; very dusky red (10R 2/2), resistant, blocky fractures, very fine grained, very well sorted and well rounded, thin bedded (5-15 cm), one part cross-bedded, cemented with silica	11	1213
55 - Siltstone; dusky brown (5YR 2/2), non-resistant, brittle fractures, thickly laminated (5-8 mm)	3	1216
56 - Sandstone; dusky brown (5Y 2/2), resistant, blocky fractures, very fine grained, well sorted, well rounded, very thick to massive bedded (150-200 cm), cross-bedded	10	1226
57 - Sandstone; dusky brown (5Y 2/2), resistant, blocky fractures, very fine grained, well rounded, well sorted, mica abundant, thick to massive bedded (10-150 cm), cross-bedded, cemented with silica	5	1231

	Layer Thickness (in meters)	Cumulative Thickness
58 - Interbedded sandstone and siltstone; dusky brown (5YR 2/2), resistant to non-resistant, blocky to brittle fractures. Sandstone is very fine grained, well rounded, well sorted, thin bedded (10-25 cm). Siltstone is thickly laminated (5-8 mm), cemented with silica	9	1240
59 - Sandstone; dusky brown (5YR 2/2), resistant, blocky fractures, very fine grained, well rounded, well sorted, very thick to massive bedded (80 - 120 cm), cemented with silica	2	1242
60 - Interbedded sandstone and siltstone; dusky brown (5YR 2/2), non-resistant, blocky to brittle fractures. Sandstone is thin bedded (10-25 cm) and cross-bedded. Siltstone is thickly laminated (5-8 mm)	6	1248
61 - Covered	38	1286
62 - Siltstone; grayish red (5Y 4/2), resistant, blocky fractures, thin bedded (10-40 cm), some parts cross bedded, upper 3 meters thickly laminated (0.5-1 cm), some plant fossils present	12.5	1289.5
63 - Mudshale; grayish red (5Y 4/2), non-resistant, brittle fractures, thickly laminated (5-10 mm), mica abundant, fissile parting	1.5	1300
64 - Sandstone; very dusky red (10R 2/2), resistant, blocky fractures, very fine grained, well rounded, well sorted, mica abundant, thick bedded (20-50 cm),		

	Layer Thickness (in meters)	Cumulative Thickness
upper part thin bedded (10-20 cm), cemented with silica	5	1305
65 - Siltstone; grayish red (5R 4/2), non-resistant, blocky fractures, thin bedded (10-25 cm), cemented with silica	5.5	1310.5
66 - Sandstone; grayish red (5R 4/2), non-resistant to resistant, blocky fractures, thin bedded (10-25 cm), very fine grained, well rounded, well sorted, cemented with silica	7.5	1318
67 - Sandstone; blackish red (5R 2/2), resistant, blocky fractures, mica abundant, very thick to massive bedded (120 - 200 cm), very fine grained, well rounded, well sorted, cemented with silica	6	1324
68 - Siltstone; grayish red (5R 4/2), non-resistant, brittle to blocky fractures, thickly laminated (5-8 mm) to thin bedded (10 25 cm)	7	1331
69 - Covered	3	1334
70 - Siltstone; dark yellowish brown (10R 3/4), resistant to non-resistant, blocky to brittle fractures and thin bedded (2-4 cm)	3	1337